

NATURAL CONVECTION ANALYSIS OF THE MITR-II
DURING LOSS OF FLOW ACCIDENT

by

FARID BAMDAD HAGHIGHI

S.B. Pahlavi University 1974

Submitted in partial fulfillment of
the requirements for the degree of
Nuclear Engineer
and

Master of Science in Nuclear Engineering

at the

Massachusetts Institute of Technology

August 1977

Signature redacted

Signature of Author

Department of Nuclear Engineering
Signature redacted

Certified by

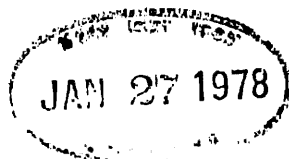
Thesis Advisor

Accepted by

Signature redacted

Chairman, Department Committee on Graduate Students

Archives



NATURAL CONVECTION ANALYSIS OF THE M.I.T.R. II
DURING LOSS OF FLOW ACCIDENT

by

FARID BAMDAD-HAGHIGHI

Submitted to the Department of Nuclear Engineering,
Massachusetts Institute of Technology in partial fulfillment
of the requirements for the degree of Nuclear Engineer.

ABSTRACT

The natural convective cooling of the MITR-II, in a transitory period due to loss of electrical power to the main panel is studied in this work.

The transient behavior of the Reactor after scram due to loss of flow is examined for an infinite operation at the steady state power of 5 MWth. The shutdown energy due to fission of the delayed neutrons, decay of fission products and the activated core materials is transferred by the pump coast down and natural convection flow.

A series of incore temperature measurements were made as part of the reactor startup procedure to full licensed power. A computer program was written to compare the nominal calculation of the average core temperature distribution with the experimental values. The calculated and measured temperatures are in general agreement except that the calculations predict the peak temperature at an earlier time than observed experimentally. The analysis is expanded to the hot channel temperature evaluation during loss of primary forced flow.

A single channel model is used to simulate the hot channel for calculation of temperature distribution in five possible cases that the accident might occur.

It is calculated that the hottest point in the core, due to loss of flow accident for steady state power of 5 MWth will be below the saturation temperature, even if one of the natural convection valves remains in the closed position.

In the case that two of the incore check valves do not open after the accident, boiling will occur about 10 seconds following the accident. Although the fuel surface temperature

exceeds saturation at a height of approximately 12 inches from the bottom of the fuel plate, it is still far below the softening point of aluminum, (450°C).

Increasing the core inlet temperature encourages the onset of nucleation boiling. The fuel surface temperature increases to 104.5°C. Boiling will occur for a few seconds on the uppermost part of the fuel plate if the primary heat exchanger outlet temperature is increased to 52°C.

Thesis Supervisor: David D. Lanning

Title: Professor of Nuclear Engineering

TABLE OF CONTENTS

ABSTRACT	2
LIST OF FIGURES	7
LIST OF TABLES	10
ACKNOWLEDGMENTS	11
Chapter 1. INTRODUCTION	12
1.1 General	12
1.2 Description of the MITR-II	14
1.3 Natural Convection Loop	25
Chapter 2. REACTOR BEHAVIOR AFTER LOSS OF FLOW ACCIDENT	27
2.1 General	27
2.2 Pump Coast Down and Loss of Flow	29
2.3 Energy Release by Delayed Neutrons	32
2.4 Heat Generation from Decay of Fission Products	37
2.5 Heat stored in Activated Core Materials	38
2.6 Heat Distribution in the Core	39
2.7 Dissipation of Decay Energy in the Reactor	45
Chapter 3. THERMAL HYDRAULIC ANALYSIS IN STEADY STATE AND TRANSIENT	48
3.1 General	48
3.2 Conservation Equations and Their Applica- tion to Natural Convection	49

3.3	Containment Tank Mixed Temperature Evaluation	59
3.4	Onset of Nucleation Boiling and Two Phase Flow	63
3.5	Heat Transfer Coefficient in Laminar and Turbulent Flow	66
3.6	System Geometry	67
3.7	Friction Coefficients and Form Factors	70
Chapter 4. STARTUP NATURAL CONVECTION TEST		75
4.1	General	75
4.2	Experimental Procedure	78
4.3	Preliminary Calculations	81
4.4	Natural Convection Test Measurements	86
Chapter 5. COMPUTER RESULTS		94
5.1	General Assumptions	94
5.2	Pump Coast-Down and Natural Convection Flow	97
5.3	Core Temperature Calculations	98
5.4	Steady State Operation with Natural Convective Cooling	122
Chapter 6. CONCLUSION		125
6.1	Summary and Conclusion	125
6.2	Recommendations for Future Works	128

Appendix A	COMPUTER CODE DESCRIPTION AND FLOW CHARTS	132
A.1	Code Description	133
A.2	Transient Pressure Drop in the Down Commer	135
A.3	Transient Core Calculations	138
A.4	Calculation of Core Entrance Properties	140
Appendix B		143
B.1	Input Data Cards	144
B.2	Nomenclature to the Computer Code LOFA	155
Appendix C		165
C.1	Computer Code Listing	166
C.2	Sample Output	195
Appendix D	TWO PHASE FLOW ANALYSIS	212
D.1	Friction Coefficient	213
D.2	Void Fraction	215
D.3	Boiling Criteria	215
Appendix E	STARTUP INCORE TEMPERATURE MEASUREMENTS	218
	REFERENCES	238

LIST OF FIGURES

Figure

1.1	Vertical Cross Section of the MITR-II	15
1.2(a)	Core Section of the MITR-II	19
1.2(b)	Core I with Cadmium as Fixed Absorber	20
1.3	Core II with No Fixed Absorber	22
1.4	Core III with Hafnium as Fixed Absorber	23
1.5	Core IV with No Fixed Absorber	24
1.6	Natural Convection Loop	26
2.1	Flow and Pressure at MF-1 After Pump Coast Down in MITR-II	30
2.2	Core Power Distribution with Shim Bank at 7.9 inches	44
3.1	Summary of Transient Calculation	60
3.2	Boiling Phenomena in Convective Heat Transfer	64
3.3	Core Cooling in Steady State Operation	68
3.4	Natural Convection Valve	71
4.1	Incore Thermocouple Position	77
4.2	Thermocouple Calibration Factor	85
4.3	Transient Temperature Measurements of the Incore Thermocouples (4 MWth for 11.5 hrs.)	87
4.4	Transient Temperature Measurements of the Incore Thermocouples (4 MWth for 10 min.)	88
4.5	Wall Temperature Evaluated at Hot Spot	90

Figure

4.6	Wall Temperature at Hot Spot in Fuel Element C-13	91
4.7	Outcore Temperature Measurements	92
4.8	Medical Facility Temperature Measurements for Long-Term Operation	93
5.1	Core Flow After Pump Coast Down	99
5.2	Core Bulk Temperature for Average Power Distribution	100
5.3	Hot Channel Bulk Temperature for Case-1 (4 Valves Open and $T_{in} = 40^{\circ}\text{C}$)	104
5.4	Hot Channel Fuel Surface Temperature for Case-1 (4 Valves Open and $T_{in} = 40^{\circ}\text{C}$)	107
5.5	Hot Channel Temperature and Heat Flux Distribution at Peak for Case-1	109
5.6	Hot Channel Bulk Temperature for Case-2 (3 Valves Open and $T_{in} = 40^{\circ}\text{C}$)	110
5.7	Hot Channel Fuel Surface Temperature for Case-2 (3 Valves Open and $T_{in} = 40^{\circ}\text{C}$)	111
5.8	Hot Channel Bulk Temperature for Case-4 (4 Valves Open and $T_{in} = 47^{\circ}\text{C}$)	116
5.9	Hot Channel Fuel Surface Temperature for Case-4 (4 Valves Open and $T_{in} = 47^{\circ}\text{C}$)	117
5.10	Hot Channel Bulk Temperature for Case-5 (4 Valves Open and $T_{in} = 52^{\circ}\text{C}$)	119
5.11	Hot Channel Fuel Surface Temperature for Case-5 (4 Valves Open and $T_{in} = 52^{\circ}\text{C}$)	120
5.12	Hot Channel Fuel Surface Temperature Distribution at the Peak Point for Case-5	121
5.13	Average Core Channel Temperature for Natural Convection at 100 KWth Steady State Power Operation	124

Figure

A.1	Flow Diagram of MAIN Program	134
A.2	Flow Diagram of Subprogram DOCO	137
A.3	Flow Diagram of Subprogram TRANS	139
A.4	Flow Diagram of Subprogram TANK	142

LIST OF TABLES

Table

2.1	Decay Constant and Yield of the Delayed Neutrons	34
2.2	Half-Lives and Yields of Photoneutrons from U-235 Fission Products in D ₂ O	35
2.3	Ratio of Epithermal to Thermal Fission Cross Section for Different Fuel Specifications	43
4.1	Thermocouple Position in Core-4 Startup Test	76
STARTUP INCORE TEMPERATURE MEASUREMENTS		
E.1	Steady State Power of 2.50 MWth for 3 hrs.	219
E.2	Steady State Power of 3 MWth for 3 hrs.	220
E.3	Steady State Power of 3.50 MWth for 6 hrs., 37 min.	222
E.4	Steady State Power of 4.00 MWth for 10 min.	224
E.5	Steady State Power of 4.00 MWth for 11.5 hrs.	226
E.6	Steady State Power of 4.50 MWth for 3.25 hrs.	229
E.7	Steady State Power of 4.90 MWth for 10 min.	232
E.8	Steady State Power of 4.83 MWth for 18 hrs.	235

ACKNOWLEDGEMENTS

I would like to dedicate this work to my wife, Cindy, whose loving support, patience, and encouragement during many months is deeply felt.

I am grateful to Professor D.D. Lanning for his guidance and consultation as supervisor of this Thesis.

I wish to thank Professors L. Wolf and J.E. Meyer for their participation and interest in the discussion of some of the approaches.

The assistance of the entire staff of MIT Reactor, in particular, J. Bernard, G. Dooley, and T. LaFontaine is greatly appreciated.

I also extend my thanks to the Atomic Energy Organization of Iran for their financial support in completion of this degree.

CHAPTER I

INTRODUCTION

1.1 General

The modified Massachusetts Institute of Technology Research Reactor, MITR-II, is cooled with H_2O that is circulated by two primary pumps. Sufficient cooling is provided in order to operate at five thermal megawatts steady state power within the acceptance criteria. The heat generated is transferred to the secondary water system and is rejected into the atmosphere by force draft cooling towers.

The MITR-II is designed to function within a safety limit in all possible ways with regard to loss of coolant flow. The reactor will scram whenever there is a reduction in primary coolant flow or pressure below a set point. There is a backup low level scram protection in the containment tank to keep the water not any lower than three inches below overflow. Two antisiphon valves which are maintained in the closed position by the primary pumps pressure, open automatically to prevent siphoning of the main tank water in the unlikely event of pipe break. Four incore check valves are designed and installed to remove the after scram heat generation due to loss of flow accident.

These valves open to produce a loop for natural convection heat removal as soon as the pressure on both sides of them balances.

As part of the Safety Analysis Report of the MITR-II, loss of flow accident was studied by Choi (Ref. 1.1 and 1.2) and it was shown that "cooling by natural convection flow after a shutdown is sufficient to prevent the wall temperature from reaching the boiling point during the first 50 minutes".

To demonstrate that the decay heat resulting from long term operation at 5 MWth can be removed by natural convection, a series of temperature measurements were made as part of the startup procedure. A thermocouple fuel element was inserted into a central position (A-2) to measure fuel wall temperatures at 0.1 and 4.0 inches from the bottom of the fuel plates. Spider hole inlet and fuel element average outlet temperatures were also measured. The transient experiments above 2 MWth were done based on the assumption of loss of electrical power to the main panel. Therefore both primary pump switches as well as the reactor minor scram button were pushed at the same time. The temperature measurements were made for loss of flow accident up to 2 MWth. In this

case the primary pumps were stopped and the reactor was scrammed automatically due to flow coast down. The MITR-II, Core-4, transient behavior is studied in this work analytically and compared with the experimental results. A computer code is written to analyze the reactor function after a scram due to loss of flow accident. It is capable of solving transient problems involving loss of primary flow such as loss of electrical power, pump trip or breakdown, and pipe break in the reactor inlet system. To compare with the startup experiments, the first case is considered here and it is assumed that before the accident the reactor was operating at steady state conditions. A single channel model is used to analyze the average core power distribution or hot channel separately. It is also shown how the computer program could be modified for multi-channel calculations.

1.2 Description of the MITR-II

The MITR-II is a light water cooled and moderated and heavy water reflected nuclear reactor which uses flat plate-type, finned aluminum clad highly enriched uranium fuel elements. It is designed to operate at a steady state power of five thermal megawatts. Figure 1.1

shows a vertical cross sectional layout of the MITR-II.

The reactor is located at the center of a gastight cylindrical steel building equipped with a controlled pressure relief system. The reactor is located inside of two concentric tanks and a core shroud. The outermost tank is a four foot diameter D_2O reflector tank and is used to maintain a D_2O level for neutron reflection. Heat generated in the core is removed by primary light water forced convection system. Primary coolant enters the reactor through the inlet plenum and into the annular area between the core tank and the core shroud. It then flows downward through the upper plenum to the bottom of the hexagonal core support housing assembly where it is directed upward through the fuel elements. It then moves slowly within the chimney and core shroud to the three exit ports which form the outlet plenum, just above the level of the inlet plenum.

The fuel is arranged in a compact core configuration to minimize the thermal neutron flux in the reflector region where the experimental beam ports are located. Because of rather high heat generation in the core, the fuel plates are finned to augment heat transfer. The fuel element consists of fifteen fuel plates assembled

between two grooved side plates. The fuel plates are slightly over 2.5 inches wide with 110 longitudinally-milled square fins on either side; 0.01 inches high and 0.01 inches wide grooves. More detail about fuel elements can be found in Reference 1.3. The fissionable material consists of uranium enriched to approximately 93% U-235. Each fuel element contains about 445 grams of U-235.

The control blades come down around the outside of the core and are effective by cutting off thermal neutron transport between the reflector and the core. The control blades are made of Cadmium in an aluminum sandwich.

On August 14, 1975, MITR-II reactor went critical for the first time with 20 fuel elements loaded which was considerably less than the 27 positions available in the core. Because of the small control bank worth, only one additional element could be added to the core without exceeding the shutdown margin required by Technical Specifications. However, a twenty-one element core would not have sufficient heat transfer area for 5 MWth operation and also the empty fuel position would allow too much bypass flow and unacceptable power peaking.

In order to be able to load more fuel into the reactor, the fixed absorber was lowered and the reactor went critical for the second time, with a loading of 22 active fuel elements, 3 solid dummy elements, and one sample assembly containing a neutron source. Two additional active elements were loaded and one dummy was removed. The Core-I loading at the beginning of power distribution measuring is shown in Figure 1.2.

In February, 1976, when an attempt was made to remove a fuel element from the core, it was discovered that about $2/3$ of the reactor fuel elements were stuck in the core because the cadmium fixed absorber sandwiches were swollen beyond the acceptable tolerances for the compact core arrangement. Water had leaked into the sandwich from the seal weld and corroded the cadmium. Hydrogen from the corrosion process had built up a gas pressure inside the sandwich and caused swelling, (Ref. 1.4).

In order to prevent damage to the fuel elements, the fixed absorbers were removed. Core-II was designed to contain fewer fuel elements and more solid dummies in order to counter balance the positive reactivity effect of removal of the fixed cadmium absorbers. To minimize the power peaking effect of the water gap produced by

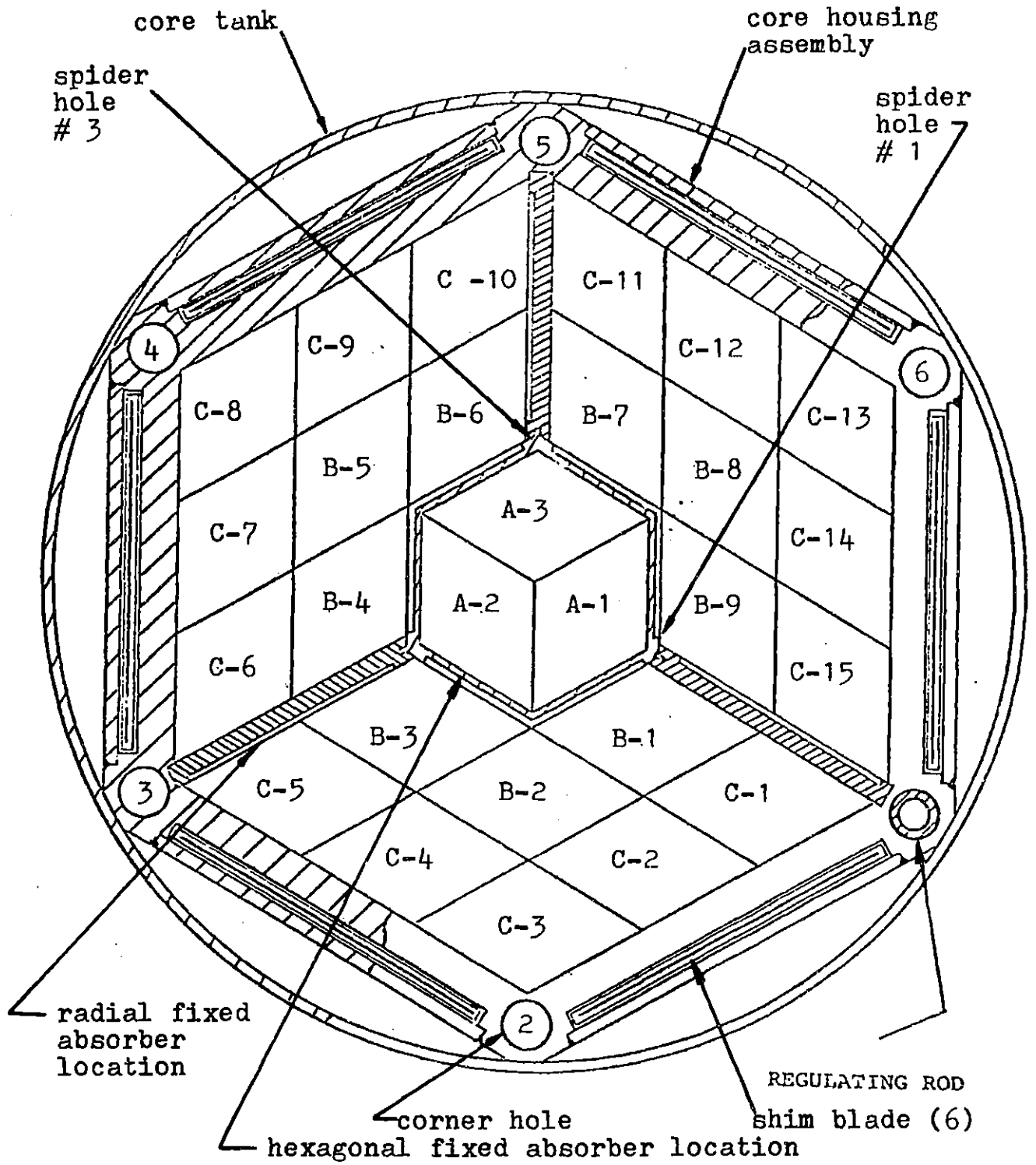
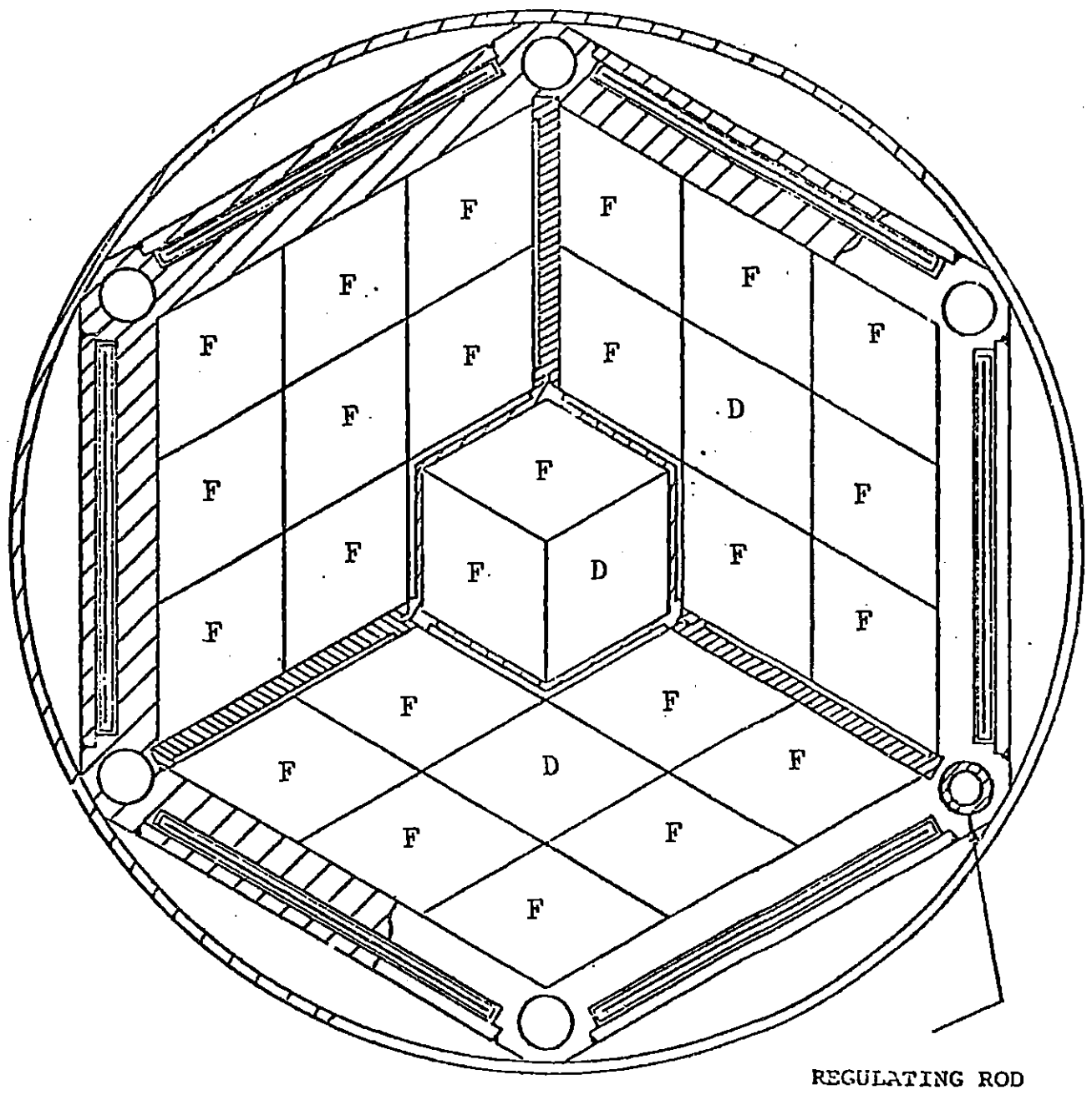


FIG. 1.2 (a) Core Section of MITR- II



F - Fuel Element
D - Dummy Element

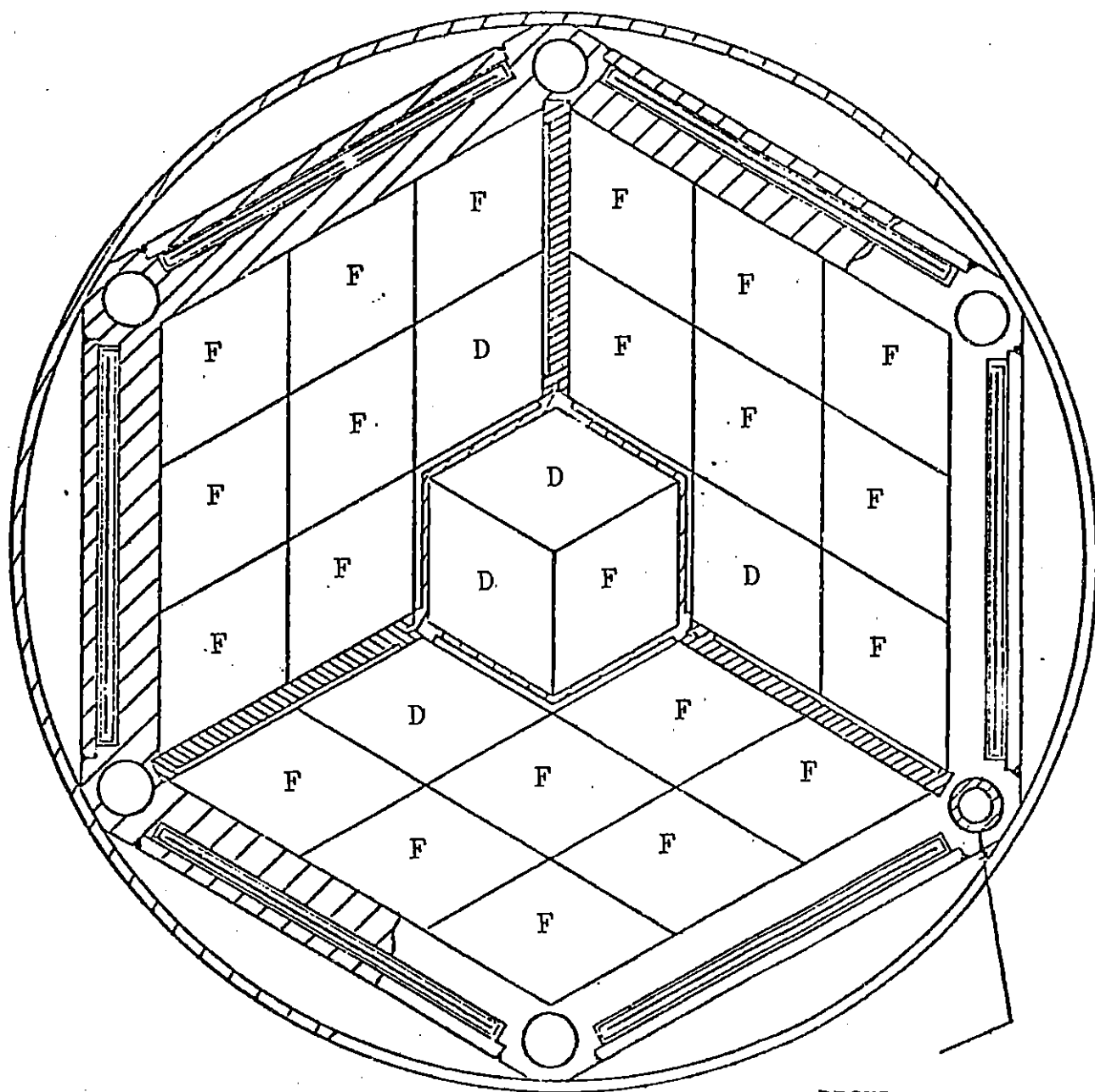
FIG . 1.2 (b) Core I with Cd as fixed absorber

removing the fixed absorbers, and to decrease the worth of solid dummies in the B ring they were loaded into positions B-3, B-6 and B-9 , as is shown in Figure 1.3. By placing solid dummies in these positions and because of "notch up" plate arrangement, no single plate was directly against the water gap caused by removal of the fixed absorbers.

To prevent swelling, Hafnium was selected as the absorber material for the fixed absorber. In November, 1976, Core III went critical with the same loading as Core I. Calculations showed that for long term operations, only 2 dummies could be placed in the core. Therefore the final Core III loading had 25 fuel elements and 2 dummies as is shown in Figure 1.4.

Core III had all the requirements of Technical Specifications, except that due to high negative reactivity of hafnium, too many fuel elements were loaded into the core. Since the MITR-II is a research reactor, it was decided to provide more space in the core for experimental facilities. Therefore the hafnium fixed absorbers were removed to be able to put more dummy elements in the core.

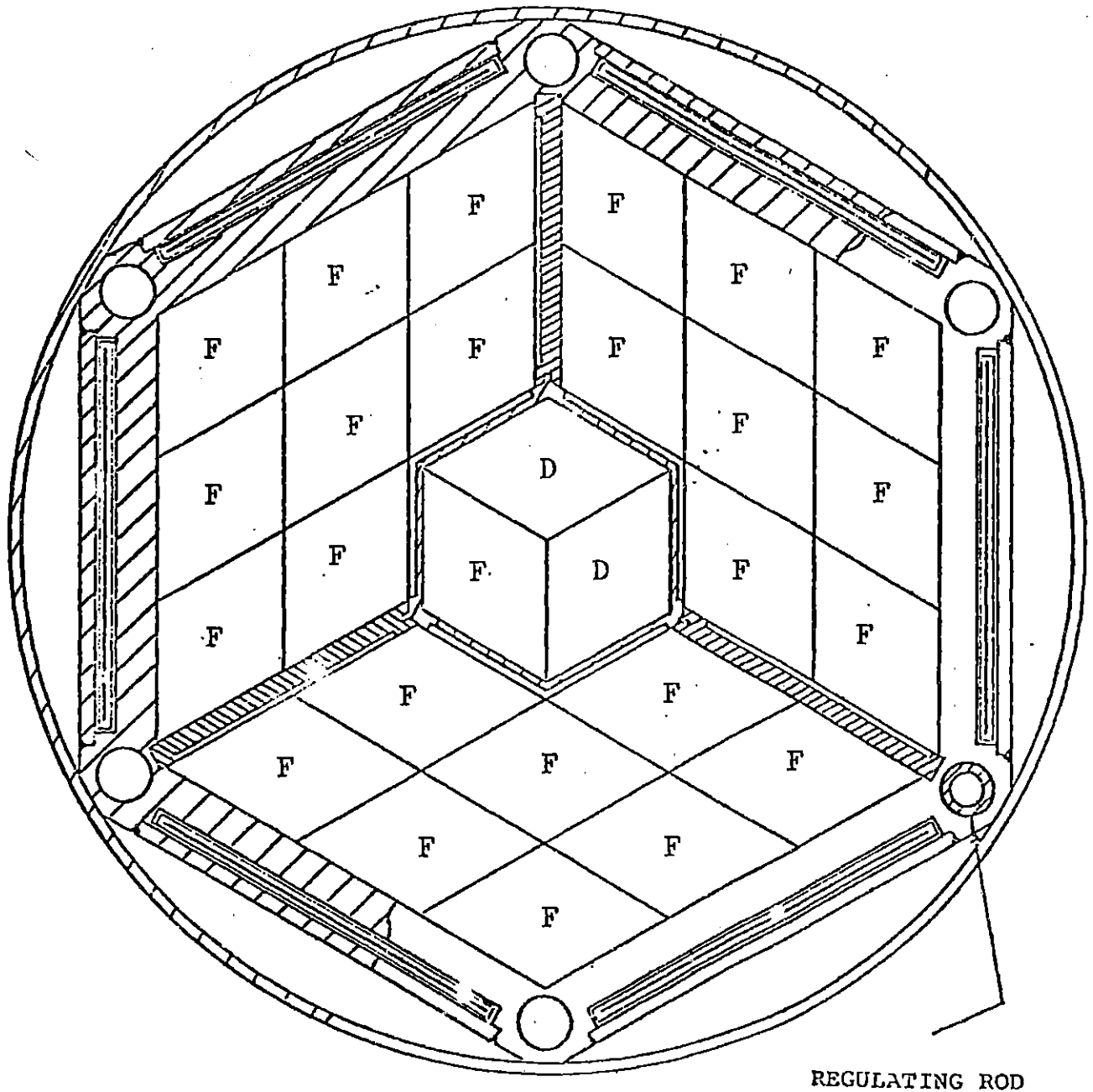
Core IV was designed with 4 dummies and 23 fuel elements with no fixed absorber, to be the final core configuration for long term operation at full licensed power of 5 MWth. Figure 1.5 shows Core IV loading at the time of startup natural convection measurements.



F - Fuel Element
D - Dummy Element

REGULATING ROD

FIG. 1.3 Core II with no fixed absorber

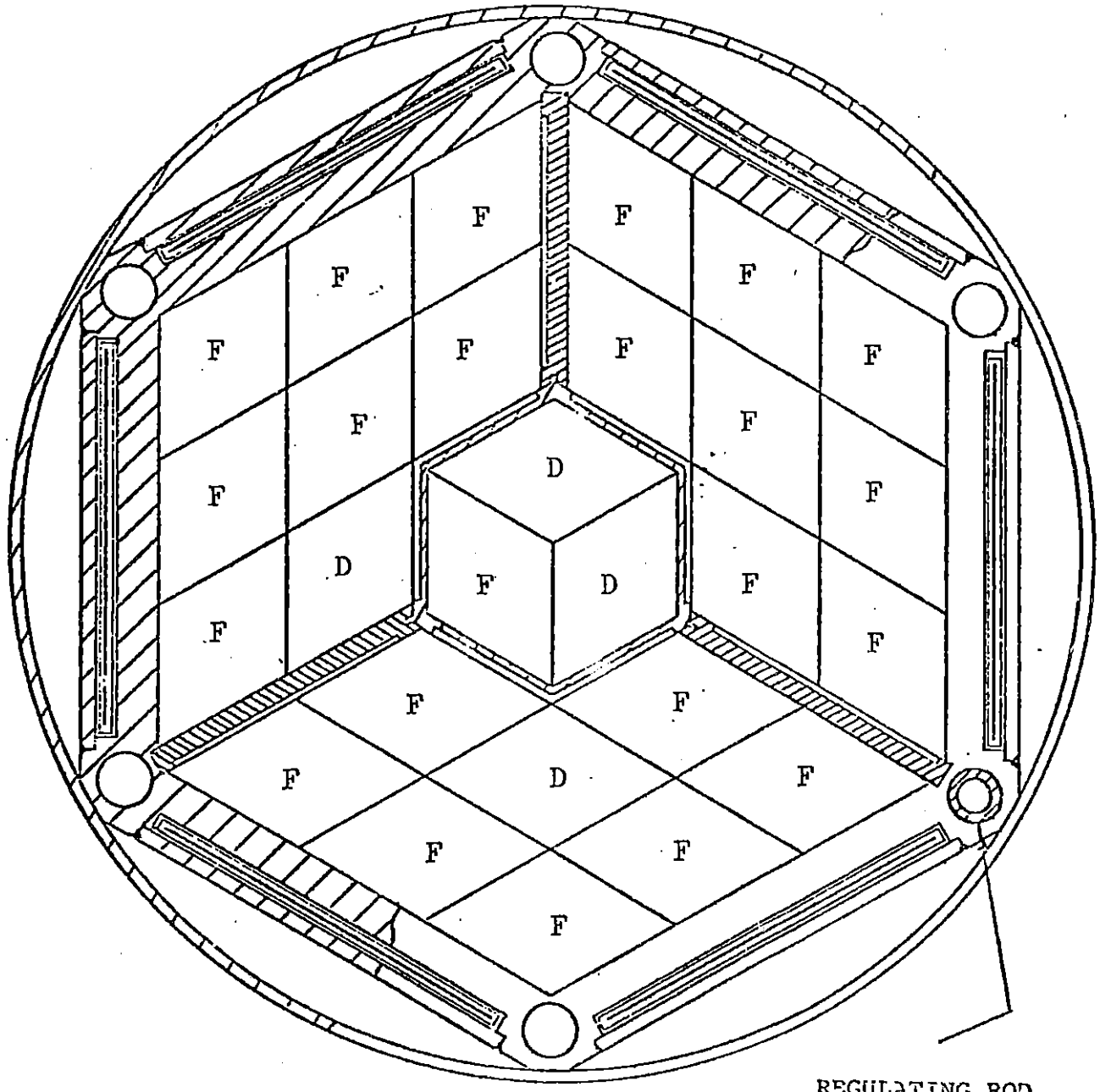


REGULATING ROD

F - Fuel Element

D - Dummy Element

FIG. 1.4 Core III with H_f as fixed absorber



REGULATING ROD

F - Fuel Element

D - Dummy Element

FIG. 1.5 Core IV with no fixed absorber

1.3 Natural Convection Loop

A natural convective cooling loop is predicted in the Safety Analysis Report to be produced in the case of primary pump failure, to remove the decay heat from the core. This loop as is shown in Figure 1.6, is maintained closed by natural convection valves due to primary coolant pressure and opens automatically when the flow decreases. In the case that the pump forced flow is not considerable and natural convection valves are opened, the decay heat released into the channels produces a density difference between the core and the downcomer which transfers the cold water in the lower plenum up into the core cooling channels. As this proceeds, the heat exchanger outlet water from the annular space between the core tank and the core shroud mixes with the containment tank water coming through the chimney in the upper plenum and enters the core

The chimney was installed at the top of the core to protect the shim blades from turbulence of the core outlet. It also helps to increase the driving pressure in the natural convection. The hot water outlet of the core goes up through the chimney and mixes with the containment tank water before entering the natural convection loop.

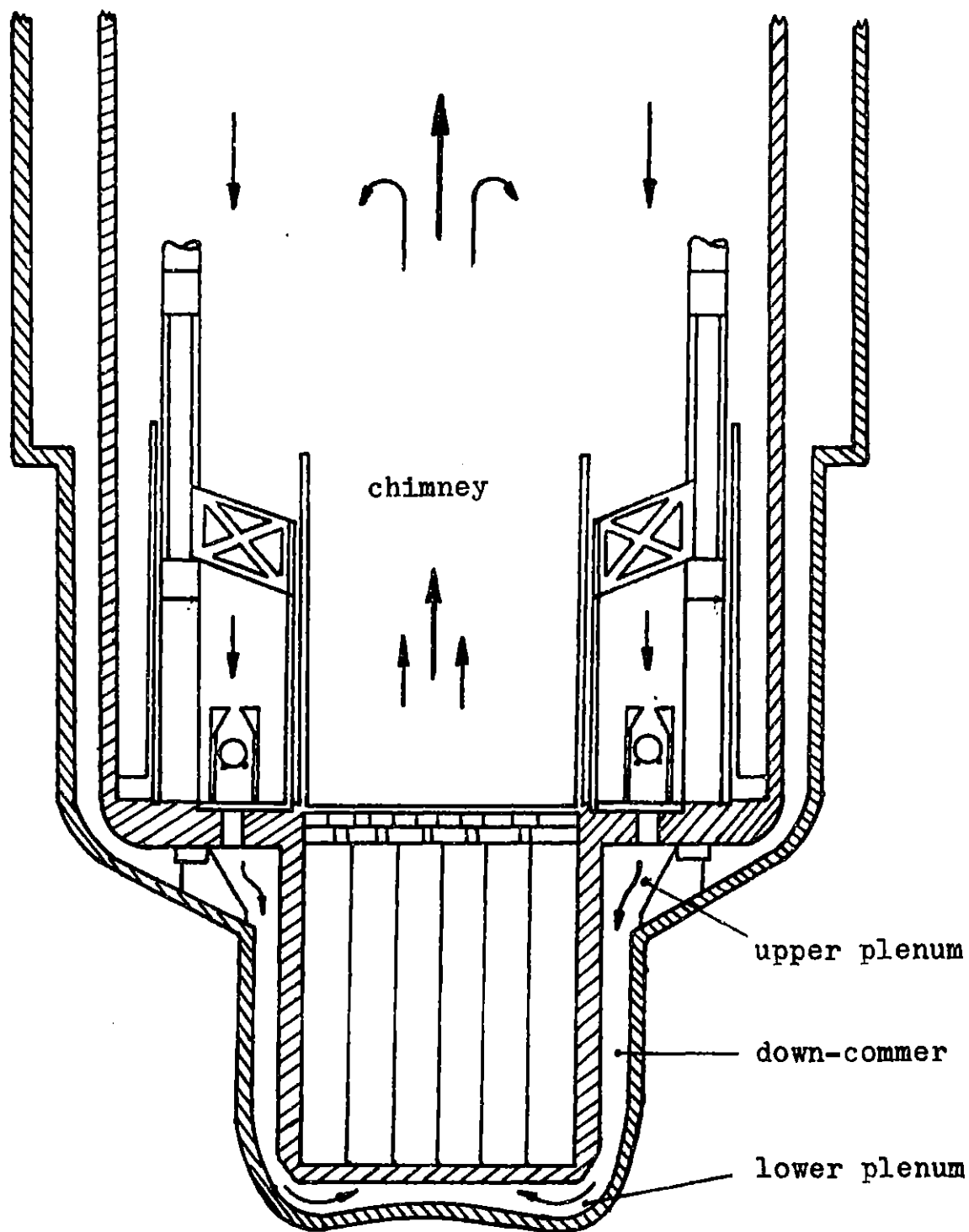


FIG. 1.6 Natural Convection Loop

CHAPTER II

REACTOR BEHAVIOR AFTER LOSS OF FLOW ACCIDENT

2.1 General

Startup Natural Convection Tests, at power level above 2 MWth, were done based on the assumption of loss of electrical power to the main panel. This loss of power would trip both primary pumps at the same time that the magnets holding the shim blades are disabled and therefore scram the reactor.

Choi (Ref.1.2) estimated the maximum release time of the magnetic clutches in the control rods to be 0.06 seconds. Weekly startup procedure sheet shows that it takes about 0.45 seconds for the shim bank to reach 80% of full insertion.

In startup natural convection tests above 2 MWth, both the minor scram and primary pump switches were pushed at the same time. Assuming a scram delay time of 0.41 seconds (Ref.1.2) it takes about 0.86 seconds from the time of scram to 80% of full insertion of the shim bank. To be more conservative a value of 0.9 seconds is assumed where in reality it takes about 0.51 seconds.

Shim bank integral reactivity measurements shows a reactivity worth of 4.8β for 80% full insertion of the shim bank for a critical height of 7.9 inches. This value is smaller than the individual blade worth measurements due to perturbation of shim bank on them.

Although it takes about one second to insert all the control blades, the power does not die rapidly. After a sudden shutdown, about 90% of the neutron population dies off in about 0.01 seconds (Ref.2.2), but only a few percent of the precursors decay in that time. Then the rest of the neutron and precursor population dies away with a decay period of more than 10 seconds. This decay period depends on the half life of the longest delayed neutron group.

Energy released from fission products in the form of beta and gamma radiation, contributes to the energy sources after the scram.

Decay heat from activated core materials can be considered as one of the other shutdown energy sources.

2.2 Pump Coast-Down and Loss of Flow

The coolant flow rate during a coast-down transient was measured for MITR-I (Ref.1.1) and it was found that after about 3.25 seconds the pump flow rate was almost zero. In MITR-II the transient flow rate is larger due to the differences in core and piping design. The flow rate and pressure drop have been measured in the MITR-II by using differential pressure transmitters and a voltage recorder. These values are normalized according to the calibration curve of flow v.s. voltage, (Ref.2.3). The results are calculated at the flow meter MF-1, for reference.

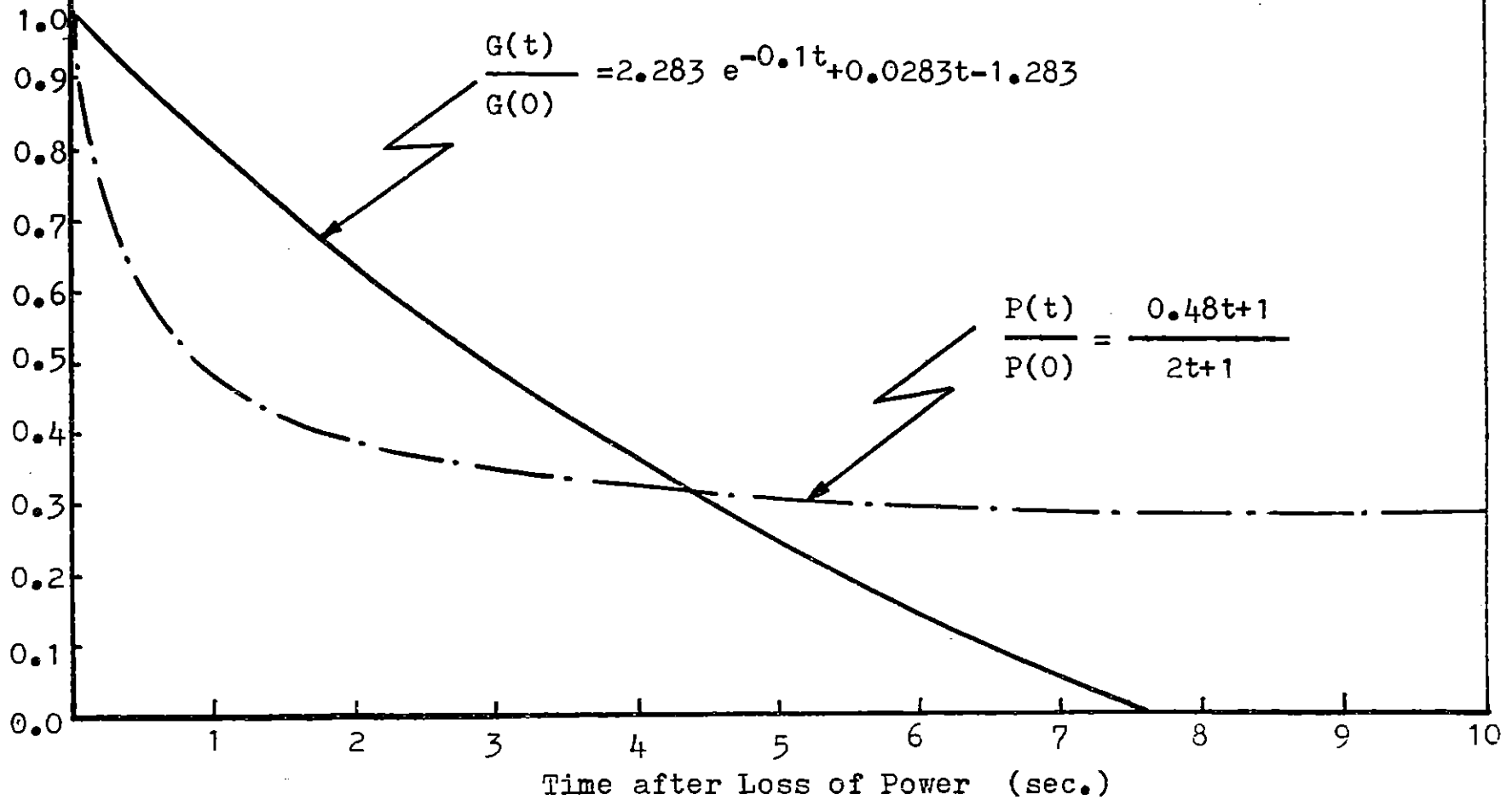
It is found that in MITR-II the pump flow goes to zero after about 7.5 seconds, as shown in Fig.2.1, and pressure at MF-1 reaches infinite value after 7.0 seconds.

In order to be able to use flow rate and pressure coast-down values in calculations related to the initiation of natural convection, the following equations are used where the constants are values chosen to fit the experimental values.

$$G(t)/G(t_0) = 2.283 \exp(-0.1t) + 0.0283t - 1.283 \quad (2.1)$$

$$P(t)/P(t_0) = [0.48t + 1]/[2t + 1] \quad (2.2)$$

FIG. 2.1 Flow and Pressure at MF-1 after Pump Coast-down in MITR-II



where,

t is the time after loss of power in seconds,

$G(t)$ and $P(t)$ are flow rate and pressure at time t at MF-1 respectively, and

$G(t_0)$ and $P(t_0)$ are those values at steady state condition.

It is noted that the maximum deviation from true value is 8.5% for flow rate and 4.0% for pressure.

As the flow coasts down in the primary loop, pressure in the upper plenum decreases to a value that balances the pressure at the top of the natural convection valves. This valve balancing pressure is the sum of atmospheric pressure, static head of water in the containment tank, and pressure due to weight of the natural convection ball. At this time the ball drops and the pressure at the bottom of the valve exceeds the static pressure at the top by some amount equal to the weighted value of the ball. This causes some flow forced up through the natural convection valves which decreases with the pressure in the upper plenum, and stops as soon as the transient pressure balances the static head above the natural convection valves.

The total time that this reverse flow takes is found to be less than 0.1 seconds due to; fast pressure drop in the upper plenum, small contribution of the balls to the static pressure, and large pressure drop in the natural convection valves. As will be shown by the calculations, the contribution

of the natural convection to heat transfer from the core is not significant before the valves are opened. Even then, the coast-down flow still remains dominant until it decreases to a value of about 10 lbs./ft**2/seconds. Thereafter natural convection takes over and transfers the decay heat from the core.

2.3 Energy Release by Delayed Neutrons

Energy released by delayed neutrons can be found by solving the non-stationary neutron diffusion equation. If the neutron flux in the reactor is ϕ_0 up to the moment of shutdown, equation 2.3 will give the thermal neutron flux as a function of time, t , after shutdown:

(Ref.2.6):

$$\phi(t)/\phi_0 = \sum_{j=0}^m A_j \exp(\omega_j t)$$

$$\sum_{j=0}^m A_j = 1 \quad (2.3)$$

$$\sum_{j=0}^m \lambda_i A_j / (\omega_j + \lambda_i) = 1 \quad i = 1, 2, \dots, m.$$

where m is the number of neutron precursors,

β_i is the fraction of the total number of neutrons emitted from the precursor ,

$$\beta = \sum_{i=1}^m \beta_i ,$$

λ_i is the decay constant for fission products of i th group,

and ω_i is the eigen value of the inhour formula.

Equation 2.3 is simplified for the cases that:

$$\rho/K_{\text{eff}} \approx \rho \quad \text{and} \quad \lambda_i \ll 1/T$$

and the following equation is found:

$$\phi(t)/\phi_0 = \sum_{i=1}^m (\beta_i/(\rho + \beta)) \exp[(-\rho/(\rho + \beta))\lambda_i t] \quad (2.4)$$

where K_{eff} is the effective neutron multiplication factor,
 T is the neutron lifetime in the reactor, and
 ρ is the instantaneous reactivity reduction at the moment of shutdown.

Equation 2.5 is therefore suggested (Ref. 2.7) for decay energy due to delayed neutrons:

$$\frac{P(t)}{P_0} = \frac{\beta_{\text{eff}}}{\beta} \sum_{i=1}^m \left[\frac{\beta_i}{\rho + \beta_{\text{eff}}} \exp\left(\frac{-\lambda_i \rho t}{\rho + \beta_{\text{eff}}}\right) \right] \quad (2.5)$$

Where the value for effective total delayed neutron fraction, β_{eff} , is taken to be 0.00786 (Ref.2.1), and six delayed neutron precursors are chosen with β_i and λ_i for U-235 as shown in Table 2.1 (Ref.2.8).

The effect of delayed photoneutrons produced in the D_2O reflector, due to fission of U-235, is not considered in equation 2.5.

The half-lives and yields of photoneutrons from fission products of an atom of U-235, in an infinite medium of D_2O , is shown in Table 2.2, (Ref.2.14). Summation of the numbers presented in the last column shows that a total number of

Group	Decay constant λ_i (sec. ⁻¹)	Yield, β_i , (nt/fiss.)
1	0.0124	0.000215
2	0.0305	0.001424
3	0.1110	0.001274
4	0.3010	0.002568
5	1.1400	0.000748
6	3.0100	0.000273

Table 2.1

Decay Constant and Yield Of the Delayed Neutrons

Table 2.2

j	Half-life	Decay con. λ_j	Photoneutron yield 22 s. delayed nt. yield	$y_j = \frac{\text{Photoneut. } 10^{-5}}{\text{Fission}}$
1	2.5 s	2.77×10^{-1}	0.469	158.00
2	41.0 s	1.69×10^{-2}	0.147	49.50
3	2.4 m	4.81×10^{-3}	0.0504	17.00
4	7.7 m	1.50×10^{-3}	0.0242	8.14
5	27.0 m	4.28×10^{-4}	0.0149	5.01
6	1.65 h	1.17×10^{-4}	0.0168	5.65
7	4.37 h	4.37×10^{-5}	0.00232	0.78
8	53.00 h	3.63×10^{-6}	0.00074	0.25

Sum = 244.33×10^{-5}

Half Lives and Yields of Photoneutrons from U^{235} Fission Products
in D_2O

2.44×10^{-3} photoneutrons are produced per fission of U-235. This is even less for finite system as in the case of MITR-II because of the leakage of a considerable number of photons out

Yarmen (Ref.2.14) showed that about 0.093×10^{-3} photoneutrons are generated by photons having had one and only one collision, in the time interval of 2-1000 seconds after fission, and the rest ($2.44 \times 10^{-3} - 0.093 \times 10^{-3}$) is due to those photoneutrons produced by the uncollided photons, (with an approximation of about 12%).

The threshold energy for photoneutron reaction is 2.23Mev and the maximum photon energy in MITR-II can be assumed to be six Mev (Ref.2.13). For a uniform photon energy, the number of photoneutrons produced per second, per fission of U-235, at time t after fission, can be found in the Equation 2.6 :

$$N(t) = \sum_{j=1}^J Y_j \lambda_j e^{-\lambda_j t} \quad (2.6)$$

where λ_j is the decay constant of the time-wise group j

($j=1,2,\dots,j$), and

Y_j is the total number of photoneutrons of group produced per fission of U-235.

Note that the total number of 2.44×10^{-3} photoneutrons per fission can be obtained by intergrating $N(t)$ over the infinite time after fission.

The energy released by photoneutrons at time t after shutdown is therefore found from the following equation :

$$\frac{P_{ph}(t)}{P(0)} = \int_0^t \left[\sum_{j=1}^J Y_j \lambda_j e^{-\lambda_j t} \right] dt \quad (2.7)$$

where $P(0)$ is the steady state power, and

$P_{ph}(t)$ is the power released by photoneutrons at time t after shutdown.

2.4 Heat Generation From Decay of Fission Products

The power emitted by fission products is evaluated in the form of a curve as a function of time after shutdown, (Ref. 2.7).

For infinite reactor operation Dudziak (Ref.2.8) fits the following equation to experimental curves :

$$\frac{P(t)}{P_0} = 5 \times 10^{-3} A t^{-a} \quad (2.8)$$

Where t is the time after shutdown in seconds,

$P(t)$ and P_0 are the power at time t and the steady state power respectively.

The values of A and a are given as a function of time for U-235 as following :

Applicable Time Interval (Sec.)	A	a
$10^{-1} \leq t < 10^1$	12.05	0.0639
$10^1 \leq t < 1.5 \times 10^2$	15.31	0.1807
$1.5 \times 10^2 \leq t < 4 \times 10^6$	26.02	0.2834

The following equation is suggested when $t_0 \ll t_s$:

$$\frac{P(t_s)}{P(t_0)} = 5 \times 10^{-3} t_0^a A t_s^{-(a+1)} \quad (2.9)$$

where t_0 is steady state operational time before shutdown (sec.),
and t_s is the time after shutdown (sec.).

2.5 Heat Stored in Activated Core Materials

Aluminum is the major metal used in the core structure. It becomes radioactive and decays with emitting β and γ rays.

Choi, (Ref.1.1) derived the following equation for the decay power of activated aluminum in the core for an average thermal flux of $= 1 \times 10^{14}$ (n/cm² sec.).

$$P(t) = 1.94 \times 10^4 e^{-0.0052t} \quad (\text{Btu/hr})$$

Three-dimensional CITATION calculation for no fixed absorber in the core and shim bank at 7.9 inches from the bottom shows an average flux of 2.0×10^{13} (n/cm². sec.), in the core. This value does not change significantly for a critical shim bank height of 10 inches. The average thermal neutron flux is assumed reasonably to be 3×10^{13} n/cm². sec.

Therefore :

$$\frac{P(t)}{P_0} = 3.41 \times 10^{-4} e^{-0.0052t} \quad (2.10)$$

where t is time after shutdown in seconds,

$P(t)$ & P_0 are decay power due to activated core material and the steady state reactor power respectively.

2.6. Heat Distribution in the Core

By comparing the energy sources during reactor steady state operation and shutdown transient condition, one will find out that γ rays contribute to a larger extent in after scram decay sources, whereas in fission 80% of the energy comes from fission products. In other words 80% of the energy is produced within a very short range of the source in reactor at power. But in a shutdown reactor, due to long range of γ radiation, energy production appears far from the source and therefore has a smoothing effect on the heat flux distribution in the core.

Since the spatial heat distribution in the core has a relatively smooth shape, the power distribution after the scram can be assumed to have the same shape as in the steady state operation.

Core power distribution was first evaluated by a finite difference diffusion code, Exterminator II (Ref.2.11), and then by using Computer Code CITATION, (Ref.2.12). Radial peaking factor, for the shim bank at a height of 10 inches from

the bottom was found to be 1.30 for center plate, and 1.22 for a plate at the edge of the core next to the D₂O reflector.

Removing the fixed absorbers from the core has changed the power distribution in the core.

Axial flux distribution was measured by copper wire activation analysis. Copper wires of 0.0252 inches diameter were covered with 0.01 inches clear polyolefin, (unsaturated ethylene) and placed in coolant channels between fuel plates. They were irradiated at 200 nominal watts for one hour and then left for at least one more hour for Cu⁶⁶ to decay. The wires were scanned and activities due to Cu⁶⁴ isotopes at various axial positions were recorded. The activities were corrected for decay and background countrate, and different irradiations were correlated to one power.

The following equation is suggested by Allen(Ref.1.4) for initial countrate calculation :

$$C_0 = \frac{C_t - B}{e^{-\lambda t}} \frac{SMCOB}{COB(K)} \quad (2.11)$$

where t is the time from the end of irradiation to the beginning of the count,

C_t is the raw countrate at time t ,

B is the background countrate,

λ is the decay constant for Cu⁶⁴,

SMCOB is the reference cobalt countrate from plate scanning,

COB(K) is the cobalt foil countrate for the Kth irradiation, and

C₀ is the normalized initial countrate.

The activity induced in the copper wire was caused by both thermal and resonance neutrons. To find the fission rate in U²³⁵, Equation 2.11 should be multiplied by a factor f defined as :

$$f = \frac{\text{fission rate in U}^{235}}{\text{activity due to Cu}^{64}}$$

$$f = \frac{\Sigma_{f3} \phi_3 + \Sigma_{f2} \phi_2 + \Sigma_{f1} \phi_1}{\Sigma_{Cu3} \phi_3 + \Sigma_{Cu2} \phi_2 + \Sigma_{Cu1} \phi_1} \quad (2.12)$$

where ϕ is the neutron flux,

Σ_f is the macroscopic fission cross section for U²³⁵

Σ_{Cu} is the macroscopic absorption cross section for Cu, and subscripts 3,2, and 1 refer to thermal (0.0025 ev-0.4 ev), epithermal (0.4 ev -3 kev) and fast neutron energy group in CITATION, respectively.

Using the following approximations;

$$\frac{\sigma_{Cu1}}{\sigma_{Cu3}} \ll \frac{\sigma_{Cu2}}{\sigma_{Cu3}}$$

$$\frac{\sigma_{Cu1}}{\sigma_{Cu3}} \approx \frac{\sigma_{f1}}{\sigma_{f3}}$$

and since $\frac{\sigma_{Cu}}{\sigma_{Cu3}} > \frac{\sigma_{f2}}{\sigma_{f3}}$, Equation 2.10 can be simplified

as follows:

$$f = 1 - \frac{\frac{\phi_2}{\phi_3} \frac{\sigma_{Cu2}}{\sigma_{Cu3}} - \frac{\sigma_{f2}}{\sigma_{f3}}}{1 + \frac{\phi_2}{\phi_3} \frac{\sigma_{Cu2}}{\sigma_{Cu3}}}$$

where σ is the microscopic cross section, and

$$\frac{\sigma_{Cu2}}{\sigma_{Cu3}} = \left[\frac{[\sigma_{Cu3}]_{1/v \text{ resonance}} + [\sigma_{Cu3}]_{\text{non } 1/v \text{ resonance}}}{\sigma_0 \text{ Cu3}} \right] \frac{\sigma_0 \text{ H}_2\text{O}}{\Sigma_3^- \text{ H}_2\text{O}}$$

and a subscript $_0$ (zero) refers to 2200 m/sec. neutron energy group.

Substituting the values for cross sections, Equation 2.13 is found :

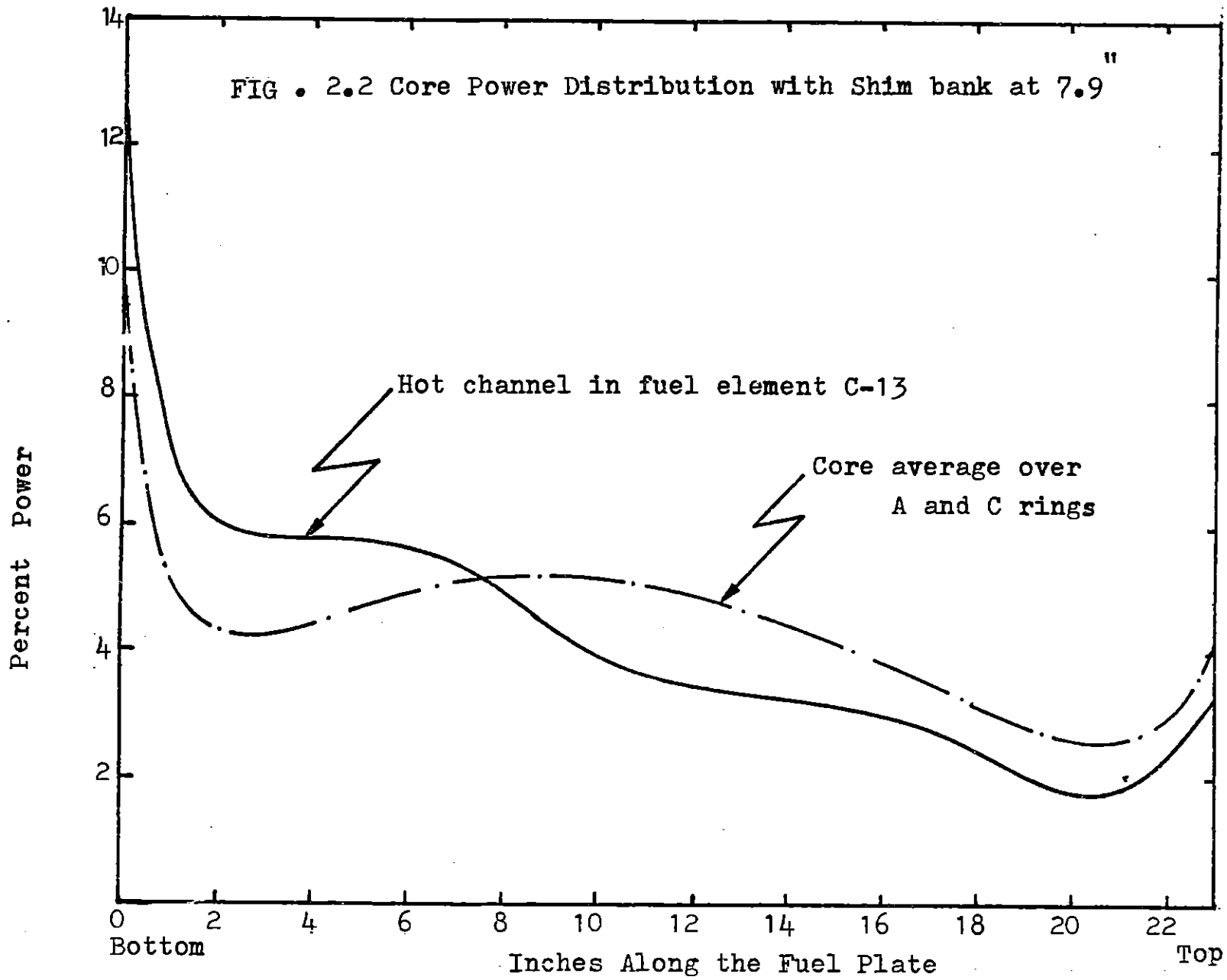
$$f = 1 - \frac{\frac{\phi_2}{\phi_3} (0.1729 - \frac{\sigma_{f2}}{\sigma_{f3}})}{1 + 0.1729 \frac{\phi_2}{\phi_3}} \quad (2.13)$$

Table 2.3

Region	Fuel Element	$\sigma_{f2} / \sigma_{f3}$
1	C	0.07733
3	A	0.07711
4	A	0.09153
5	C	0.09080
6	C	0.07690
13	A	0.09130
14	C	0.09210

Ratio of Epithermal to Thermal Fission Cross section
for Different Fuel Specifications

FIG . 2.2 Core Power Distribution with Shim bank at 7.9"



The neutron flux ratio ϕ_2 / ϕ_3 is obtained by taking the ratio of epithermal to thermal flux at each wire position from the three-dimensional CITATION computer calculation. The value of $\sigma_{f2} / \sigma_{f3}$ is found from Table 2.3, where the Region number is the one used in CITATION for fuel specification.

Figure 2.2 shows axial heat flux distribution measured by copper wire for different heights of shim bank and different positions in the core with no fixed absorber in the core.

2.7 Dissipation of Decay Energy in the Reactor

The three different kinds of decay energy produced in the core after shutdown are transferred to the containment tank by pump coastdown and natural convection flow. One can assume that the steady state power is removed by primary heat exchangers, i.e. the temperature in the containment tank is the same as steady state core outlet temperature. Therefore due to decay heat addition to the tank, the temperature of the water increases. Although part of the energy is transmitted to the outside through the reactor shielding and the off-gas monitoring system, and since the rate of enthalpy increase in the containment tank is slow (about 0.02 Btu/lbm per minute) heat transfer from the tank can be neglected. Energy dissipated in the reflector and the shielding is estimated by Choi (Ref.1.1), and it is found that about 5.31% of the fission energy is deposited in the D₂O reflector, and only

0.91% in the shielding. This value is not considerable in the shutdown reactor. On the other hand due to high thermal resistance of the helium gap it can be assumed that no heat is transmitted through the gap from the relatively hot graphite into the reflector.

Therefore after the natural convection begins and the hot water in the tank starts flowing down into the lower plenum, there might be some heat convection between the down-commer and the D₂O reflector. Due to high conductivity of the aluminum walls (188 Btu/hr/ft²°F), free heat convection can be considered between the hot water flowing down into the down-commer and relatively stagnant flow in the D₂O reflector tank.

In the steady state operation a pump and heat exchanger remove the heat deposited in the reflector with a flow rate of about 140 gpm. Heavy water enters the reflector tank at a temperature of 36°C and leaves at about 38°C. Therefore after scram, due to loss of electrical power, D₂O is left enclosed between the core and the reflector tank at the exit temperature.

Natural convection flow in the down-commer will lose some heat by free convection to the reflector through the core tank wall. Eckert (Ref.2.10) suggests Equation 2.14 for natural convection to a fluid enclosed between two vertical walls;

$$\dot{q}'' = \frac{k_e}{b} (T_h - T_c) \quad (2.14)$$

where \dot{q}'' is the average heat flow per unit time and area,
 b is the normal distance between the two walls,
 T_h and T_c are the temperatures on the hot and cold
sides of the system, and
 k_e is equivalent heat conductivity.

The values of k_e are found experimentally and plotted versus a dimensionless factor $Gr_b Pr$, Grashof's number times Prandlt's number. For the special case of interest with :

- containment tank mixed temperature, $T_h = 125^\circ F$
- D_2O reflector tank outlet temperature, $T_c = 100^\circ F$
- reflector thickness next to the down-commer, $b=1.114$ ft.,

the ratio k_e/k for heavy water reflector is found to be 1.38. Therefore the rate of heat flux transmitted to the reflector is about 10.836 Btu/ft²/hr, or the total leakage power from the down-commer after scram is only about 33.77 watts.

CHAPTER III

THERMAL HYDRAULIC ANALYSIS IN STEADY STATE AND TRANSIENT

3.1 General

Although natural convection valves are closed in steady state operation, the buoyancy of relatively hot water in the core will also help to remove the heat insignificantly.

Average core outlet temperature is about 50°C at 5 MWth steady state power and 2050 gpm flow rate. This energy is removed from the water in two primary heat exchanges and water enters the core at 40°C . When natural convection valves open, a loop is produced ; cold water coming from the heat exchangers is in one leg, and decay heat is being added to the core coolant channels in the other leg. The density difference between the two legs initiates a small flow which is directly proportional to the driving force. Decay heat addition to the core flow increases the driving force and therefore the natural convection flow. Since shutdown energy generation decays exponentially, a time is reached that natural convection flow is just enough to remove the decay heat without increasing the enthalpy. Thereafter the flow rate decreases with decay power.

During the normal reactor operation, a flow disparity is observed at the core inlet (Ref.1.4). This flow disparity is more uniform during natural convection because the down-coming flow is laminar, so each of the n channels

should take $1/n^{\text{th}}$ of the total flow. But the flow rate in natural convection depends on the heat flux, or in other words, on the amount of energy released into the channel.

Eselgroth and Griffith (Ref.3.1) show that "for an array of channels, the pressure drop across any individual channel is independent of the flow through it" and is common to all channels, for the case flow passing from one header to another through n identical channels with low flow rate.

In natural convection both flow rate and pressure drop are governed by heat flux in different channels. Therefore if there is a uniform pressure distribution in the lower plenum at the core inlet, right above at the core outlet, there should be both pressure and flow distribution due to density variation. These different temperature and flow streams will mix due to turbulency, and a height will be reached where there is a mixed temperature, density, and pressure. This point can be well considered to be at the top level of the chimney.

3.2 Conservation Equations and Their Application to Natural Convection

The natural convection loop described in the last section, can be analyzed as a single channel. Momentum Integral Model is applied to one dimensional transient fluid flow. In this model, variation of mass flow rate with position

in the channel due to axial changes in density and vapor content with time is considered. Also because of small pressure difference along the core (less than 1 psia), single pressure can be used for evaluating all fluid properties (Ref.3.2).

The following equations express the conservation of mass, momentum and energy in the constant area channel with z being the axial direction from bottom to top of the core (Ref.3.2) :

$$\frac{\partial \rho}{\partial t} + \frac{\partial G}{\partial z} = 0 \quad (3.1)$$

$$\frac{\partial G}{\partial t} + \frac{\partial}{\partial z} (vG^2) = - \frac{\partial P}{\partial z} - \frac{fvG^2}{2D_h} - \rho g \quad (3.2)$$

$$\rho \frac{\partial H}{\partial t} + G \frac{\partial H}{\partial z} = (\phi + rq'') / l_1 \quad (3.3)$$

where ϕ is fuel surface heat flux per unit time

q'' heat generation rate per unit fuel surface area,

r is fraction of q'' directly produced in the collant,

l_1 is the half channel thickness,

G is the mass flow rate per unit area,

D_h is hydraulic diameter (4 flow area/ wetted perimeter),
 g is component of acceleration of gravity in the negative z direction,
 P is absolute pressure and
 ρ , v , and H are thermal properties; density, specific volume and enthalpy respectively with $\rho = \rho(H)$ and $v = v(H)$.

Substituting Equation 3.3 into Equation 3.1 will give a more convenient form of mass conservation :

$$\frac{\partial \bar{G}}{\partial z} = - \frac{1}{\rho} \left(\frac{\partial P}{\partial H} \right) \left[\frac{\phi + r q''}{k_1} - G \frac{\partial H}{\partial z} \right] \quad (3.4)$$

where it is assumed that: $\partial P / \partial t = (d\rho/dH)(dH/dt)$

Momentum Equation 3.2 should be integrated over the entire loop, L , to be consistent with the assumption of single reference pressure. This yields Equation 3.5 for average mass velocity, \bar{G} :

$$\frac{d\bar{G}}{dt} = \frac{1}{L} (\Delta P - F) \quad (3.5)$$

where $\bar{G} = \frac{1}{L} \int_0^L G ds$

Δp is pressure difference between core inlet and outlet
 F is the total resistance to fluid flow, composed of friction, shock, elevation, and spacial acceleration portions of channel pressure drop.

Axial and radial heat conduction in the fuel plates are neglected. All the energy is assumed to be deposited in the coolant because of small thickness and high conductivity.

Steady State Solution - Conservation equations for steady state condition can be obtained from Equations 3.1 to 3.3:

$$\partial G / \partial z = 0 \quad (3.1a)$$

$$\frac{\partial}{\partial z} (v G^2) = - \frac{\partial P}{\partial z} - \frac{f v G^2}{2D} - \rho g \quad (3.2a)$$

$$G \frac{\partial H}{\partial z} = \frac{\phi + r q''}{\ell_1} \quad (3.3a)$$

where all the parameters were defined before.

Mass conservation will give constant flow rate through the channels which are forced by primary pumps at G_0 lbm/ft²/sec.

Application of first order forward difference method to energy equation gives enthalpy at every mesh point, j , knowing the steady state core inlet enthalpy, H_1 :

$$H_{j+1} = H_j + \frac{Q_j + 1/2}{k_1 G_0} \Delta Z_j$$

where ΔZ_j is the selected mesh distance , and

$$Q_{j+1/2} = 1/2 (\phi_{j+1} + \phi_j) + 1/2 [(rq'')_{j+1} + (rq'')_j]$$

then the fuel wall temperature can be found directly from enthalpy as following :

$$T_{w_j} = H_j / C_{p_j} + \phi / h_j$$

where h_j and C_{p_j} are heat convection coefficient and specific heat at constant pressure, and they are evaluated as functions of enthalpy at mesh point j . In appendix A the values for C_p are normalized to the constant pressure specific heat at the enthalpy corresponding to 100°F . Therefore wall temperature is found in $^\circ \text{F}$ from Equation 3.6, where H_j ; (Btu/lbm), C_{p_j} ; (Btu/lbm $^\circ \text{F}$) and ϕ and h are evaluated in corresponding dimensions:

$$T_{w_j} = \frac{1}{C_{p_j}} (H_j - 68.05) + \phi_j / h_j + 100^\circ \text{F} \quad (3.6)$$

Determination of Time-Step Size - To proceed the calculations

in transient from known values at time t^i to unknowns at t^{i+1} , a correct evaluation of time step $t^i = t^{i+1} - t^i$ should be made.

Minimum fluid transport time is determined by :

$$\Delta t_{tr}^i = \text{Min}_{j=1 \text{ to } N} \left[\frac{\Delta Z_j (\rho_j^i + \rho_{j-1}^i)}{(G_j^i + G_{j-1}^i)} \right] \quad (3.7)$$

where this quantity differs from time-step to time-step in transient calculations.

The time-step size will finally be chosen the smaller value of Equation 3.7 and the specified time interval t_0 .

Transient Enthalpy Calculation - Having the time-step size, the enthalpy at the advanced time may be determined by applying any finite difference method to Equation 3.3. Integration of this equation, using the Cuachy polygon formula (3.4), will give the following three-point equation :

$$H_j^{i+1} = H_j^i - \alpha_{j-1/2}^i (H_j^i - H_{j-1}^i) + 2\Delta t^i Q_{j-1/2}^i / \rho_{j-1/2}^i \quad (3.8)$$

$$\left. \begin{aligned} \text{where } G_{j-1/2}^i &= \frac{1}{2} (G_j^i + G_{j-1}^i) \\ \rho_{j-1/2}^i &= \frac{1}{2} (\rho_j^i + \rho_{j-1}^i) \\ Q_{j-1}^i &= \frac{1}{2\ell_1} (\phi_j^i + \phi_{j-1}^i) + \frac{1}{2\ell_1} [(rq'')_j^i + (rq'')_{j-1}^i] \\ \alpha_{j-1/2}^i &= G_{j-1/2}^i \Delta t^i / \rho_{j-1/2}^i \Delta Z_j^i \end{aligned} \right\} \quad (3.9)$$

For the first node, H_1 is determined from down-commer enthalpy in pump coastdown or mixed containment tank enthalpy calculation in natural convection as is described in appendix A. This method, known as characteristic explicit method, is stable for positive and negative flow rates, and values of α such that $|\alpha| \leq 1$. The characteristic values of α for natural convection are less than 0.2.

The wall temperature can be found from energy balance between the fuel plate and fluid enthalpy. This allows the fuel plate to be an energy sink in some region, usually in the top of fuel, where the heat flux is small. Normalizing the constant pressure specific heat to enthalpy at 100°F, the fuel wall temperature may be found from Equation 3.10 :

$$T_{wj}^i = [H_j^i - 68.05]/Cp_j^i + \phi_j^i/h_j^i + 100^\circ\text{F} \quad (3.10)$$

where $\phi_j^i = q_j^i/\gamma_{ej}^i = \frac{\text{heat generation rate per unit length}}{\text{effective fuel plate parameter}}$, and

$$\gamma_{ej}^i = (\text{base channel perimeter covered by fins}) \times (\text{fin effectiveness})$$

Evaluation of Transient Flow- The total fluid resistance in the natural convection loop, shown as F in Equation 3.5, may be decomposed in terms as following;

$$F = \sum_{loop} K \bar{G}^2/2\rho + \sum_{loop} (1-\sigma^2)\bar{G}^2/2\rho + \oint \frac{f\bar{G}^2}{2D\rho} ds + \oint \rho g ds \quad (3.11)$$

where the terms on the right hand side are recognized as shock, spacial acceleration, friction and elevation pressure drop in the loop. K is loss coefficient, σ is the area ratio ($\sigma < 1$) at cross-sectional area changes, and f is Darcy friction factor.

In steady state and pump coast-down, ΔP in Equation 3.5 is the pressure drop forced in the loop by primary pumps. In natural convection there is no hydraulic force applied to the loop, therefore $\Delta P=0$. The main driving force to natural convection flow is the density difference between the two legs, namely down-commer and core coolant channels. This is included in the last term shown in Equation 3.11. Expansion of elevation pressure drop over the loop gives:

$$\begin{aligned} \oint \rho g ds &= \int_{core} \rho g dz + \int_{tank} \rho g dz + \int_{chim} \rho g dz + \int_{d.c.} \rho g dz \\ &= - \int_0^L (\rho_{d.c.} - \rho_{core}) g dz + \int_0^h (\rho_{chim} - \rho_{tank}) g dz \end{aligned}$$

Where l is the height of the core and h is the one of the chimney. Average flow rate in the loop can now be evaluated in terms of four different components of the loop. Assuming that no heat is transferred to or from the water in the containment tank and chimney, average flow rate in this part of the loop remains constant. For the core and down-commer it can be evaluated as follows:

$$\bar{G} = \frac{1}{2l} \left[\int_0^l G dz + \int_l^0 G(-dz) \right] = \frac{1}{l} \int_0^l G dz$$

Substitution into Equation 3.5 gives the following:

$$\begin{aligned} \frac{d\bar{G}}{dt} = (1/L) & \left[\int_0^l (\rho_{D.C.} - \rho_{core}) g dz + \int_0^h (\rho_{ch} - \rho_{tank}) g dz \right] \\ & - \left[\left(\int K(G^2/2\rho) ds + \int (1-\sigma^2)(G^2/2\rho) ds + \int (fG^2/2D\rho) ds \right)_{core} \right. \\ & \left. + \left(\Sigma K\bar{G}^2/2\rho + \Sigma(1-\sigma^2)\bar{G}^2/2 + \Sigma(f\bar{G}^2/2D\rho) \right)_{d.c.} \right] \end{aligned} \quad (3.12)$$

Equation 3.12 simply states that the rate of change of average flow in the natural convection loop is equal to the difference between driving force; density difference between down-flow and up-flow, and the total pressure loss in the loop. In finite difference form Equation 3.12 may be written as follows:

$$\bar{G}^{i+1} = \bar{G}^i + \Delta t^i \psi^i \quad (3.13)$$

where ψ^i is the function on the right hand side of Equation 3.12 evaluated at the conditions at time i .

The finite difference solution of Equation 3.4 can be shown as:

$$G_j^{i+1} = \lambda_j^{i+1} G_{j-1}^{i+1} + \beta_j^{i+1} \quad (3.14)$$

where it is assumed that

$$\left. \begin{aligned} (d\bar{\rho}/dH)_{j-\frac{1}{2}}^{i+1} &= [(\bar{\rho}_j - \bar{\rho}_{j-1})/(H_j - H_{j-1})]^{i+1} \\ A_{j-\frac{1}{2}}^{i+1} &= (d\bar{\rho}/dH)_{j-\frac{1}{2}}^{i+1} [(H_j - H_{j-1})/\rho_{j-\frac{1}{2}}]^{i+1} \\ \lambda_j^{i+1} &= (2 + A_{j-\frac{1}{2}}^{i+1}) / (2 - A_{j-\frac{1}{2}}^{i+1}) \\ \beta_j^{i+1} &= 2(d\rho/dH)_{j-\frac{1}{2}}^{i+1} Q_{j-\frac{1}{2}}^{i+1} \Delta Z / \rho_{j-\frac{1}{2}}^{i+1} (2 - A_{j-\frac{1}{2}}^{i+1}) \end{aligned} \right\} \quad (3.15)$$

and the other notations are defined in Equation 3.9.

For determination of individual mass velocity values at the advanced time interval, $(i + 1)$, from the channel average flow rate given by Equation 3.13, Equation 3.14 may be rewritten as :

$$G_j^{i+1} = \gamma_j^{i+1} G_0^{i+1} + \delta_j^{i+1} \quad (3.16)$$

where $\gamma_0^{i+1} = 0$, $\delta_0^{i+1} = 0$

and $\gamma_j^{i+1} = \lambda_j^{i+1} \gamma_{j-1}^{i+1}$, $\delta_j^{i+1} = \lambda_j^{i+1} \delta_{j-1}^{i+1} + \beta_j^{i+1}$

In addition let:

$$\bar{\gamma}^{i+1} = \frac{1}{2\ell} \sum_{j=1}^n \Delta Z_j (\gamma_j^{i+1} + \delta_{u-1}^{i+1})$$

$$\bar{\delta}^{i+1} = \frac{1}{2\ell} \sum_{j=1}^n \Delta Z_j (\delta_j^{i+1} + \delta_{j-1}^{i+1})$$

Then

$$G_0^{i+1} = (1/\bar{\gamma}^{i+1})(\bar{\gamma}^{i+1} - \bar{\delta}^{i+1}) \quad (3.17)$$

and $G_j^{i=1}$ may be found by substitution of Equation 3.17 into Equation 3.16, or resubstitution into Equation 3.14.

Stepwise procedure for transient calculation can be summarized in a flow chart as shown in Fig. 3.1.

3.3 Containment Tank Mixed Temperature Evaluation

It was shown before that it takes about 0.41 seconds from the initiation of scram signal until the control rods start dropping. During this time interval the reactor is operating at full power, but the pump coast-down has already started and flow is decreasing. Therefore the core outlet temperature increases to a maximum

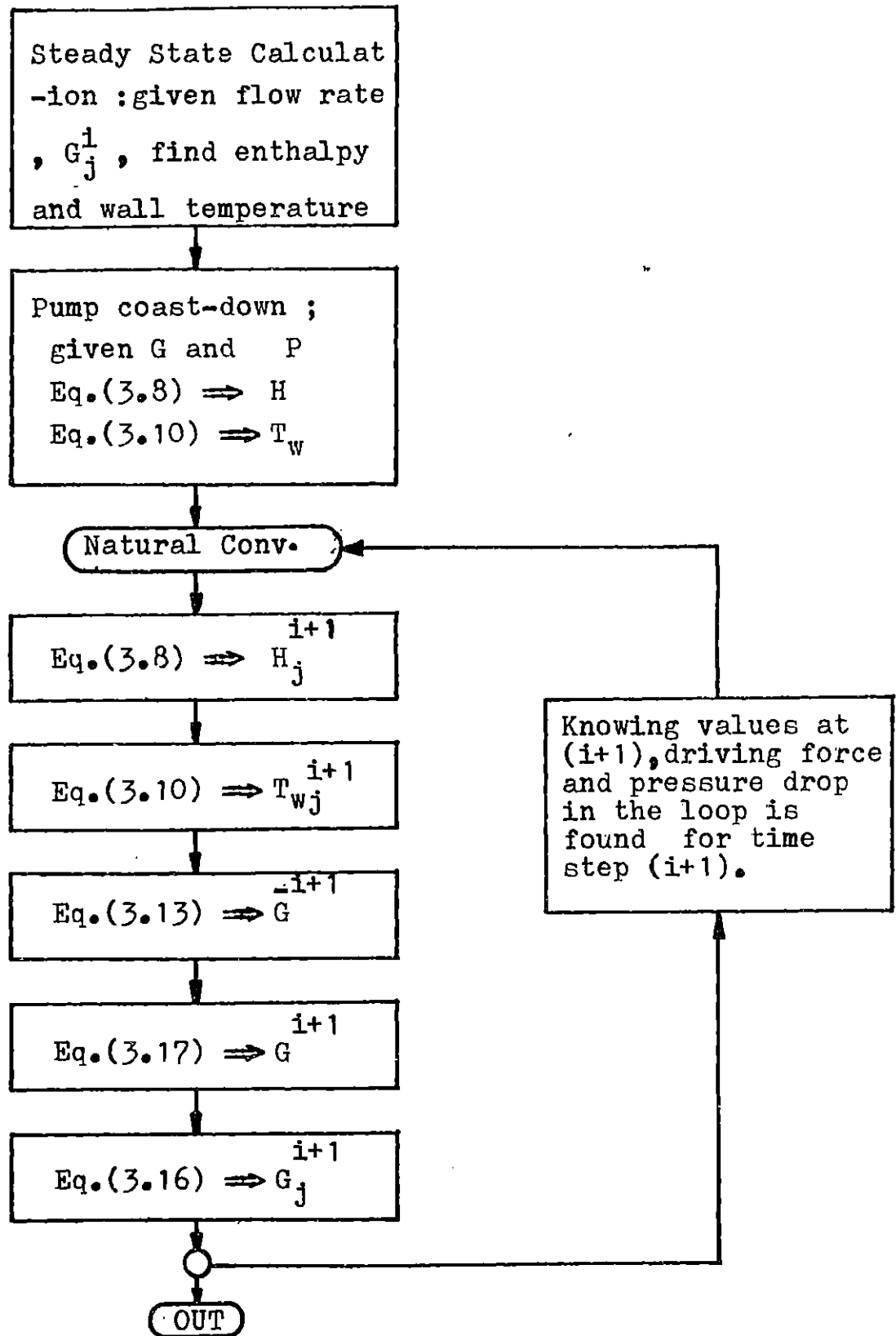


FIG. 3.1 Summary of Transient Calculation

and then decreases rapidly due to scram. As the decay heat is built up in the core, the coolant temperature increases to a point that natural convection flow can remove all the energy deposited in the core. The outlet temperature decreases then with decay of shutdown energy.

The reactor containment tank can be divided into two portions; the shroud, and chimney plus the upper part tank. In steady state operation both parts can be considered to be at the core average outlet temperature. At this time the down-commer has the same temperature as the heat exchangers outlet, namely 40°C. With the start of transient, an average tank mixed temperature, or enthalpy, can be found at any time. It may be assumed that the core outlet is mixed with the latter part of the containment tank all at once, This is of course conservative, but in reality, hot water moves up gradually in the shape of a mushroom. If the water level in the tank remains constant, from mass conservation, the amount of hot water entering the tank is equal to the amount leaving the down-commer to the lower plenum and into the core. From energy conservation the following equation can be written:

$$H_{mix}^{i+1-i} V_t = H_{NM}^{i+1, i+1} \Delta t^i + H_{mix}^{i-1} V_t - H_{mix}^{i, i+1} \Delta t \quad (3.18)$$

where $\bar{\rho}^i = \rho(H_{mix}^i)$ is the density of water at tank mixed enthalpy;
 H_{mix}^i

H_{NM}^{i+1} is core average outlet enthalpy at time t ,
 V_t is volume of the chimney plus upper tank, and
 \dot{m}^{i+1} is the mass flow rate at the core outlet
 at time .

Equation 3.18 can be written in a more convenient form:

$$H_{mix}^{i+1} = H_{mix}^i + [\dot{m}^{i+1} \Delta t / \bar{\rho}^i V_t] (H_{NM}^{i+1} - H_{mix}^i) \quad (3.19)$$

At the time that natural convection begins the down-commer, from upper plenum to lower one, has the same temperature as the heat exchangers outlet, and the water in the shroud may be assumed to have the same temperature as the containment tank at steady state operation. As soon as natural convection begins, some of the cold water in the lower plenum moves up into the core, and some relatively hot water from the tank enters the shroud. This goes on continuously with time until some time, t_1 , all the cold water is removed from the down-commer and the first wave of hot water enters the core. At some later time, t_2 , the first containment tank transient mixed enthalpy will arrive at the bottom of the core. Therefore the core inlet enthalpy is constant and has the same value as heat exchangers outlet for t_1 seconds after natural convection begins, and from time t_1 until t_2 it is constant and equal to the steady state core outlet temperature. Thereafter, depending upon the natural convection flow rate, containment tank mixed enthalpy

calculated at any time, may enter the core at some later time t_2 . This depends upon the relative mass velocity leaving the core, G_{NM}^i and the one which left the core some time ago whose mixed tank enthalpy is now entering the lower plenum, G_{NM}^{i-m} .

3.4 Onset of Nucleation Boiling and Two Phase Flow

Water coming from the heat exchangers in steady state operation is very much subcooled and its temperature is still far below saturation when it leaves the core. Therefore the only time that boiling may occur is when pump flow is lost and water temperature might exceed saturation condition. Because of relatively larger heat flux at the lower part of the fuel plates, nucleation boiling might start on the channel wall if the fuel wall temperature reaches saturation. Even then, fully developed subcooled boiling does not begin immediately. A region of "partial boiling" exists between the subsaturation condition and fully developed subcooled boiling. Fig. 3.2 shows qualitative relationship between surface heat flux and wall temperature in different zones, (Ref. 3.5). For constant inlet subcooling, the relationship between wall temperature T_w and surface heat flux, q'' , will follow the line AB in single phase liquid and then BC' until the first bubbles nucleate at C'. Then the surface temperature drops immediately to C and then further increase in q'' follows the line CDE. A higher degree of superheat is necessary to initiate the first bubble

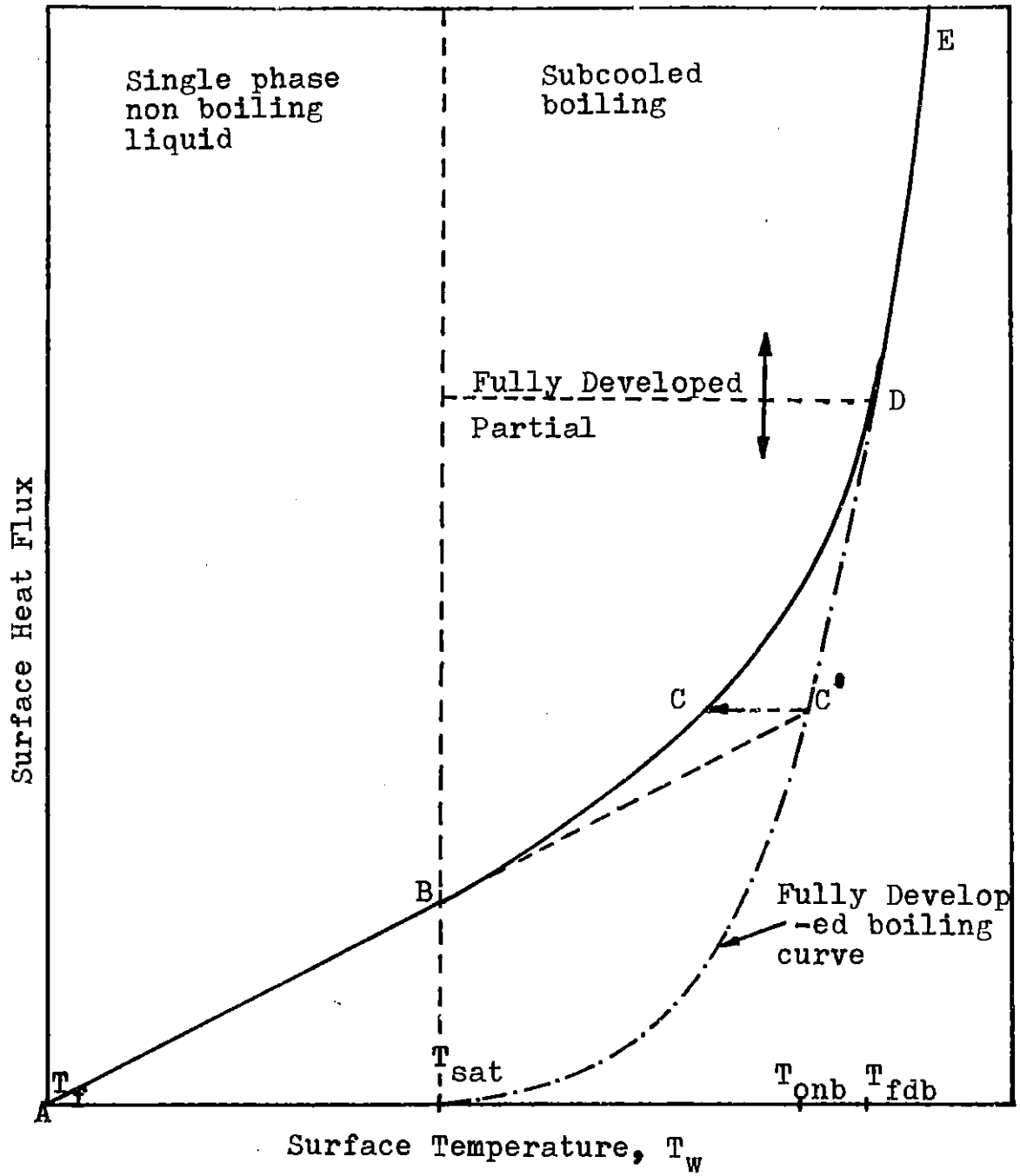


FIG 3.2. Boiling Phenomena in Convective Heat Transfer

nucleation at a given heat flux, than indicated by the curve BCD.

Bergles and Rohsenow (Ref.3.6) suggested the following equation for experimental data for water over the pressure range 15-2000 psia:

$$\phi_{\text{ONB}} = a(\Delta T_{\text{sat}})_{\text{ONB}}^b \quad (3.20)$$

where ϕ_{ONB} is the surface heat flux for onset of nucleation boiling, Btu/ft²/sec.

$(\Delta t_{\text{sat}})_{\text{ONB}}$ is the degree of superheat for wall temperature at the initiation of boiling, °F, and

a and b are given as functions of pressure, in psia:

$$a = 4.33 \times 10^{-3} p^{1.156}$$

$$b = 2.30 / p^{0.0234}$$

Natural convection tests showed that in pump coast-down even at the peak value the fuel surface, or channel bulk temperature, does not reach the saturation point if all the natural convection valves are open to flow. It will be seen in Chapter V of this work, that the first peak temperature, which occurs at about 30 seconds after the accident, all the temperatures are still subcooled and no boiling is predicted. Analytical calculations show that for 5 MWth steady state power and 40°C core inlet, the maximum bulk temperature in the hot channel will not reach saturation point even if one of the natural convection valves remains closed.

Two phase flow is analyzed in more detail in Appendix D for long term transients after loss of flow accidents due to pump trip.

3.5 Heat Transfer Coefficient in Laminar and Turbulent Flow

The best known and most widely used correlation for heat convection coefficient in turbulent regime is Dittus-Boelter equation (Ref.3.7):

$$Nu = 0.023Re^{0.8}Pr^{0.4}, \text{ for } Re \geq 4000 \quad (3.21)$$

where all the physical properties in dimensionless numbers are evaluated at the bulk temperature, and

$Nu = hD/k$	h is heat transfer coefficient
	D is hydraulic diameter of the coolant channel
	k is thermal conductivity of the coolant,
	G is mass velocity,
$Re = GD/\mu$	μ is absolute viscosity, and
$Pr = \mu C_p/k$	C_p is constant pressure specific heat.

For laminar flow a variety of theoretical relationships are available. Rohsenow and Choi (Ref.3.8) recommend a constant value of 7.0 for Nusselt number, for laminar flow in rectangular channel with aspect ratio of 25. Aspect ratio is the ratio of the larger to the smaller side of the channel.

$$Nu = 7.0 \quad \text{for } Re \leq 2300 \quad (3.22)$$

The other empirical equation based on experimental data (Ref.3.5) takes into account the effect of varying physical properties across the flow stream and the influence of free convection.

$$hD/k_f = 0.17 [GD/\mu_f]^{0.33} [Cp\mu/k]_f^{0.43} [Pr_f/Pr_w]^{0.25} [D^2\rho_f^2g\beta\Delta T_f/\mu_f^2]^{0.1} \quad (3.23)$$

$$Re < 2000$$

where β is coefficient of expansion, and subscripts f and w refer to evaluation of physical properties at film or wall temperature respectively. Film temperature is defined to be the average of wall and bulk temperature. To be more conservative, the smaller values of Equations 3.22 and 3.23 can be used in calculations.

In the intermediate transition area, $2300 < Re < 4000$, a linear interpolation on Re is made between the turbulent and laminar values of heat transfer coefficient.

To be more conservative the entrance effect on the heat coefficient is ignored.

3.6 System Geometry

Primary coolant coming from heat exchangers join into an 8" diameter pipe and after passing through a flow meter (MF-1) enters the reactor tank at the top of the core shroud Fig .3.3 . Flow cross-sectional area at core shroud is 3.648 sq.ft., and it becomes smaller to 1.193 sq.ft.. Primary water then enters the upper plenum, whose average area and volume is estimated to be about 2.206 ft² and 0.2637 ft³ respectively. The down-commer has an average flow area of 0.31 ft² for a height of about 2.026 ft. The equivalent diameter of the down-commer

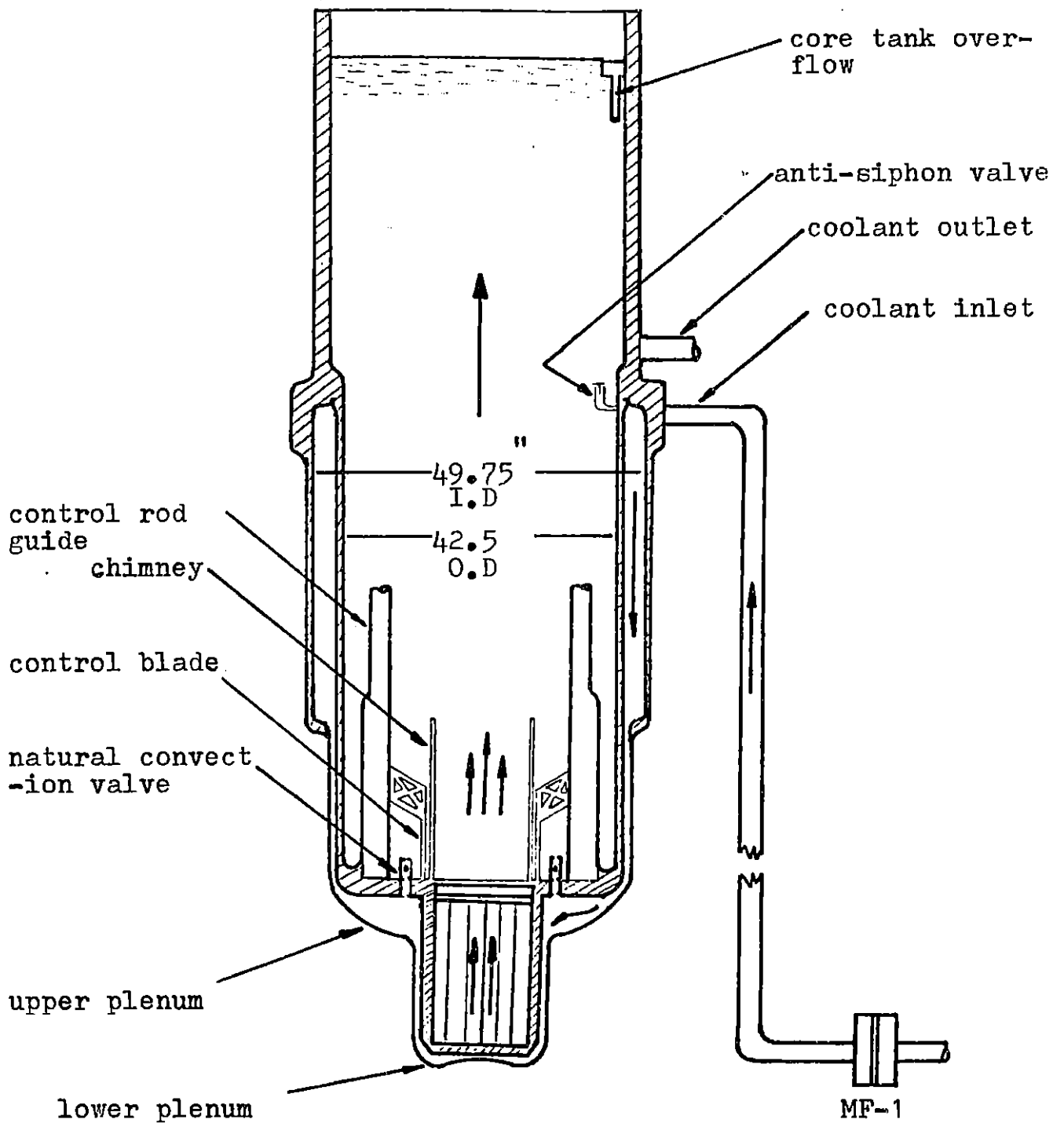


FIG. 3.3 Core Cooling in Steady State Operation

based on the definition of:

$$D_e = 4 \times \text{flow area/wetted perimeter}$$

is 0.13 ft.

Core housing has 27 spaces for orthorhombic fuel assemblies with perpendicular distance between the flats of 2.405 inches. Each fuel element has 15 cooling channels with aspect ratio of 25, flow area per channel of 0.00141 ft², and hydraulic diameter of 0.00734 ft. The core channel length is 23 inches, of which only 22.375" is heated. The distance from channel exit to hold down plate exit is 3.125 inches.

The core outlet is guided through a rectangular shaped chimney of 2.5 ft. height to prevent the shim blades from turbulency at the top of the core. The volume of the water between the fuel storage rack and chimney is estimated to be about 5.145 cu.ft.

Total volume of the containment tank, with water level at the over flow-height is 106.9 ft³ which includes the volume behind the chimney. In steady state operation, the water level in the tank is controlled by the over-flow pipe which keeps it at 3" below the top of the tank, or 10.04 ft. above the hold-down plate. The heat transfer area of fuel plates in MITR-II is increased by building longitudinally-milled square fins on both sides of them. These fins are 10 mills height with a repeating cycle of 0.02 in.. To introduce the increase in area to heat transfer, a "surface effectiveness" factor is defined as the ratio

of heat dissipated by the finned surface to heat transferred by an unfinned surface at the same wall temperature, convection coefficient and back area. Taborda (Ref.3.9) gives the following equation for heat effectiveness:

$$\eta_0 = (A_{fb}/A_B) + (A_{ft}/A_B)[\tanh m(t + w/2)/m(t + w/2)] \quad (3.24)$$

where

t is the height of the fin (0.01 in.)

w is the fin width (0.01 in.),

A_B is the repeating base area,

A_{ft} is the total fin surface area,

A_{fb} is the fin base area, and

$m = \frac{2h}{kw}$ for long fins, with h and k convection and conduction heat transfer coefficient, respectively. The average

value found for surface effectiveness using Equation 3.24 is about 1.95, which is larger than the conservative constant value of 1.486 used in SAR (Ref.2.1).

3.7 Friction Coefficients and Form Factors

Final design of the natural convection valve is composed of an aluminum housing and a stainless steel ball to reduce the chance of remaining closed after pump coast-down, Fig.3.4. The resistance made to natural convection flow is a function of mass velocity. Based on this the total height of the valve is

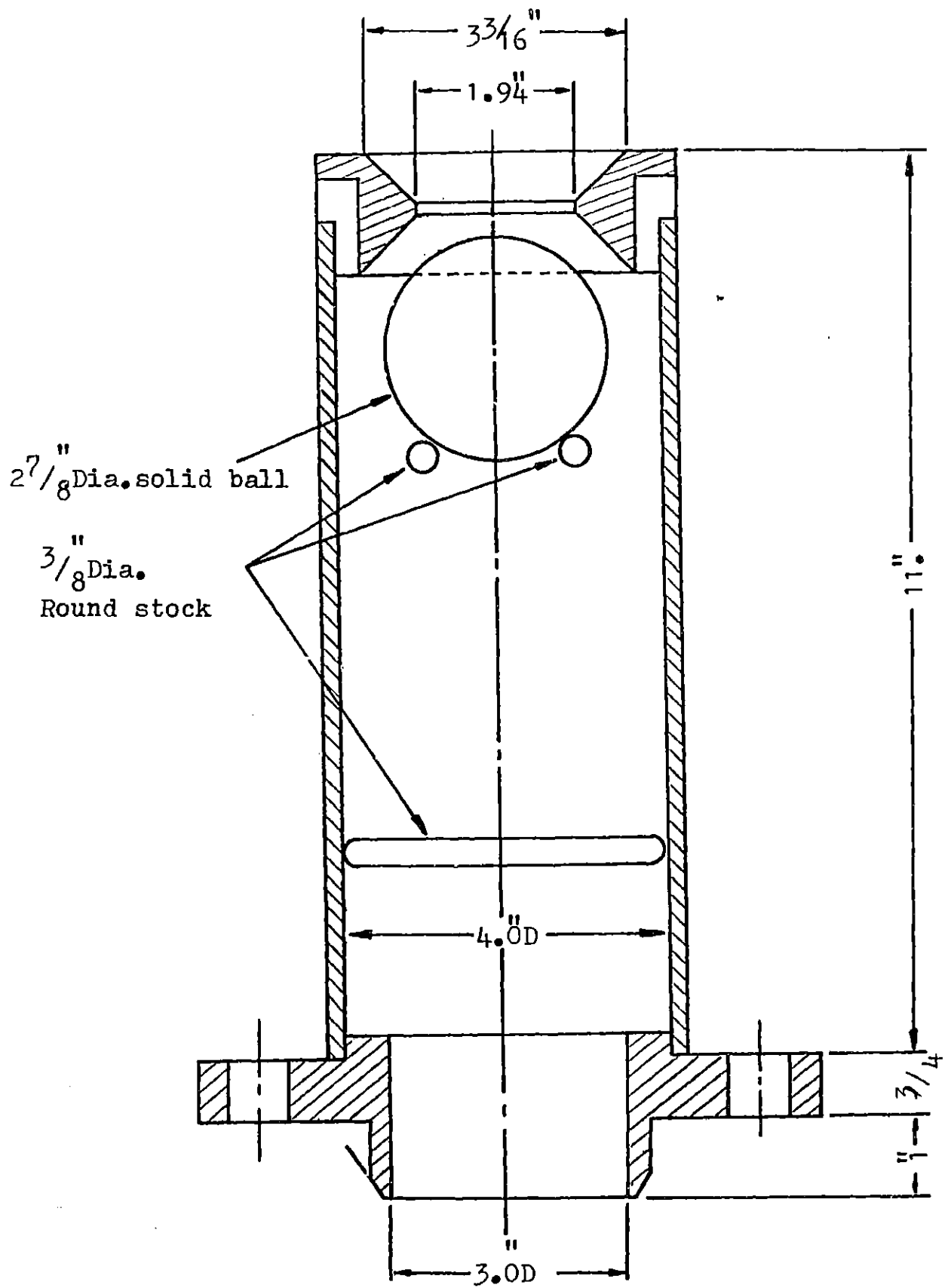


FIG 3.4 Natural Convection Valve

divided into 17 sections. The expansion and contraction coefficients are found (Ref.3.10) from charts for infinitely-wide-gap tube system at a Reynold number of 2000 which is equivalent to a flow rate of about $8 \text{ lbm/ft}^2/\text{sec.}$, that is shown to be a good number for natural convection flow. These values are normalized to the down-commer area to be able to use them more easily in loop calculations. The total natural convection form factor is found to be a function of the number of valves open to the flow as follows:

$$K = 190.38/\text{NOVO}^2$$

where NOVO is the number of valves open to flow. The numerator is found to be 160.37 for turbulent flow. Therefore even if the natural convection flow is not the same as it was estimated above the pressure drop in the valve will not differ considerably.

For the reverse flow, which might occur after the valves open, the form factor is estimated to be:

$$K_r = 57.88/\text{NOVO}^2$$

then the pressure drop could be found from standard equation:

$$\Delta P = KG^2/2\rho g_0$$

where

G	is mass velocity	$\text{lbm} / \text{ft}^2 / \text{sec}$
ρ	is density of water	lbm / ft^3 , and
g	is conversion factor,	$32.2 \text{ lbm.ft} / \text{lb}_f \cdot \text{sec}^2$.

The form coefficient at the core inlet was estimated by Morales (Ref.2.7) to be 1.05, based on the coolant velocity at the channel inlet.

Assuming that all the kinetic energy is lost at the channel exit, form factor could be taken as unit at the core exit.

Friction loss coefficient due to abrupt changes at cross-sections, are evaluated from Reference 3.11.

The Darcy-Weisbach friction factor, f , is found from the following general equation:

$$f = n Re^{-m} \quad (3.25)$$

where Re is Reynold's number and n and m are defined as as follows:

for laminar flow in circular pipes; $n = 64, m = 1$

for laminar flow in rectangular cross-section

with aspect ratio of 25, $n = 91.5, m = 1$

for turbulent flow $4000 \leq Re < 51094$; $n = 0.3164, m=0.2$

for turbulent flow $51094 \leq Re$; $n = 0.184, m = 0.20$

and in transition region, $2300 < Re < 4000$, linear interpolation is made on Reynold's number between the turbulent and laminar values.

All the values given above are for isothermal flow. In non-isothermal conditions, like those in core channels, they should be multiplied by $[1 - 0.0025 \Delta T_f]$, (Ref.3.12), where ΔT_f is the film temperature drop in °F.

For long-term transients where boiling might occur, two-phase friction multiplier is defined in Appendix D.

CHAPTER IV

START-UP NATURAL CONVECTION TEST

4.1 General

To demonstrate that the decay heat resulting from long-term operation at 5 MWth can be removed by natural convective cooling, a series of pump trip transient temperature measurements were made during the MITR-II step-wise startup to full power with Core-4. Decay heat removal performance from only the initial transient was also investigated by short power operations. The time at power was minimized, (about 5 minutes) to keep fission product inventory low. After successful completion of the short run and transient test, the test was repeated after at least three hours of power operation.




Temperature measurements were made by inserting stainless steel clad chromel-alumel type K thermocouples into various positions. Table 4.1 shows a summary of thermocouples and their places in Core-4. Figure 4.1 also shows the in-core thermocouples.

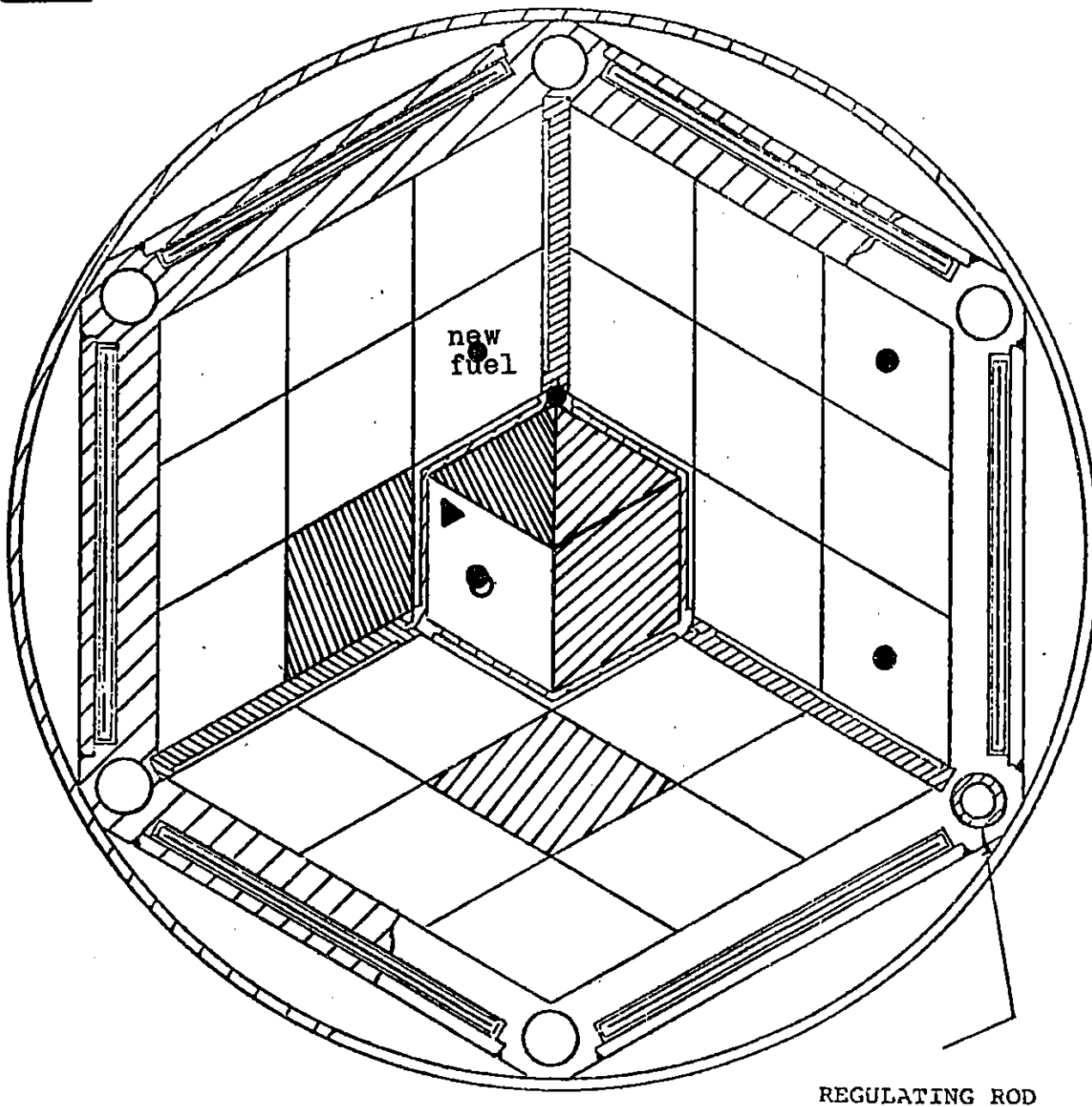
Thermocouple installation and wiring is shown in construction and startup procedure of MITR-II (Ref.2.14). The main design criteria was to affix the holder so that it could not break free during both primary pumps operation and yet would have minimum effect on the element flow.

Table 4.1

Thermocouple Position in Core -4 Startup Test

<u>T/C number</u>	<u>Position Element</u>	<u>Place</u>
6	C-13	mixed outlet
7	C-15	mixed outlet
8	A-2	mixed outlet
9	B-6	mixed outlet
10	3Gu6	graphite plug
11	spider hole #3	bottom of core inlet
12	A-2	T/C on inside of the last plate 4 " from bottom, toward A-3
13	A-2	T/C On center plate of the element 0.1" from bottom , away from A-3
16		cadmium shutter

-  Aluminum
 Molybdenum
 Stainless Steel



- - T/C for mixed temperature
 ○ - T/C #13 at 0.1" from the bottom
 ▲ - T/C #12 at 4.0" from the bottom

FIG. 4.1 Incore Thermocouple Position

To measure the fuel element outlet temperature the thermocouple tip is positioned in the element exit plenum under the end nozzle bale. Since the distance to channel exit is less than one inch, the measured temperature may not be the mixed mean element outlet temperature.

Fuel plate surface temperature was measured by using a "thermocouple fuel element". The thermocouple fuel element was inserted into position A-2, for Core-4 with two thermocouples fixed on two different plate surfaces at 0.1 and 4.0 inches from the bottom of the fuel, (Table 4.1).

4.2 Experimental Procedure

Addendums number 1 and 2 to subprocedure 5.10.1 provide procedure for raising the reactor power of Core IV to a maximum level of 2.5 and 5 MW respectively.

Both primary pumps were used to prevent overmoderation at the center of the core. An aluminum rod of 1" diameter was installed to fill at least 18" of ISCA thimble from the bottom. It was transferred from flask to core position A-1 and was locked down by the hold-down grid. Fuel element outlet and inlet plenum thermocouples were then installed. Top lid was positioned and prerequisites specified in subprocedure 5.10.1 and 5.11.2 (Ref.4.1) were completed and verified.

Reactor power was raised in steps to 200KW for radiation survey and after approval it was increased to 1 MW. At this power

the specified transient tests in subprocedure 5.10.1 and 5.11.2 were conducted. Power was raised then in 0.5 MW steps to 2.5 MWth following the subprocedures.

To increase the power from 2.5 MW to 5.0 MW three additional thermocouples were installed in graphite plug, blister tank, and medical boron water shutter.

Using the thermocouple data available at each power level, the maximum fuel plate temperature, and temperatures at hot spot during steady state and transient operation were also plotted. Correction factors should be applied as is shown in the following section, to estimate the actual surface temperature. The acceptance criteria was conservatively chosen to account for the uncertainty of fuel plate surface temperature measurement.

At any power level, two sets of measurements were made. Decay heat removal performance from the initial transient of fission power was obtained from short interval operation. The reactor was started up following normal procedure at full core water flow rate of 2000 gpm. Power was raised to 1MW and was kept constant for 5 minutes. Core inlet, outlet, temperature difference along the core, incore temperature, flow rate, and power level were recorded. Shutdown coolant pump MM-2 was stopped. The thermocouple corresponding to the fuel surface temperature at 4.0 inches was selected on the recorder at high speed and then booster pumps HM-2 and HM-2.A and secondary pumps HM-1 and HM-1A

were stopped respectively. Primary pumps MM-1 and MM-1A were stopped simultaneously right after the other pumps. At 2 MW and above by using minor scram the reactor was shutdown simultaneously with flow stopping. Data was recorded for about 60 seconds at high speed (12 in./min.), and 15 minutes at low speed (2 in./min.). The results were evaluated with acceptance criteria before proceeding with the tests.

Removing the decay heat resulting from long term operations by natural convective cooling was the other part of the startup tests. It was shown that decay heat buildup after about three hours operation was almost equal to that of infinite operation. Therefore after each short interval operation, core water pumps MM-2, MM-1 and MM-1A were restarted followed by starting up the reactor with normal procedure. The reactor power was kept constant for at least three hours before all temperatures were measured in the same way as for ten-minute operation. Thermocouple number 12 was selected on the recorder to show the transient behavior of fuel surface temperature at 4.0 in. from the bottom while all the pumps were stopped and the reactor was scrammed in the same order as in the short interval operation. This transient was observed long enough to pass the maximum wall temperature which occurred at about 30 seconds after the scram. The recorder was then switched to the other thermocouples.

This was repeated for power to increase from 1 MW to 4.9 MW in 0.5 MW steps.

At each power, the level trip was set less than 20% above the next step if the data was approved.

The acceptance criteria for decay heat removal testing is as follows:

- " 1. Measured fuel plate temperatures are equal to or less than those calculated in Section 3 of the SAR.
2. Temperatures in the reflector tank are less than 55°C and minimum flow requirements are established.
3. Temperature in the graphite region are equal to or less than those in the MITR-I.
4. Temperature of medical water shutter is less than 70°C and minimum flow requirements established.
5. Temperature of D₂O blister tank less than 60°C."

4.3 Preliminary Calculations

Aluminum melts at 660°C and begins to lose strength at 450°C, so the latter temperature could be a suitable criterion for guaranteeing the structural integrity of the fuel element. Since MITR operates at atmospheric pressure at the pool level, it is estimated that boiling occurs at the core mid-height, at about 107°C.

In startup natural convection tests, the maximum wall temperature in the hottest channel was to be estimated at any power by extrapolating the known data. Therefore from installed thermocouple readings, hot spot temperature had to be evaluated. Thermocouple number 12 measured (Table 4.1) fuel plate wall temperature at a height of 4 in. from the bottom of the element. Actual film temperature drop ($T_w - T_f$) at that point could be estimated from thermocouple reading and core average temperature increase:

$$[T_w - T_f]_{\text{act,A-2}} = (T_{12} - T_{11}) - F_r Z_q \Delta T_{\text{cav}} + \Delta T_{\text{er}} \quad (4.1)$$

where

- T_w is actual wall temperature at the point of thermocouple in A-2-15
- T_f is fluid temperature at 4 in. height in A-2 ,
- T_{12} is maximum transient temperature reading of T/C no.12
- T_{11} is maximum transient temperature reading of T/C no.11
- ΔT_{cav} is the core average temperature increase,
- ΔT_{er} is correction temperature for thermocouple installation
- F_r is radial peaking factor for fuel element A-2, and
- Z_q is fraction of power produced up to the height of thermocouple.

The wall temperature measured by a thermocouple, relative to the actual fuel surface temperature depends upon the thermocouple attachment effectiveness. A properly attached thermocouple reads a temperature close to the actual surface temperature, while a poorly attached thermocouple reads a temperature that is closer to bulk fluid temperature at that point. Thermocouple installation factor, I , was developed by Szymzak (Ref.4.2) as a function of fin effectiveness, η , and heat transfer coefficient obtained by using the Dittus-Boelter correlation, h :

$$I = (T_0 - T_f) / [Q/A] \quad (4.2)$$

where,

Q/A is the heat flux at thermocouple location,

T_0 is the temperature observed by the thermocouple, and

T_f is the bulk coolant temperature at the thermocouple location.

The actual fuel surface temperature can be obtained from the measured wall temperature by knowing the calibration factor, Z_c , used by Szymzak (Ref.4.2) as follows:

$$Z_c = [T_w - T_0] / [T_w - T_f] \quad (4.3)$$

where,

T_w is the actual surface temperature,

T_0 is the temperature measured by the thermocouple, and

T_f is the bulk fluid temperature at the thermocouple tip location.

The calibration factor is plotted against ηh , as defined before, in Figure 4.2. Equation 4.3 can be rearranged to yield:

$$T_w - T_f = (T_0 - T_f)/(1 - Z_c) \quad (4.4)$$

Figure 4.2 shows that for lower values of ηh which would be in natural convection cooling, the thermocouple would read close to the actual wall temperature even if they were poorly installed.

The correction temperature, ΔT_{er} , used in Equation 4.1 was estimated to be about 4.5°C .

The hot spot temperature in fuel element C-13, could be estimated from Equation 4.1 by evaluating the relative power produced in the hot channel, in fuel element C-13 to that of A-2 at 4" :

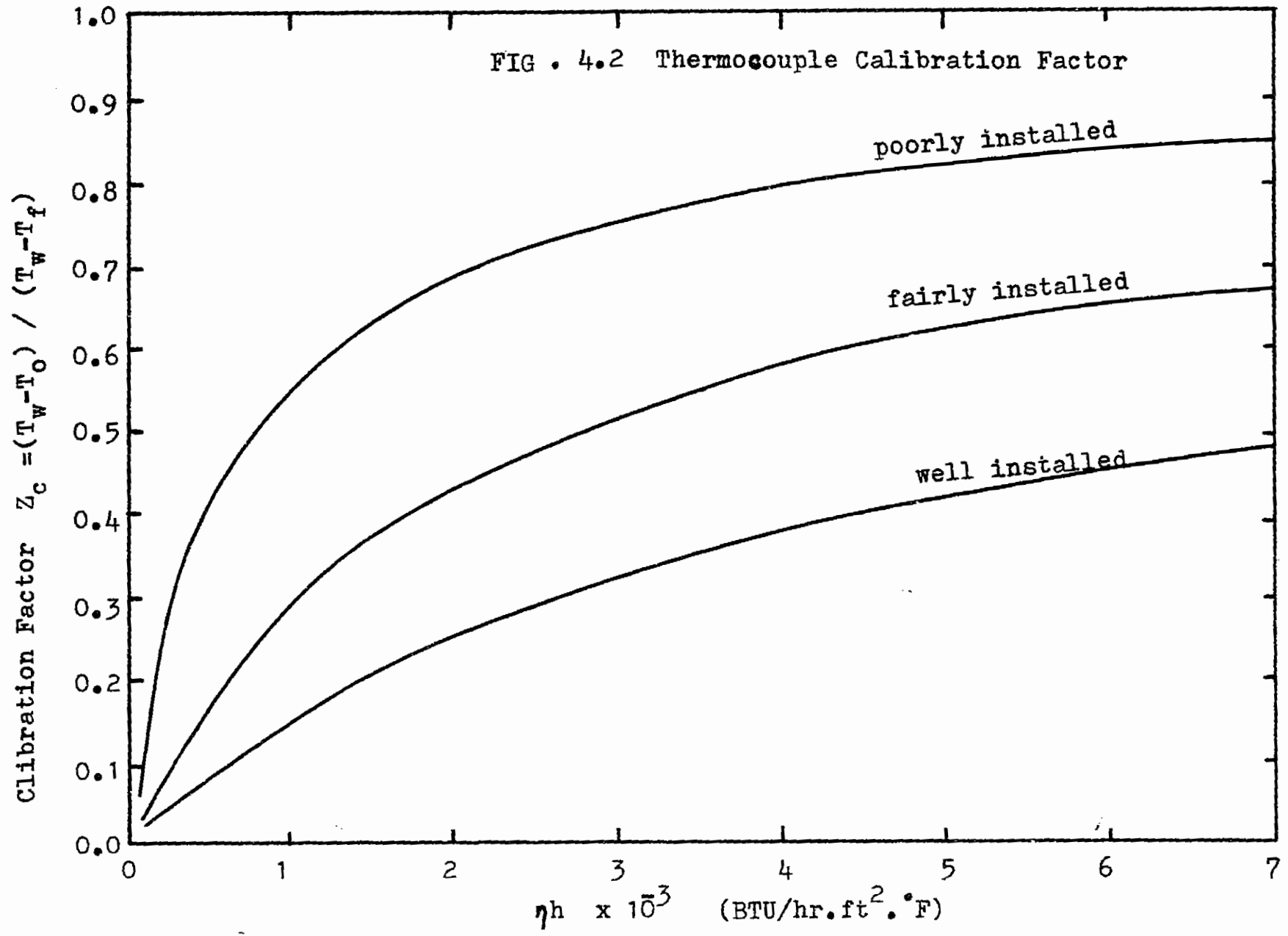
$$[T_w - T_f]_{c-13}/[T_w - T_f]_{A-2} = [F_r F_a]_{c-13}/[F_r F_a]_{A-2} \quad (4.5)$$

where F_r and F_a are the radial and axial peaking factor respectively, and the subscript C-13 and A-2 refer to their position in the core.

Fluid temperature at the hot spot, $T_{f,C13}$ in Equation 4.5 can be found by heat addition to the hot channel :

$$T_{f,c-13} = T_{in} + \Delta T_{cav} (F_r Z_q)_{c-13} \quad (4.6)$$

FIG . 4.2 Thermocouple Calibration Factor



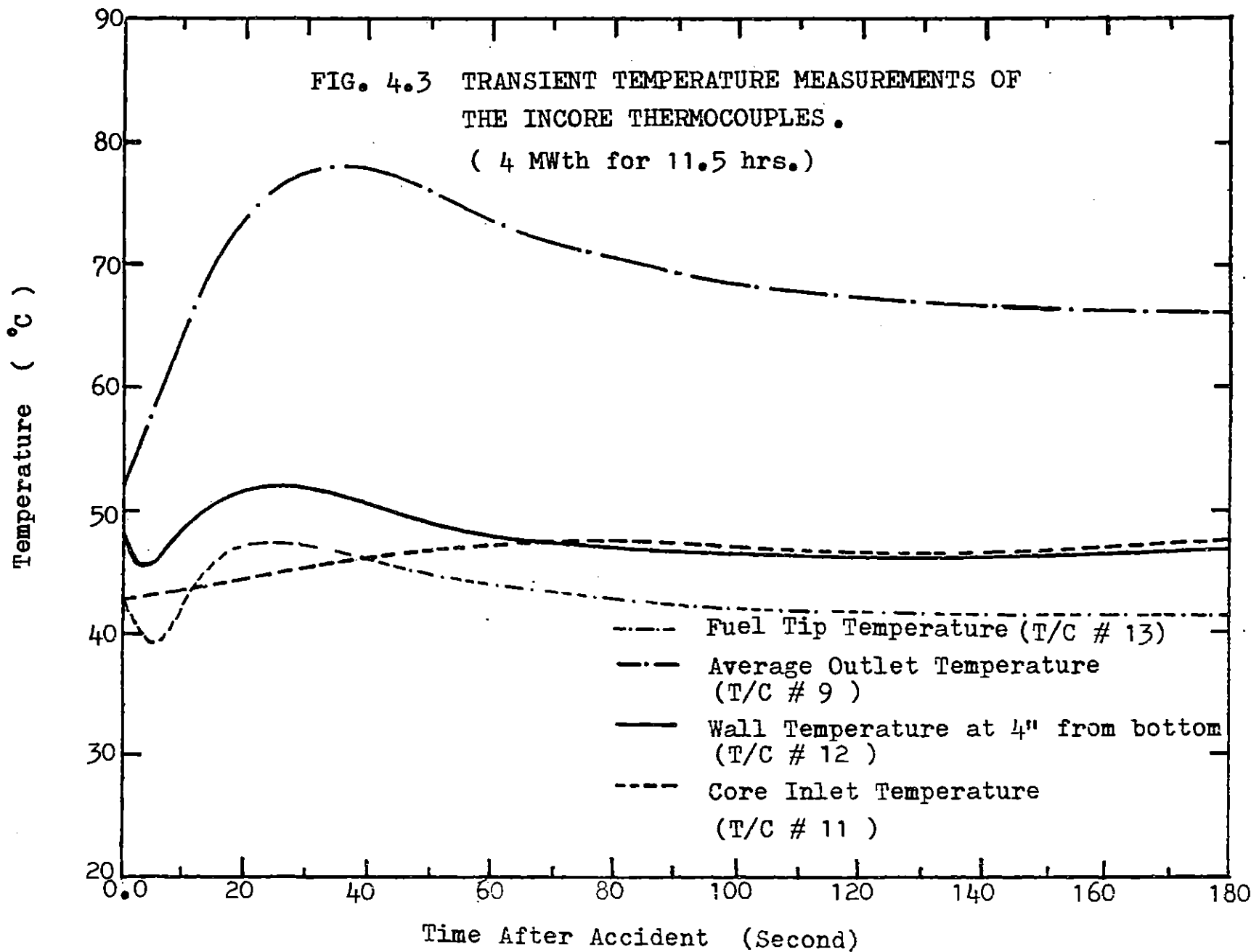
where the term in parenthesis is the fraction of power generated in the hot channel up to the height of hot spot and T_{in} is the fluid inlet temperature. Other parameters in Equation 4.6 were defined before. Assuming that the core outlet scram set is at 55°C , the core inlet temperature could be found conservatively from power balance. A temperature difference of 8°C is evaluated for 5 MWth power and 2000 gpm flow rate.

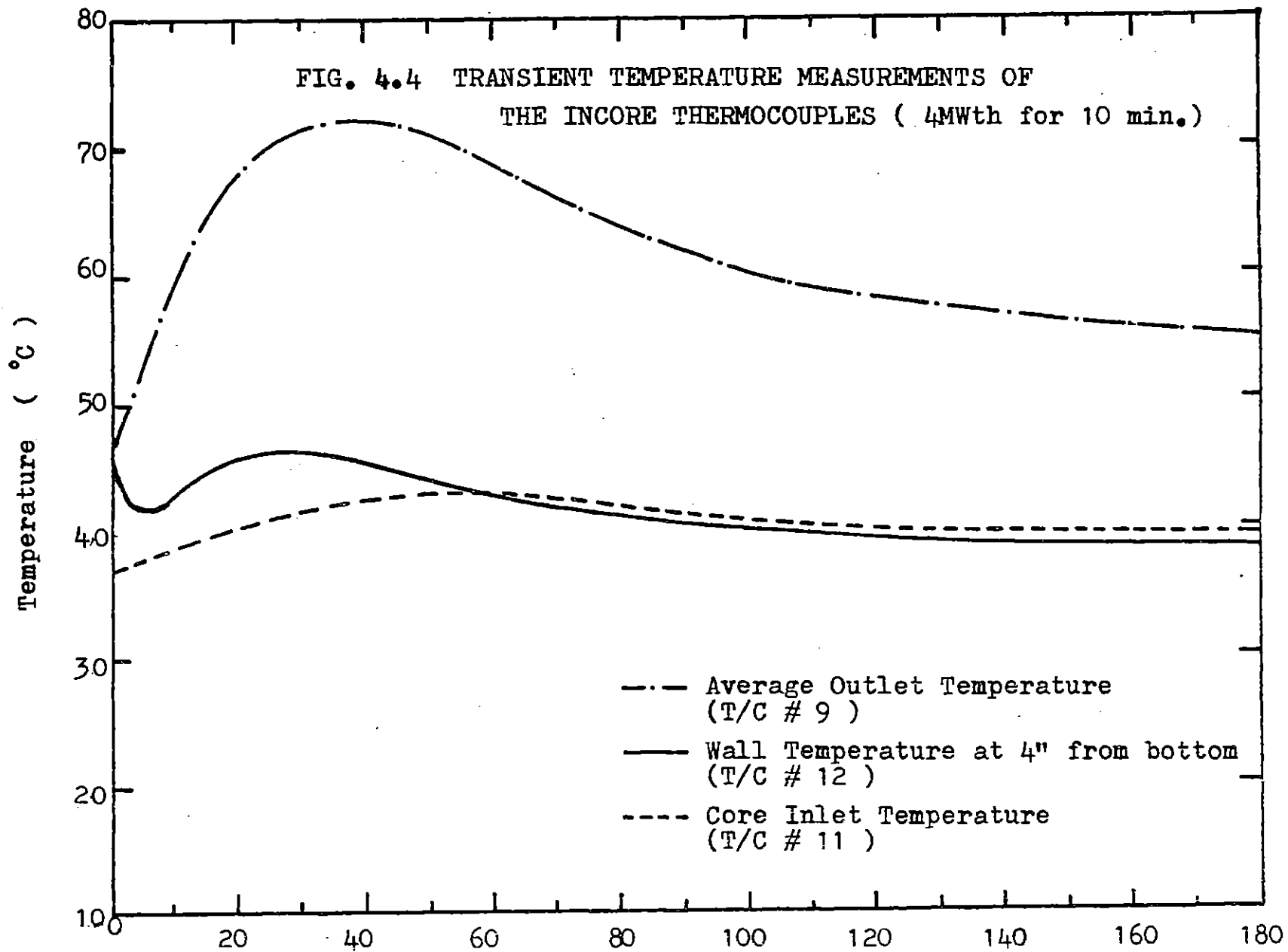
4.4 Natural Convection Test Measurements

Transient in-core temperature measurements for 4 MWth power after 11.5 hours and 10.0 minutes steady state operation are shown in Figures 4.3 and 4.4. The fuel tip temperature in the first few minutes after scram was not measured, so the dashed line shows only the shape that it would follow in short transient. Transient temperature measurements of the in-core thermocouples for other power discussed in the earlier section are shown in Appendix E.

The coolant outlet temperature increases for a few degrees right after the scram signal is initiated because of the scram delay time. This relative peak could not be measured and recorded due to delay time of the thermocoupling wiring system and relatively low speed of the recorder.

Maximum wall temperature in the hottest channel could be evaluated by combining Equation 4.1, 4.5, 4.6. These temperatures are shown in Figure 4.5 based on the peak values of thermocouples 11 and 12, inlet temperature of 47°C and the following peaking factors





at hot spot in C-13 element with shim bank and at 10" from the bottom; $F_r = 1.315$ $F_a = 1.630$

at 4.0 " from the bottom in A-2 with shim bank at a height of 8"; $F_r = 1.175$ $F_a = 1.050$.

Extrapolation of Figure 4.5 shows that the maximum wall temperature in the hottest channel during transient pump coast down will be much below saturation, even if the steady state power is 6 MWth . Figure 4.6 shows the steady state hot spot temperature for different powers evaluated from Equation 4.5.

Acceptance criteria for startup of MITR-II requires some limitations on the out core temperatures. Therefore along with the in core temperature measurements, thermocouples were installed to measure the temperatures of graphite, cadmium shutter, boron water and D₂O shutter tank. Figures 4.7 and 4.8 show the maximum transient temperatures for different reactor powers. It is shown that all temperatures are within acceptable limits.

FIG 4.5 WALL TEMPERATURE EVALUATED AT
HOT SPOT

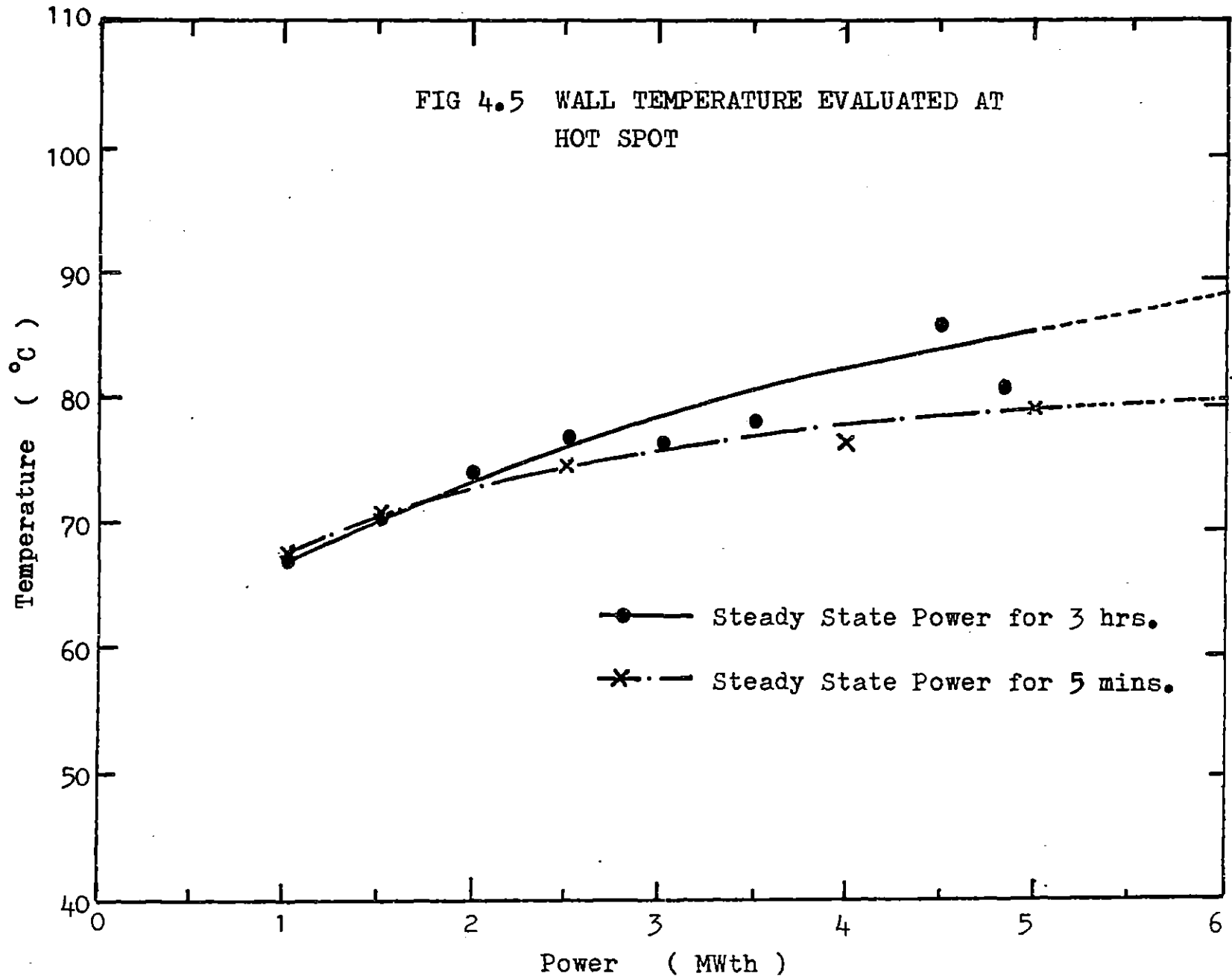


FIG 4.6 WALL TEMPERATURE AT HOT SPOT
IN FUEL ELEMENT C -13

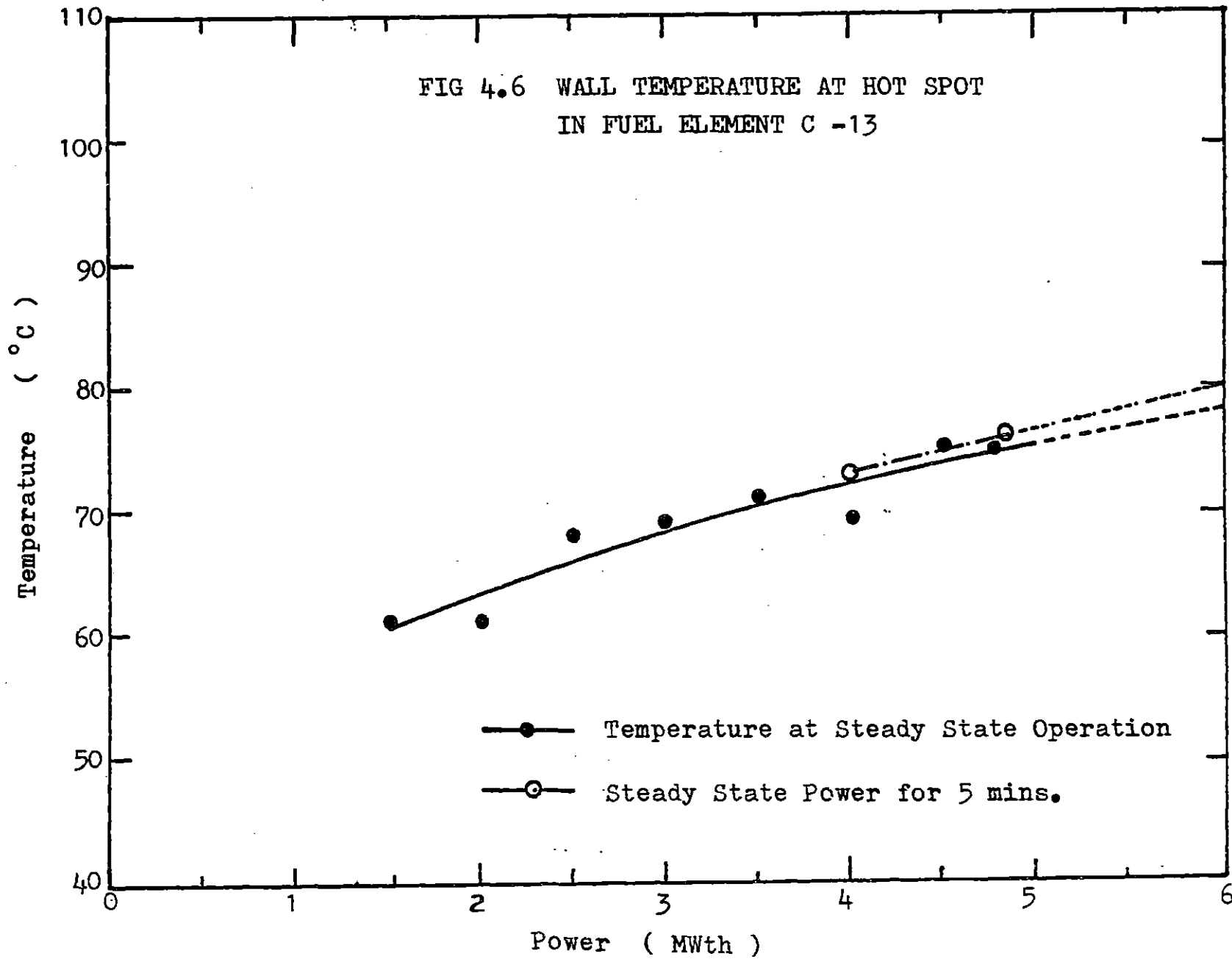


FIG 4.7 OUTCORE TEMPERATURE MEASUREMENTS

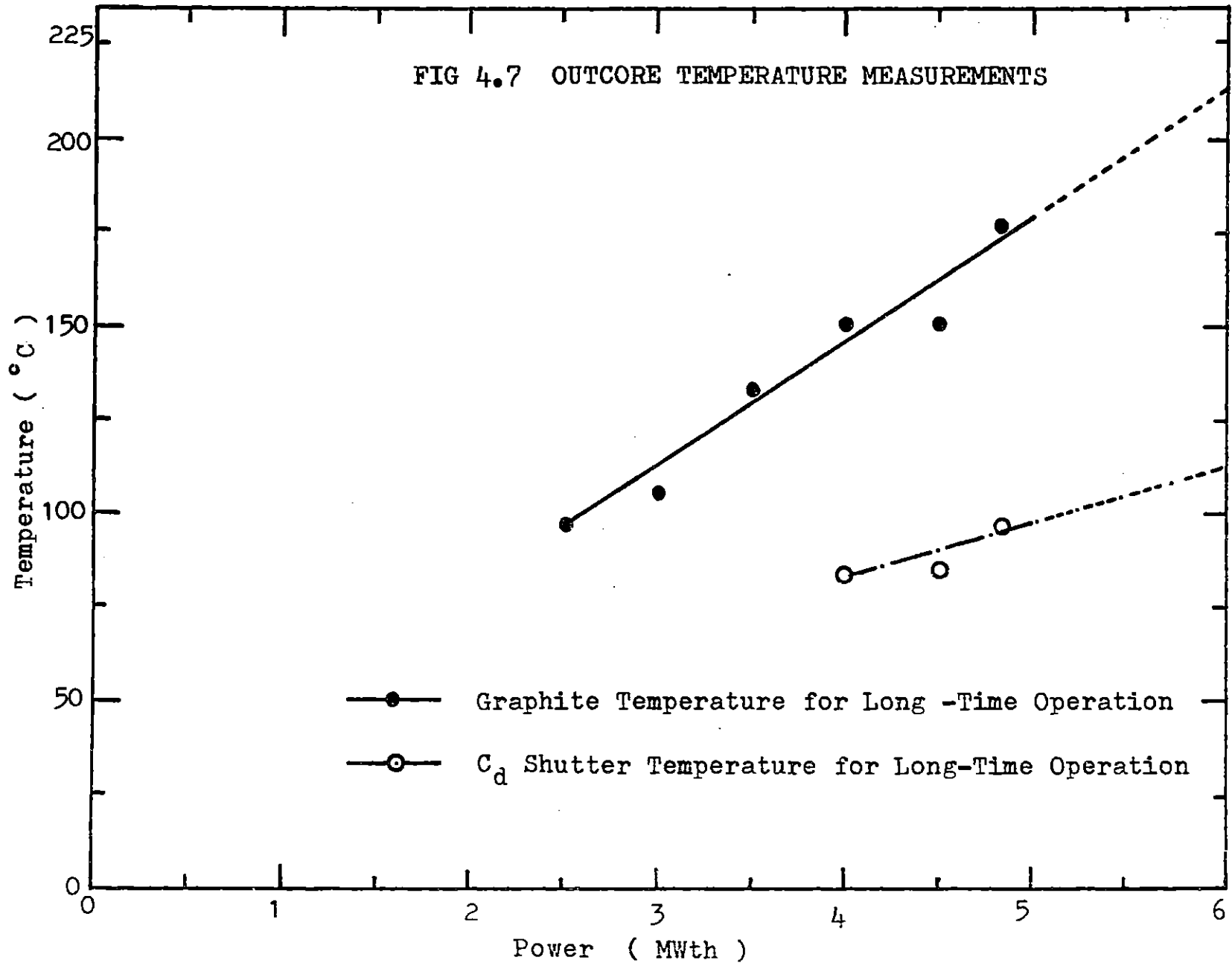
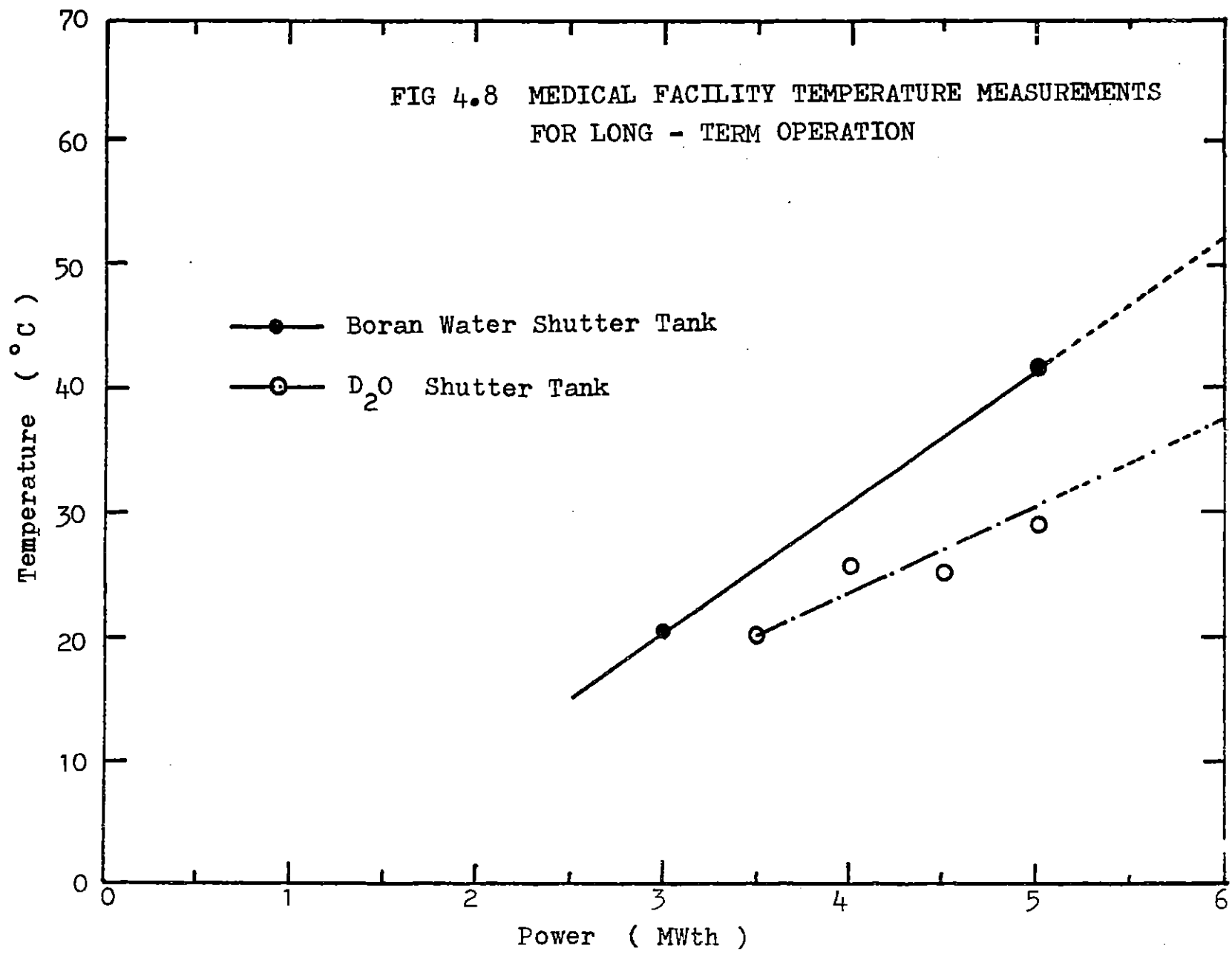


FIG 4.8 MEDICAL FACILITY TEMPERATURE MEASUREMENTS
FOR LONG - TERM OPERATION



CHAPTER V

COMPUTER RESULTS

5.1 General Assumptions

The Computer Code LOFA is written to analyze the steady state, forced flow transient, and natural convection behavior of the MITR-II during a Loss of Flow Accident. A single channel model is applied to the equations derived in previous Chapters II and III to consider the core average power distribution. The computer code output is compared with the startup temperature measurements in the fuel element B-6, in order to be able to use the code in the prediction of hot channel behavior in natural convective cooling.

The startup natural convection tests above 2MWth were based on the assumption of loss of electrical power to the main panel. The same assumption is made in all the computer code calculations which are made in this work. In other words, after steady state calculation, the reactor is scrammed at the same time that both primary pumps are stopped.

A scram delay time of 0.41 seconds is assumed for the reactor shut down. Therefore until 0.41 seconds after

the loss of electrical power, the reactor is assumed to be at full steady state power, whereas the primary coolant flow starts decreasing as soon as the power goes off. To be more conservative, the time that it takes for 80% of the shim bank insertion, is added to the scram delay time. Thus, it is assumed that a reactivity of -4.8 beta is inserted at 0.9 seconds after the accident. This is equivalent to the insertion of 80% of the shim bank worth at once.

For the time between 0.41 and 1.0 seconds after the accident, the heat deposition rate in the core is determined by interpolating on time between the values at 0.41 and 1.0 seconds.

Delayed photoneutrons produced due to gamma absorption in the D_2O reflector were discussed in Section 2.3 for infinite medium. Although those values are used here conservatively it is seen that the contribution of delayed photoneutrons to decay power is only a few percent.

In steady state operation, more than 5% of the fission energy is deposited in the D_2O reflector and shielding. This energy loss is neglected in the after scram decay heat deposition in the core.

The heat transfer from the containment tank by the tank gas system or by conduction through the wall is neglected in the tank mixed enthalpy calculations.

In Section 2.7 it was found that the heat transferred from the down comer to the D₂O reflector around it is about 33.8 watts. This could be ignored in comparison to the decay heat produced in the core which is comparatively large. The decay power at about three minutes after the scram is approximately 250 KW.

Axial power distribution in the core after shut down is assumed to be the same as that which is at steady state operation. Due to gamma ray energy contribution, the decay energy is actually more uniformly distributed along the core than normal steady state power.

Due to the small thickness of fuel plates and high conductivity of aluminum cladding, no axial or radial heat conduction is considered in the calculations.

Five percent of the total decay energy is assumed to be generated directly in the coolant. Heat produced in the core is presumed to be deposited in the coolant to allow the fuel plates to be the energy sink if the heat flux is negligibly small.

For hot channel calculations, a value of 1.265 is taken for the total radial peaking factor, (Ref.5.1).

The antisiphon valves are installed in the reactor to prevent the containment tank water from flowing out into the inlet pipes when the pressure in the primary loop drops below a specified level. As soon as the natural convection valves open, the cold water in the shroud and down comer is assumed to be mixed with the water around the chimney for core inlet calculations. The water in the primary loop will flow into the shroud due to the pump leakage, whose effect on the tank mixed enthalpy calculation is ignored.

Aside from the moderate assumptions discussed in this section, whenever an uncertainty existed in calculations or evaluations of input data, the most conservative values were chosen.

5.2 Pump Coast-Down and Natural Convection Flow

Loss of electrical power to the main panel, stops both primary pumps at the same time. Due to momentum conservation in the flywheels, the flow coasts down as is shown in Figure 2.1. Equation 2.1 is used to evaluate the flow rate due to pump coast-down for the first few seconds until natural convection flow dominates.

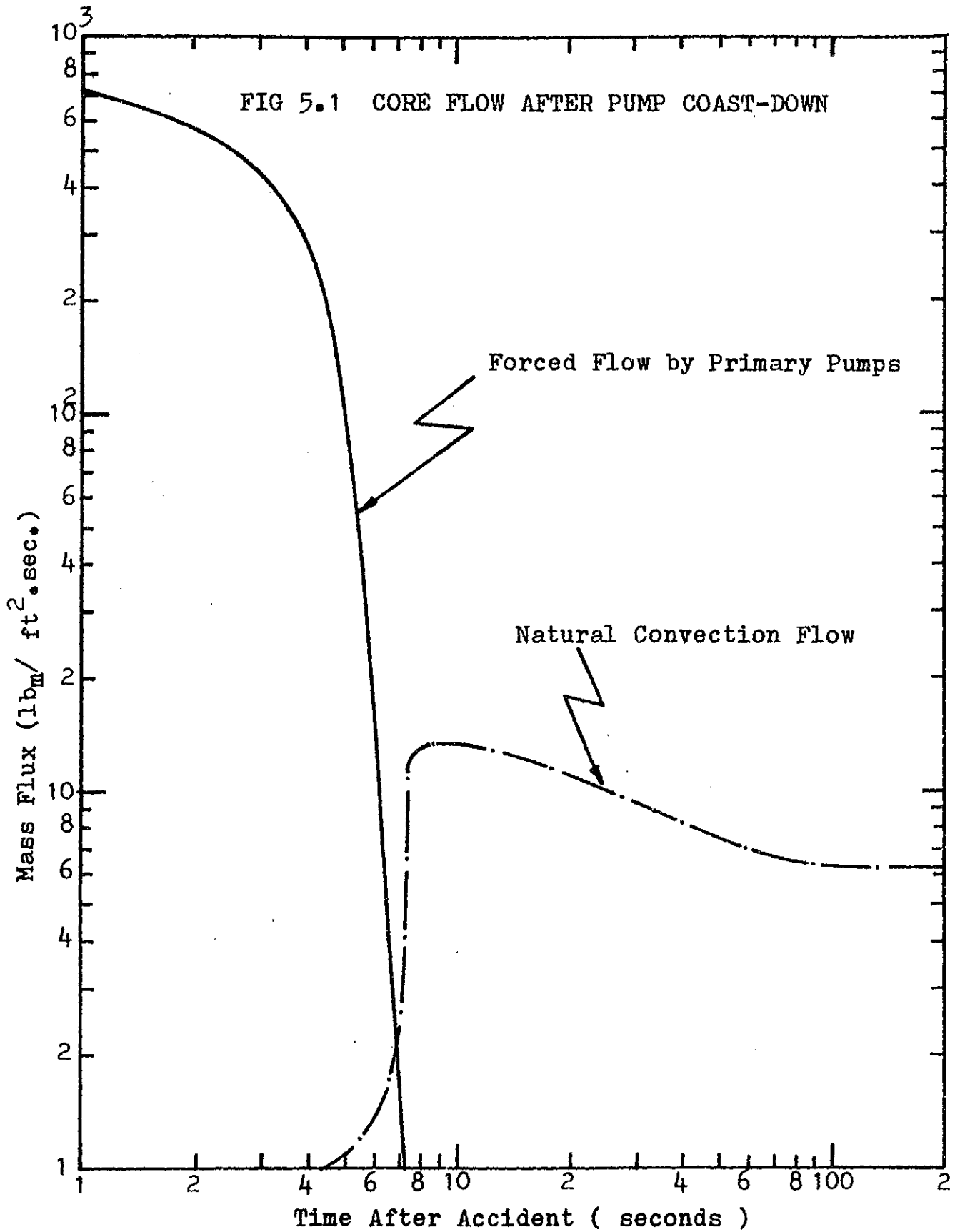
Although the natural convection valves are closed during pump coast-down, there is a small contribution to the flow due to the buoyancy of the hot water in the core. Natural convection flow increases rapidly as soon as check valves open and reaches a maximum at the same time that maximum core outlet temperature occurs. Figure 5.1 shows the flow behavior after scram for Core-4 with average power distribution. The maximum natural convection flow is about 13.65 (lbm/ft.²/sec.), which is due to small water density in the core at the time of peak outlet temperature of 81°C. Thereafter the natural convection flow decreases slowly with decay power.

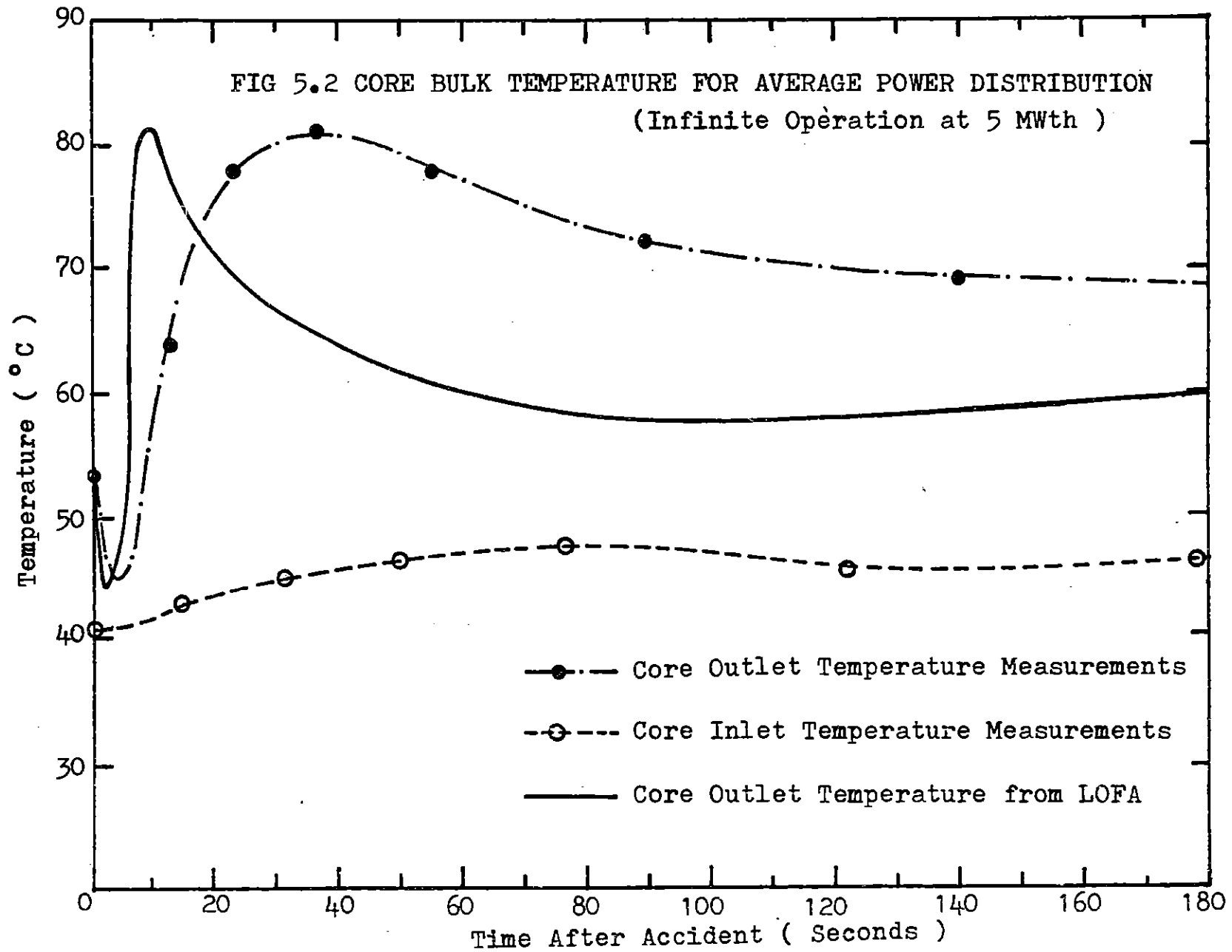
Free convection flow rate decreases less rapidly when the relatively hot water in the containment tank reaches the down comer.

5.3 Core Temperature Calculations

A comparison was made between the computer results and the temperature measurements of the startup natural convection test for the average core outlet temperature.

Figure 5.2 shows that the core outlet temperature increases to a maximum value of 81.6°C in both cases.





The difference between the computer results and the experimental values is that the calculated peak temperature values occur at a time of about 10 seconds after shutdown, while the experimentally measured peak temperature occurred at about 30 seconds. A delay time of about 20 seconds is observed between the peak outlet temperatures in Figure 5.2. Considering core inlet temperature shown in the same figure, it can be assumed that the relatively rapid increase in the core inlet temperature after the initiation of natural convection is due to heat transfer from the core to the down comer.

Decay heat could be transferred through the aluminum core housing to the down coming flow during the high decay energy release period. This would increase both the core inlet temperature and the heat deposited in the relatively thick aluminum wall. When the energy released in the core decreases, the inlet temperature and heat transfer from the core housing to the coolant become considerable. This would shift the maximum core outlet temperature to a later time than that predicted by the computer output in which the heat transfer to the core housing is not considered.

Figure 5.2 shows that the assumption of no heat transfer to the down comer and neglecting the energy deposition and release from the core housing is conservative with regard to the evaluation of the time that maximum temperature or probably the onset of nucleation boiling occurs.

Based on the average core outlet temperature calculations, a single channel model is used to evaluate the hot channel behavior in five cases of loss of flow accident in MITR-II, Core-4. In all cases the reactor is assumed to be at 5 MWth steady state power long enough to build up decay heat as if it were at full power for infinite time. The total steady state primary flow rate is taken to be 2000gpm and the containment tank is assumed to be at the core exit temperature.

Case-1 All the natural convection valves are open after the accident. Steady state primary heat exchanger outlet temperature is assumed to be 40°C.

Case-2 Core inlet temperature is the same as in Case-1 but it is assumed that one valve remains closed

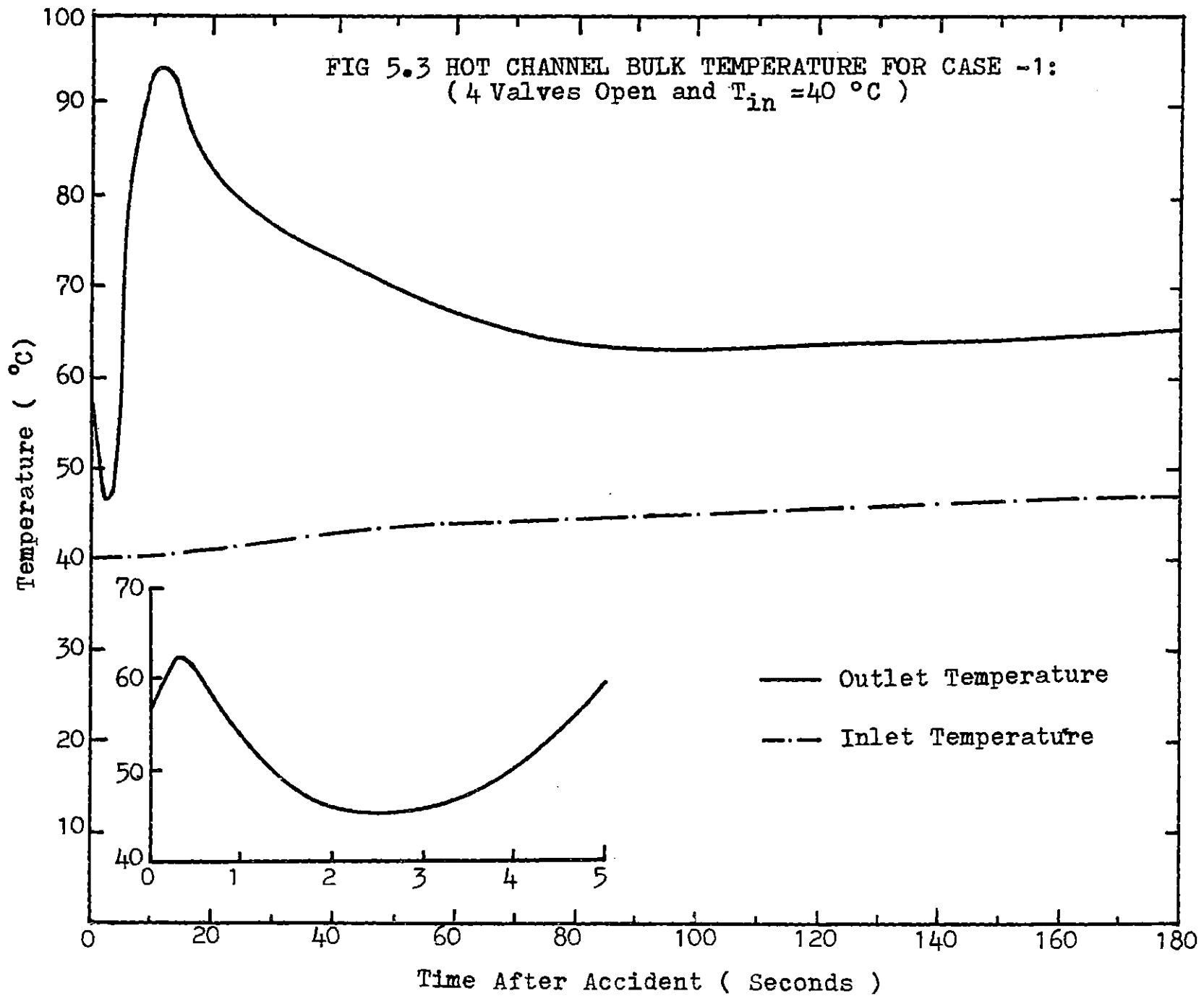
and only three natural convection valves are open to flow.

Case-3 Only two incore check valves are considered to open after loss of flow accident for core inlet temperature of 40°C.

Case-4 The core outlet temperature scram set is assumed to be at 55°C. For the steady state power of 5 MWth. This allows the primary heat exchangers exit temperature to increase to 47°C. All natural convection valves are open in this case.

Case-5 The core inlet temperature is considered to be 52°C, this is equivalent to setting the core exit temperature scram at 60°C. Four natural convection valves are allowed to open after the accident.

1. Case-1 is natural convection analysis of the hot channel in normal conditions at 40°C inlet temperature and all the valves open to flow. Figure 5.3 shows the inlet and outlet transient temperature calculations of the computer code LOFA for Case-1. The inlet temperature



increases slowly after the pump coastdown due to mixing of the relatively hot water between the chimney and the shroud and the cold water in the down comer.

The hot channel outlet temperature increases to a value of about 63°C rapidly right after the accident due to the scram delay time of 0.41 seconds. It then decreases with the insertion of the shim bank. When the coolant flow is not enough to remove the decay heat due to pump coast-down, the fluid outlet temperature increases rapidly to an absolute maximum of about 94°C . This augments the natural convection flow rate to about $11 \text{ (lbm/ft.}^2\text{sec.)}$, which is enough to remove the decay heat and decreases the channel outlet temperature. With the decrease in the fluid temperature, the free convective coolant flow rate decreases to a value which is not able to remove the decay heat from the core at the same constant rate. Therefore the fluid temperature starts increasing with a very small slope after going through a minimum.

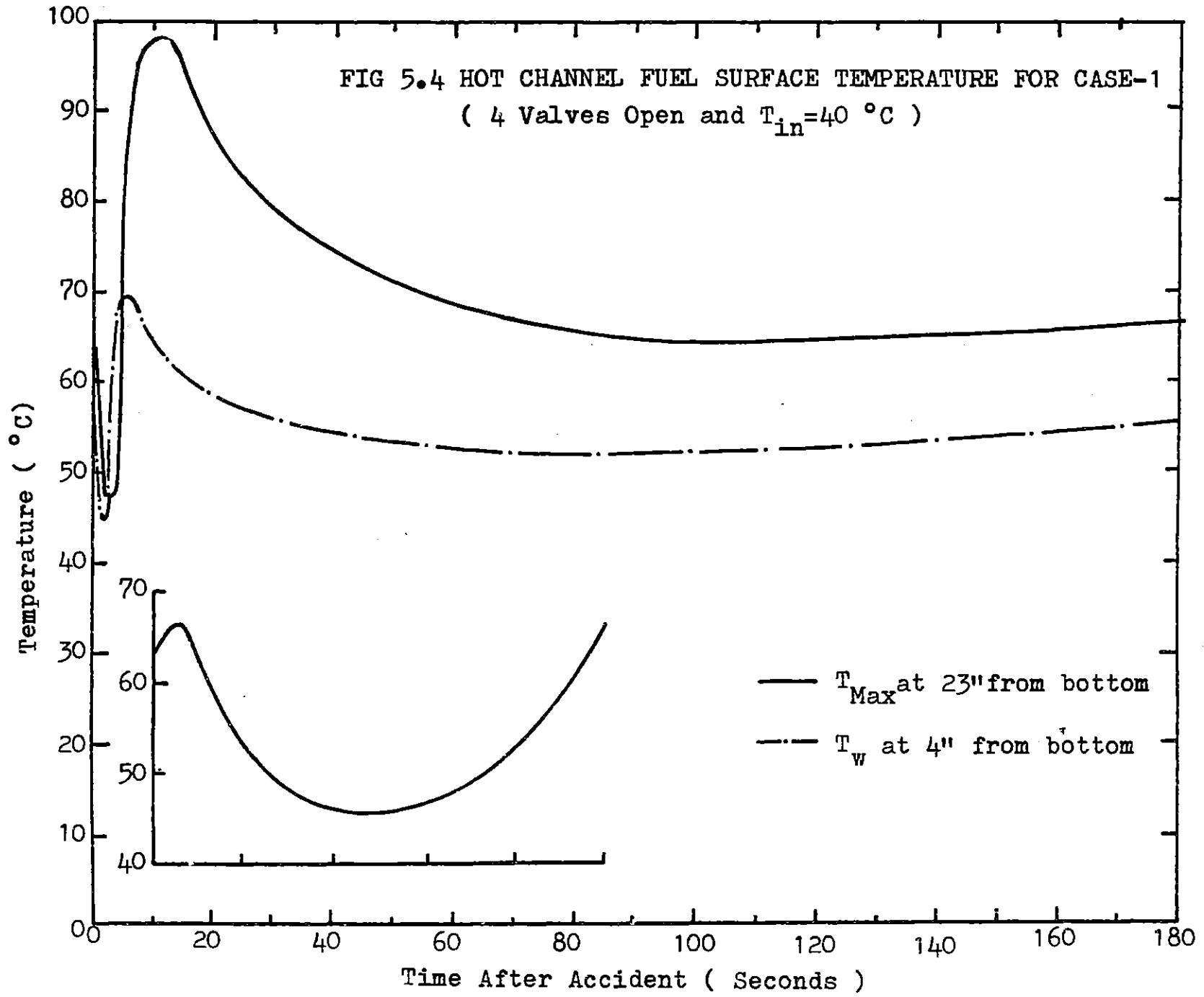
From Figure 5.3 it can be predicted that the bulk boiling will occur at about 58 minutes after the accident at the top of the hot channel assuming no heat transfer to the D_2O reflector.

Fuel surface temperature calculations for Case-1 are shown in Figure 5.4 for the hot spot and also at a mesh point at four inches from the bottom of the fuel plate.

The maximum fuel surface temperature occurs at the top of fuel plate for Core-4. Figure 2.2 shows the axial power distribution in hot channel for MITR-II Core-4. Due to removal of the fixed absorber, the heat flux at the top of the fuel plate is large compared to the Core-1. This shifts the maximum temperature to the top of the fuel plate unless the heat production per unit area is very small.

At twelve inches from the bottom of the fuel plate, the surface temperature goes to a relative maximum due to the shim bank height.

Figure 5.4 shows that the fuel plate surface temperature follows the same shape as the fluid bulk temperature in the hot channel. The hot spot temperature increases to a maximum of about 98°C at about 10 seconds after the accident. This is still far below saturation temperature. The onset of nucleation boiling on the wall is predicted to occur at about 64 minutes after loss of flow accident. This is a little later than initiation of bulk boiling at the top of hot channel because the



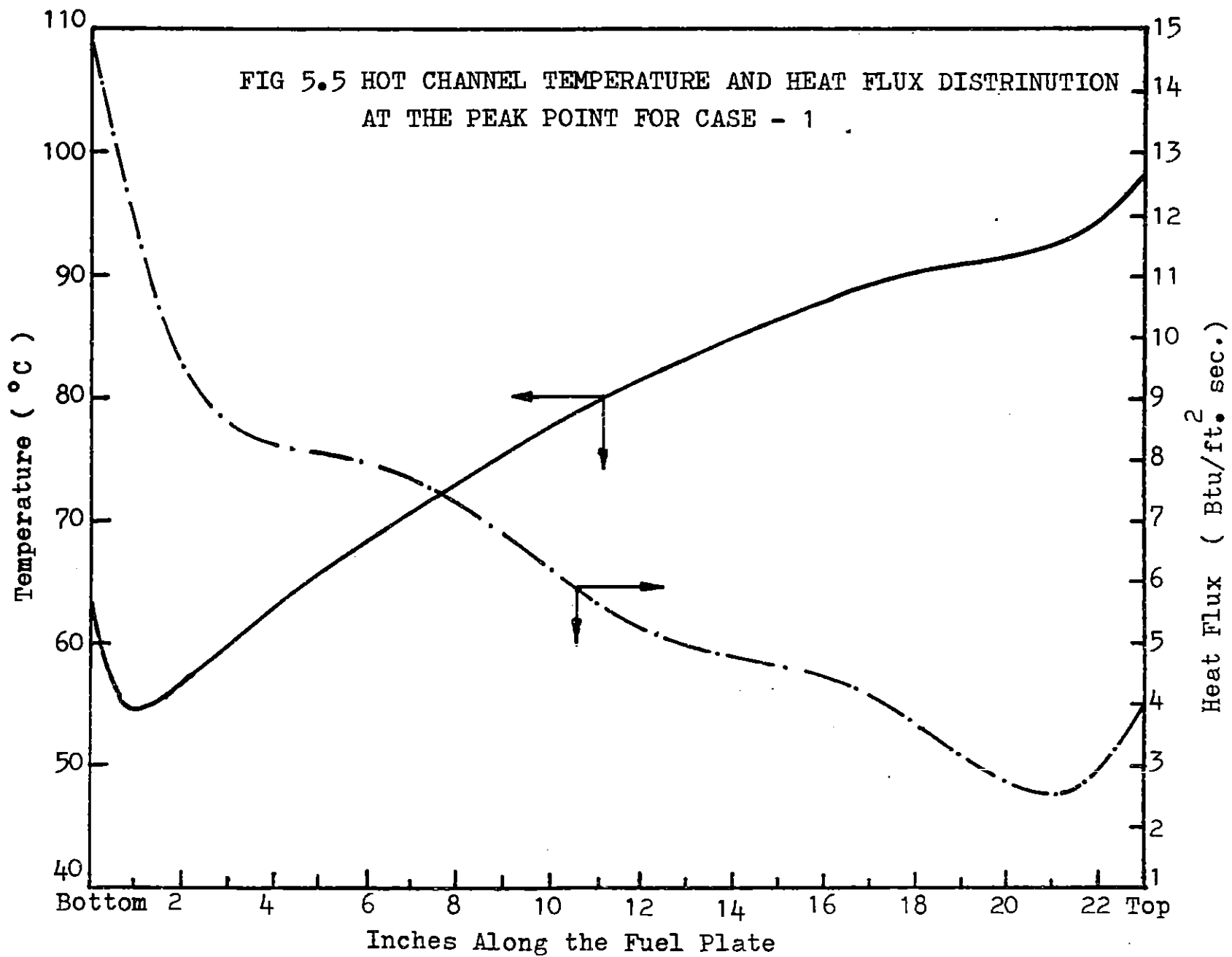
fuel surface temperature increases with a smaller slope than the fluid bulk temperature.

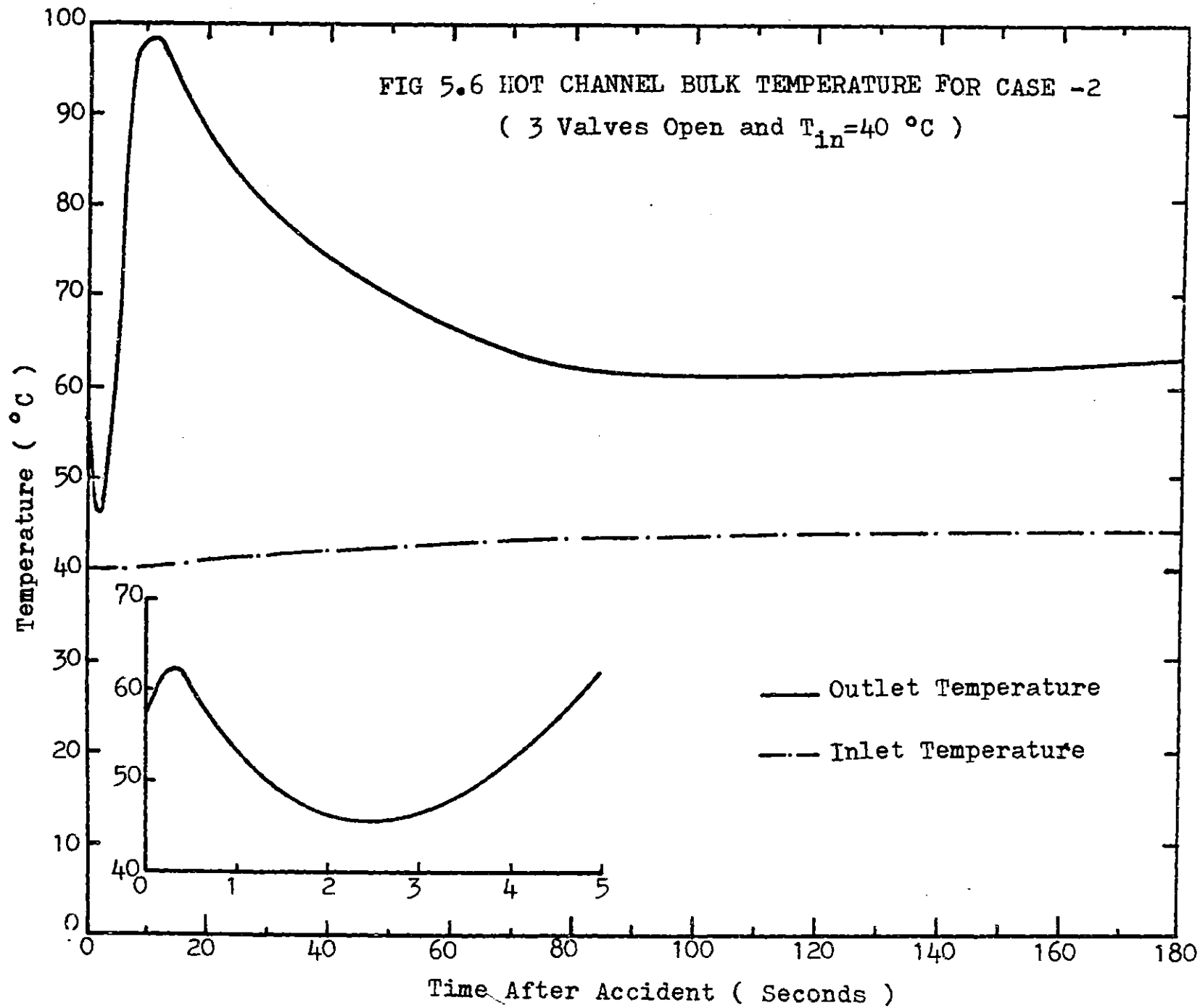
The top part of the fuel plate changes from heat source to energy sink after a long time following the accident. This is due to small contribution of the heat flux at the top of the fuel plate long after the accident. This makes the bulk fluid hotter than the fuel surface at the top of the hot channel.

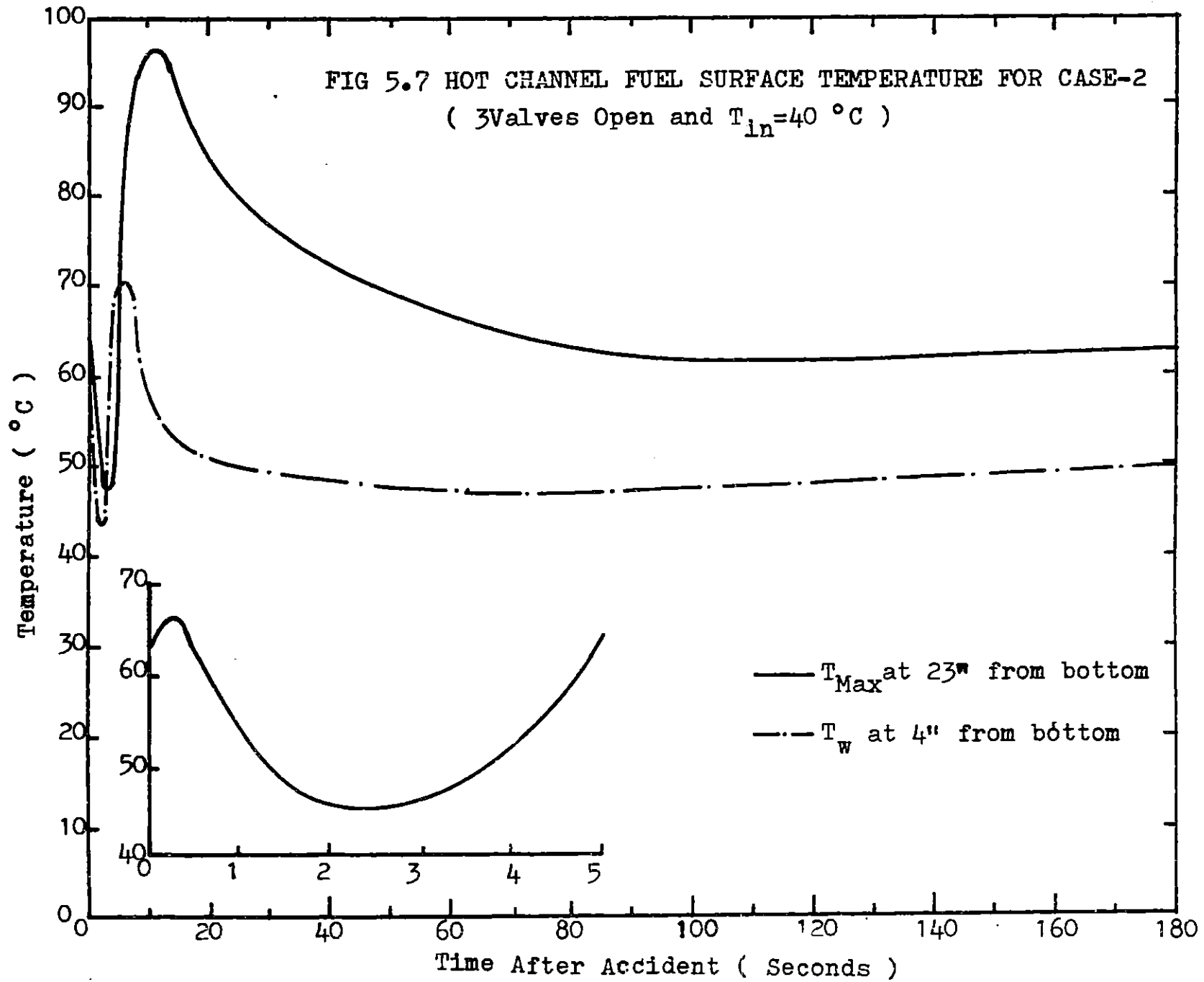
Figure 5.5 shows the axial fuel surface temperature and the heat flux distribution in the hot channel at the peak value.

2. The effect of closing one natural convection valve is studied in Case-2. The Computer Code LOFA is used to calculate the hot channel behavior with a core inlet temperature of 40°C and only three natural convection valves open to flow.

Figures 5.6 and 5.7 show the transient fuel surface and fluid bulk temperature for Case-2. The maximum channel outlet temperature occurs at almost the same time as in Case-1. However its value is increased to about 98°C . The combination of increase in the core enthalpy and pressure drop in the down comer augment the natural convection flow rate to a







value of about 13 (lbm/ft/sec.). The maximum surface temperature, which is at the top of the fuel plate is 97°C. At this point the top of the fuel plate could be considered an energy sink.

The assumption of closing one of the incore check valves, delays the start of natural convection for a few seconds. When there is no forced flow due to pump coast-down, for a very short period of time the water is stagnant in the core and therefore allows the enthalpy to increase. Natural convection begins and increases rapidly as soon as the driving force balances the pressure drop in the loop.

In this case, because of relatively high natural convection flow, long term transient bulk temperature increases with a smaller slope than Case-1. It is predicted that when one natural convection valve remains closed, the bulk boiling occurs after about 87 minutes from the time of the accident.

3. In Case-3 it is supposed that when the accident happens, two of the natural convection valves remain closed after pump coast-down. The reactor is assumed to be at steady state power with the primary heat exchanger

outlet temperature of 40°C at the time of loss of electrical power to the main panel.

Closing two of the valves increases the pressure drop in the down comer. To start natural convection flow, this relatively large pressure drop should be balanced by the driving force, which is the density difference between the two legs of the loop.

Computer calculations show that the core flow rate goes to zero with pump coast down, and it takes a while for natural convection to begin. During this short time, the decay heat released into the water increases the bulk temperature rapidly.

Although natural convection starts after a few seconds, the water flow is not enough to remove the decay energy from the core before boiling occurs. About 10 seconds after the accident, fuel surface temperature exceeds saturation at a height of 12 " from the bottom of the fuel plate in the hot channel. The natural convection mass flux at this time is about $7.8 \text{ (lbm/ft.}^2\text{sec.)}$. This flow rate is not enough to remove decay heat and boiling proceeds to the top of the channel.

The fuel surface temperature at the time of boiling is found to be 137.5°C at 12 inches from the bottom and 145.5°C at the top of the fuel plate. The sudden increase in the wall temperature is due to single phase heat convection coefficient used in the computer code. The correlation between the heat transfer coefficient of single phase, h_{sp} and two phase flow, h_{tp} could be shown as follows (Ref.3.5):

$$\frac{h_{tp}}{h_{sp}} = \frac{1}{1-\alpha} \quad (5.1)$$

where α is the void fraction.

Using the right heat transfer coefficient, suggested in Appendix D, would give a better and more correct answer for the fuel surface temperature above the saturation point.

4. Natural convection behavior of the MITR-II, Core-4 is also studied for higher core outlet temperature scram set. In Case-4 it is supposed that scram point is set at 55°C for an average core exit temperature at steady state power of 5 MWth. This is equivalent to a maximum temperature of 47°C for the primary heat exchangers outlet temperature.

Figure 5.8 shows the hot channel inlet and outlet temperatures. Although the fluid outlet temperature reaches 100°C at the very top of the core, boiling does not occur because the saturation temperature at the corresponding pressure is 106°C .

The water temperature passes the peak point at about 10 seconds after the accident. At this time the fuel surface temperature is 104.5°C which is still a few degrees below saturation, Figure 5.9. Natural convection flow rate at the peak temperature is about $12 \text{ (lbm/ft.}^2\text{sec.)}$, which decreases slowly with time.

The hot channel outlet temperature decreases to a minimum of 73°C and then increases slowly as the natural convection flow decreases. It is predicted that bulk boiling will occur at the top of the channel about 27 minutes after the accident.

Fuel surface temperature will reach saturation a few minutes later, about 32 minutes after the accident due to low energy production at the top of the fuel plate.

5. The computer analysis of the hot channel shows that boiling will occur at the top of the fuel plate if the core exit temperature scram set is at 60°C .

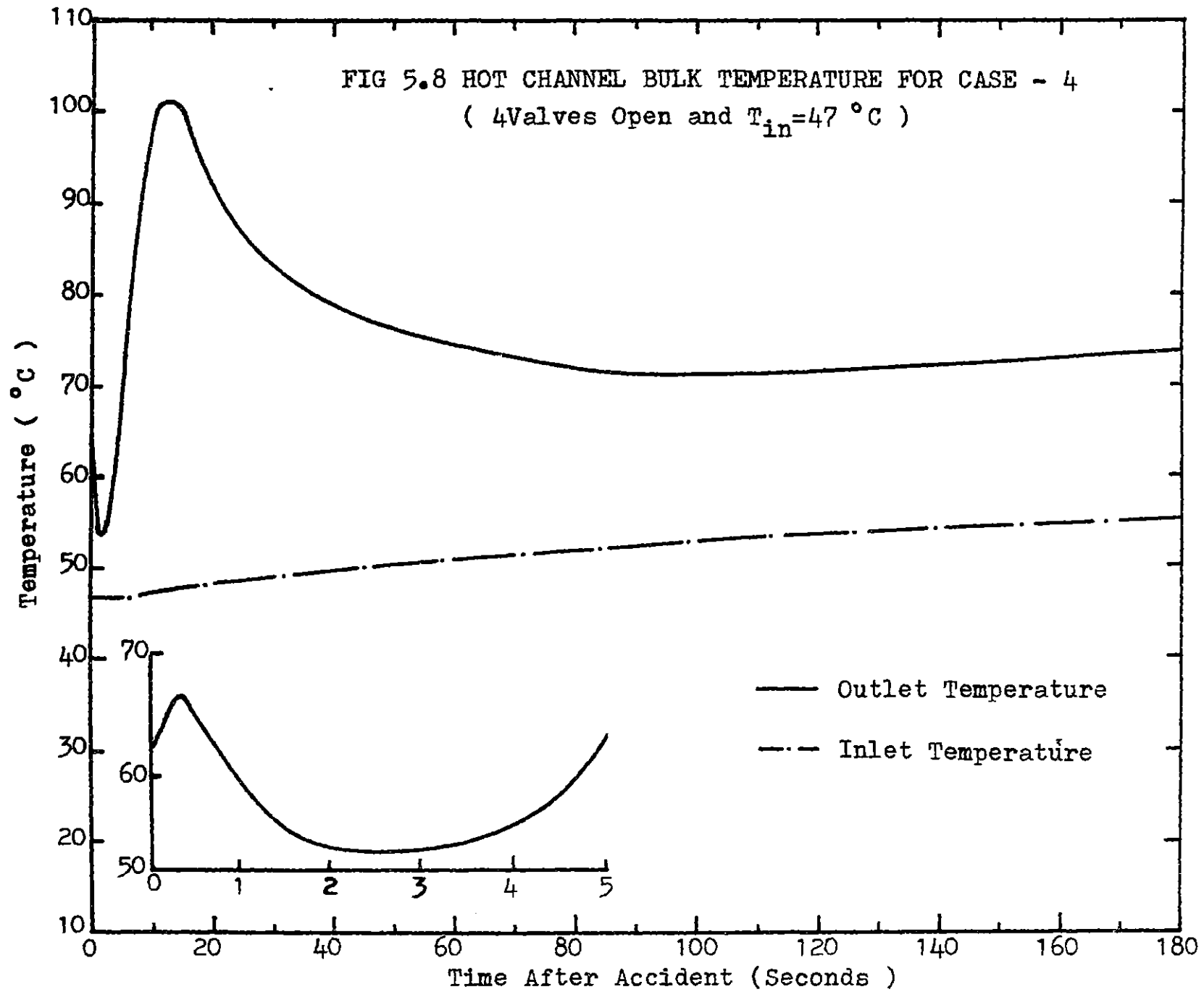
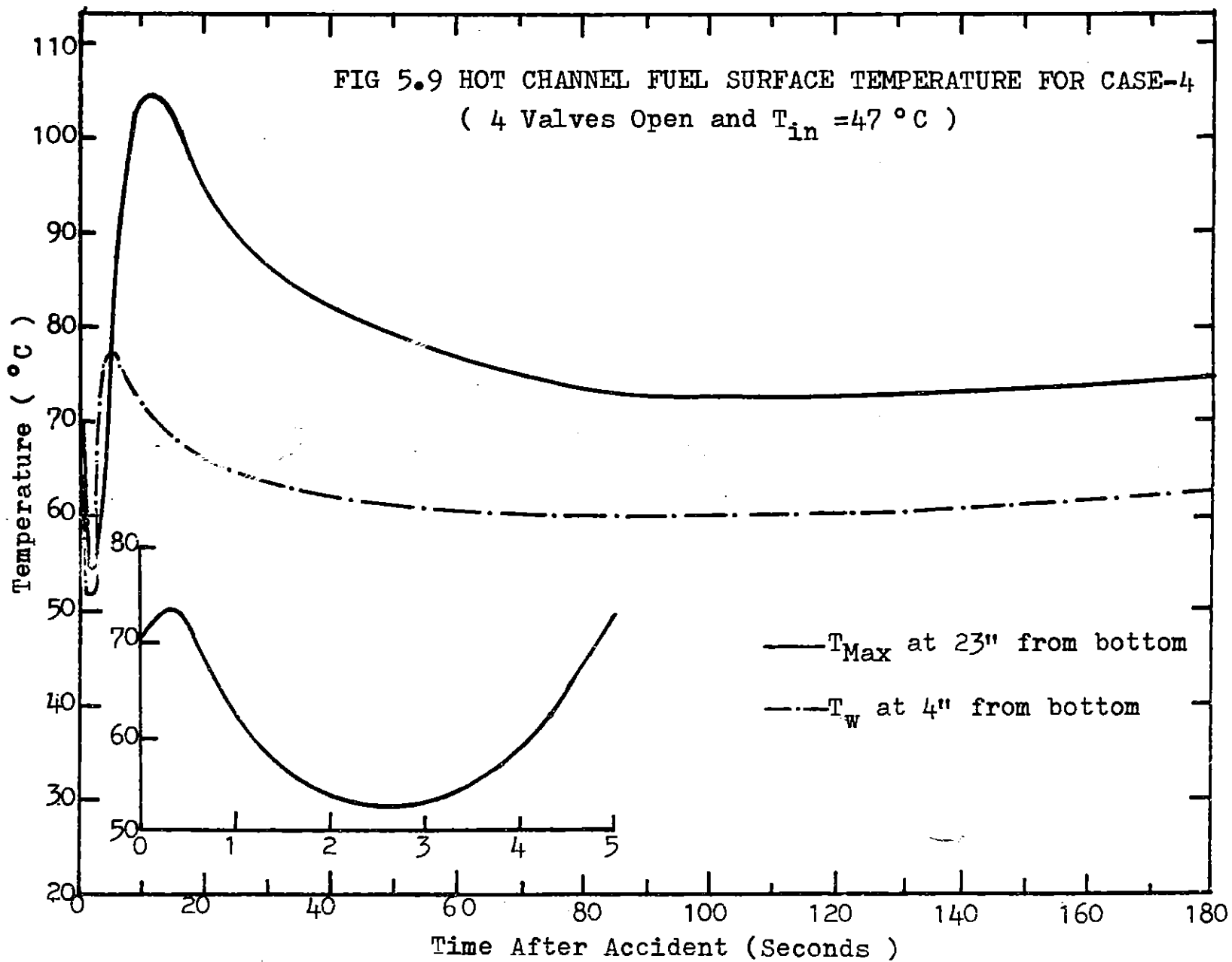


FIG 5.9 HOT CHANNEL FUEL SURFACE TEMPERATURE FOR CASE-4
(4 Valves Open and $T_{in} = 47^{\circ}C$)



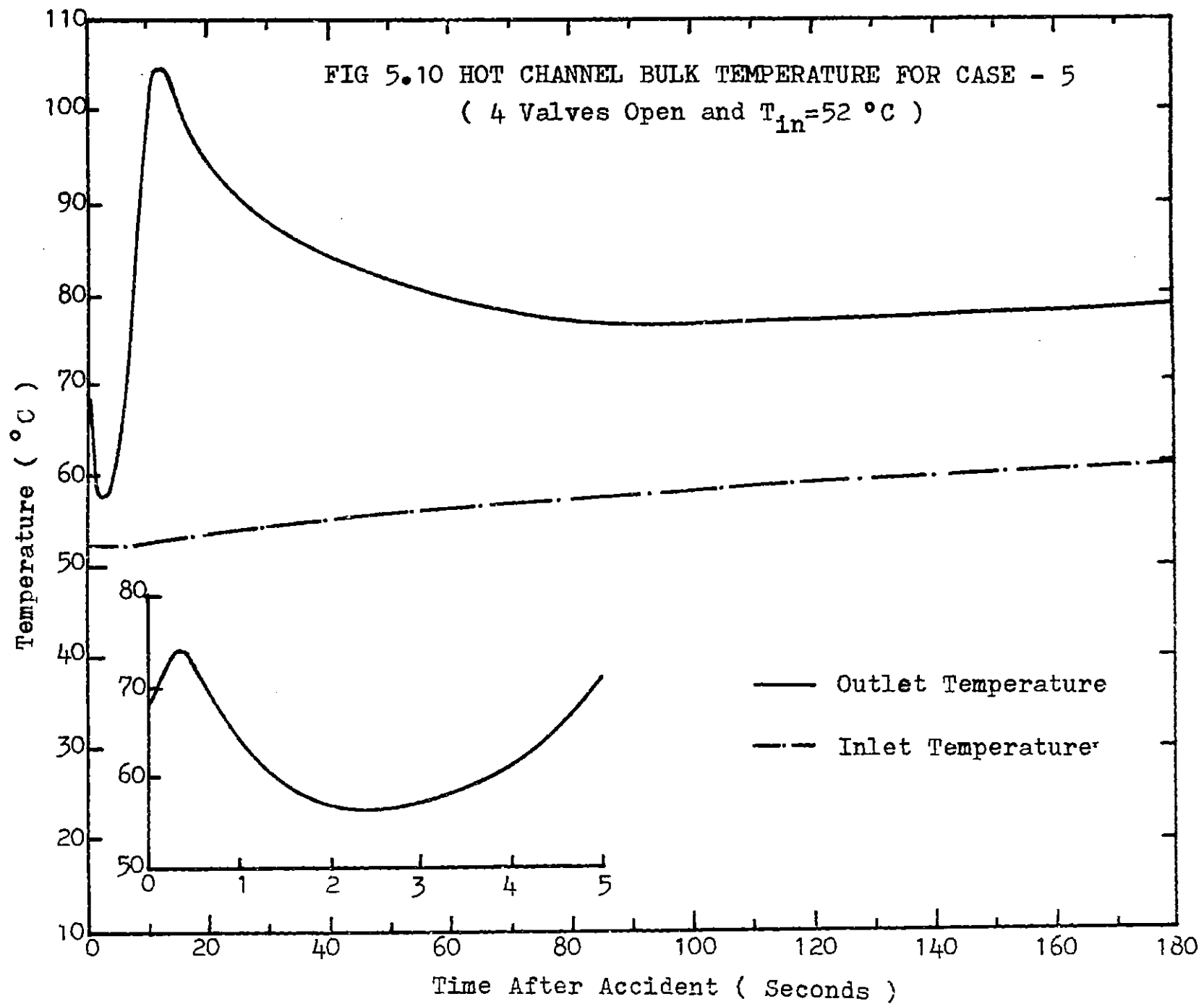
Figures 5.10 and 5.11 show the hot channel transient calculations for the core inlet temperature of 52°C which gives an average outlet temperature of 60°C for 5 MWth steady state power.

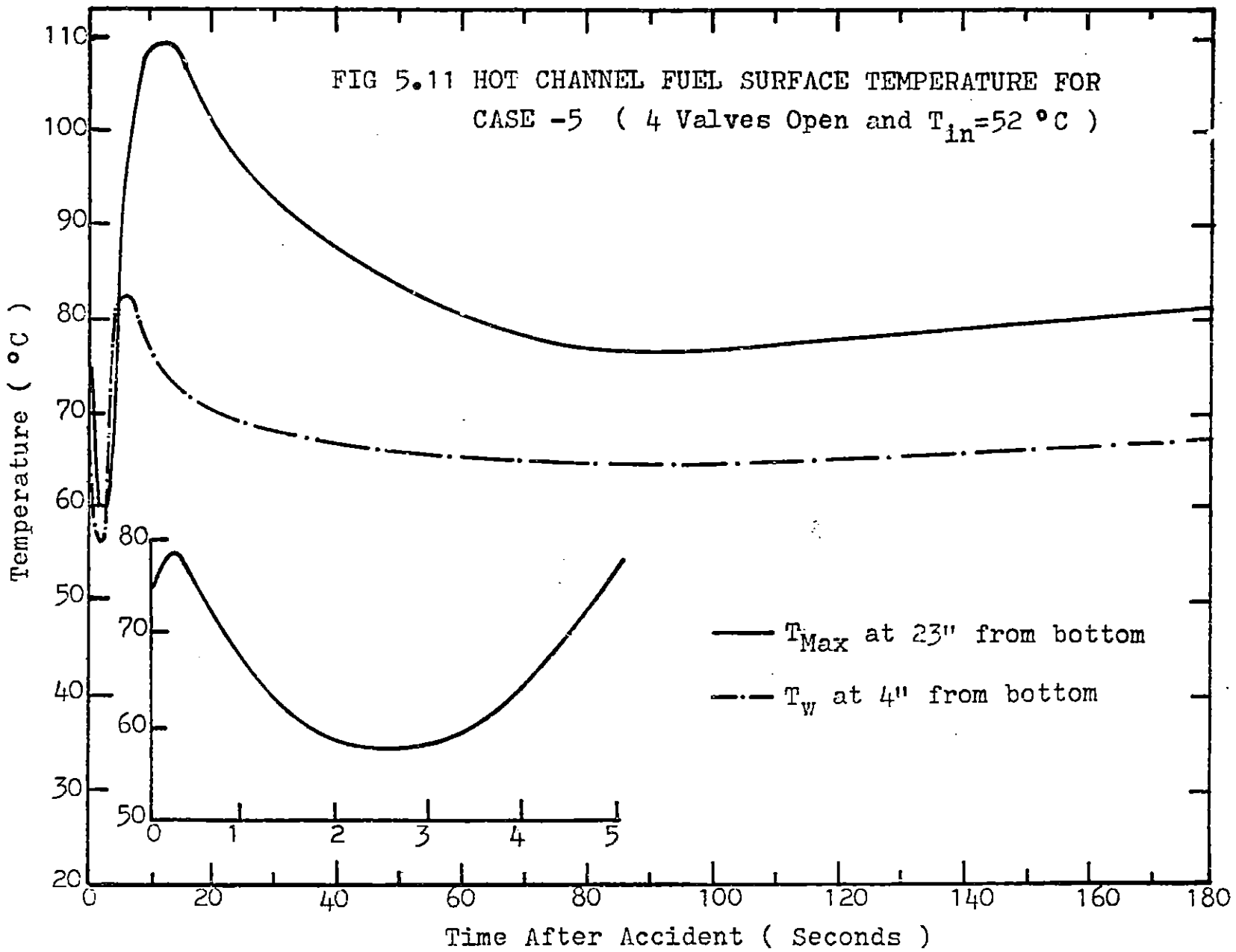
Although all the natural convection valves are open to flow, the fuel surface temperature exceeds saturation point for one inch at the top of the fuel plate. Figure 5.11 shows that the wall peak temperature occurs at about 10 seconds after the accident. It can be seen in Figure 5.12 that nucleation boiling starts at a height of 22 inches from the bottom of the fuel plate at a temperature of 106.2°C . The maximum fuel surface temperature, at this time, is 109.1°C which is at the top of the fuel plate.

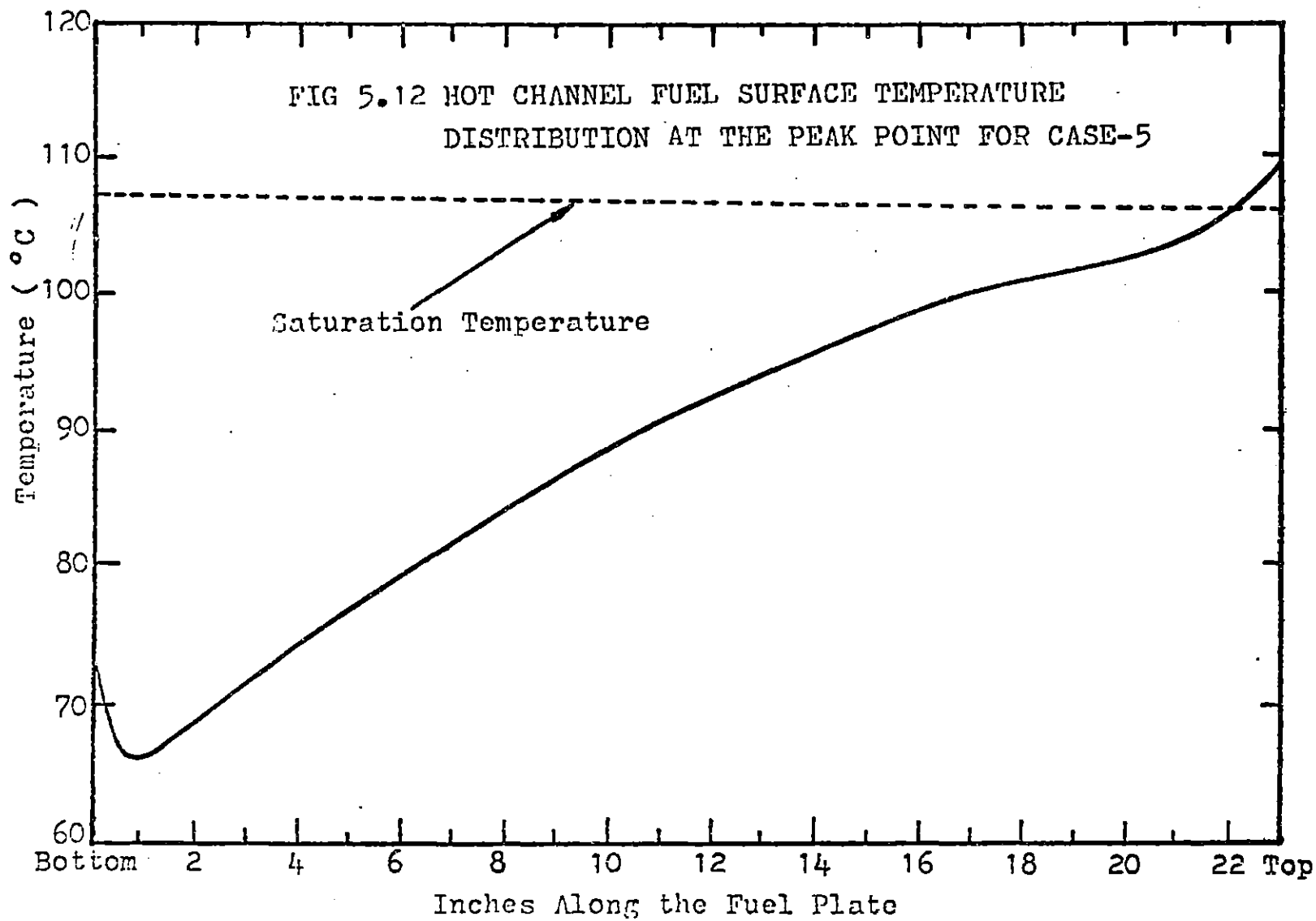
Boiling does not proceed in time and the wall temperature decreases rapidly due to exponential decay of the after scram heat generation.

The natural convection flow at the peak temperature is about 13.2 ($\text{lbm}/\text{ft}^2\text{sec.}$) which decreases with decay heat.

The slow increase in the fluid temperature due to natural convection flow reduction, leads to boiling approximately 21 minutes after the accident. Wall temperature reaches saturation a few minutes later, at 23.5 minutes after the loss of flow accident.







5.4 Steady State Operation with Natural Convective Cooling

The previous section analyzed natural convection and its efficiency during a loss of flow accident.

In order to measure the power removal capacity of the natural convective cooling system in MITR-II, a case will be considered of steady state low power (100 KWth) operation with no forced flow in the core.

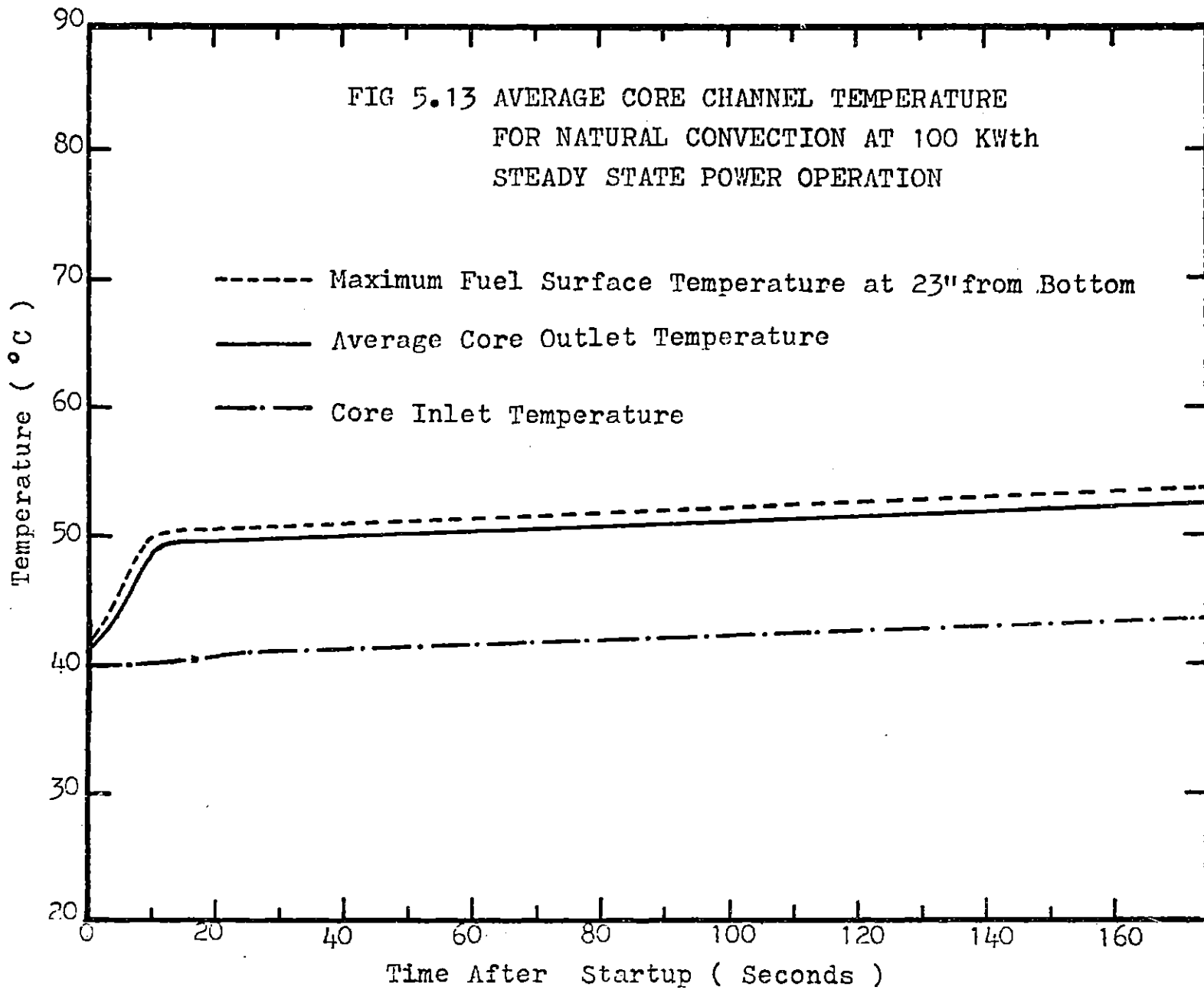
To be able to use Computer Code LOFA for this analysis, the initial conditions of a short term operation of 5 MWth is assumed in calculations. That is to say, it is supposed that the reactor was at full power long enough to give a containment tank mixed temperature equal to that of the core exit. Meanwhile, there was not a considerable decay heat buildup in the reactor prior to the test.

The reactor power, it is assumed, is lowered to 100 KWth at the same time that both primary pumps are stopped. Figure 5.13 shows the transient temperature calculation for average core power distribution. The rapid increase in the bulk and fuel surface temperature is due to pump coast-down. The natural convection flow rate increases to a maximum of 4.5 (lbm/ft.²sec.) about 9 seconds after the pumps are stopped. Thereafter it decreases with a very small slope (0.004 lbm/ft.²sec./sec.)

due to the temperature increase in the down comer.

From Figure 5.13 it can be predicted that boiling will begin on the surface at the top of the fuel plate about 49.5 minutes following the low power startup. Bulk boiling occurs one minute later at the top of the channel.

Although Figure 5.13 gives the transient temperature for average core distribution, the onset of nucleation boiling could be assumed to occur at the same time as in the hot channel. Figure 2.2 shows that the heat flux produced at the top of the average core channel is about 1.27 times that of the hot channel. This ratio is almost equal to the radial peaking factor for the hot channel. Therefore it can be assumed that nucleation boiling will occur at the same time in the hot channel as well as in the average core channel on the surface at the top of the fuel plate.



CHAPTER VI

CONCLUSION

6.1 Summary and Conclusion

The comparison between the computer code output and the startup natural convection test measurements for 5 MWth steady state power showed that single channel code LOFA could be used for transient hot channel calculations following a loss of flow accident.

The maximum temperature in the hot channel due to loss of flow accident will not exceed saturation during the first 58 minutes after the accident, even if one of the natural convection valves remains closed.

For the primary heat exchanger outlet temperature of 40°C, 5 MWth steady state power and 2000 gpm flow rate, bulk boiling will start at the top of the hot channel approximately 58 minutes following the accident, if all the natural convection valves are opened.

In the case that one valve remains closed, the hot channel fluid temperature increases immediately to 98°C, however boiling will not occur any sooner than 87 minutes after the accident. In this case natural convection flow goes to zero and then reaches

a maximum of 13 (lbm/ft.²sec.) at about 7 and 10 seconds respectively after loss of flow.

Boiling will occur about 10 seconds following the loss of flow accident, if two of the natural convection valves remain closed. Fuel surface temperature exceeds saturation point at a height of 12 inches from the bottom of the fuel plate. For steady state power of 5 MWth and core inlet temperature of 40°C, the driving force after pump coast-down is not enough to dominate the pressure drop in two of the incore check valves. Boiling starts before natural convection flow becomes large enough to remove the decay heat.

Changing the core outlet temperature to 55°C will not cause boiling immediately after loss of flow accident, if all the natural convection valves are opened to flow. The maximum bulk temperature occurs about 10 seconds after the accident and is 100°C which corresponds to a wall temperature of 104.5°C which is still below saturation.

The bulk boiling, for core inlet temperature 47°C at 5 MWth steady state power, begins approximately 27 minutes after the accident.

Increasing the core exit temperature scram set to 60°C will initiate boiling at the top of the fuel

plate about 10 seconds after loss of flow accident, even if all the natural convection valves are opened to flow. The fuel surface temperature exceeds saturation by a few degrees C on the uppermost one inch of the top of the fuel plate. This nucleation boiling disappears due to exponential decrease in the decay heat.

Bulk boiling will start about 21.7 minutes following the accident for 5 MWth steady state operation if the containment tank scram set is at 60°C and all the natural convection valves are opened.

It is noted that long term transient boiling occurs in the bulk fluid at the top of the hot channel rather than on the fuel surface due to small contribution of that part of the fuel to the decay heat production.

Natural convective cooling is able to remove the steady state low heat generation in the core as well as the decay heat after loss of flow accident. The MITR-II could be operated for about 49 minutes at a steady state power of 100 KW with no forced flow before nucleation boiling starts. The operating time may be increased by decreasing the containment tank temperature. The time interval is for steady state full power tank temperature.

Low power natural convection steady state operation leads to nucleation boiling on the fuel surface at the top of the fuel element.

6.2 Recommendations for Future Works

The natural convection analysis of the MITR-II was previously studied by D.Choi (Ref.1.1) and by A.Morales (Ref.2.5). The accidents were considered to be primary pumps failure and reactor inlet coolant pipe rupture, respectively.

The present work is one step closer to the final analysis of the problem. It has the capability of being used as a basis program for future works. The computer code LOFA is written for single channel calculations of the MITR-II during Loss of Flow Accident. This includes loss of primary coolant due to pump trip, reactor inlet pipe rupture, and failure in the electrical power to the main panel.

A suitable finite difference model is used to be able to consider the reverse flow in the case of multi-channel calculations. It is found that Explicit Cauchy Polygon Method which is used to integrate the energy equation is stable and applicable for both upflow and reverse flow in the core.

The method used for natural convection flow calculation, allows the coolant channel not to contribute to the flow circulation, partially or as a whole. This happens when the driving force is just enough to balance the friction pressure drop or when the flow oscillation or reversal is about to occur.

A two dimensional array is used for major thermal properties such as enthalpy, temperature, density, vapor quality, heat flux and mass flow rate. The dimensions are on axial mesh points and transient time after the accident. Variables J and I are used for space and time, respectively.

In order not to use too much memory of the computer for long term transient calculations, only 100 spaces are specified for I. The computer program locates the new 100 transient calculations in the past memory storage as they are evaluated. This could be reduced to 20 positions in the memory, but it was found that 100 was the best condition for the down comer temperature and density calculations.

A sensitivity analysis of the computer code showed that 25 mesh points should be taken along the fuel plate to yield the most stable enthalpy calculations. This corresponds to a mesh distance of one inch.

A third dimension could easily be added to the thermal properties to take into account the multi-channel effect. In other words a three-dimensional array could be used for transient variables to consider; time, axial position, and the corresponding channel location.

It is found in this work that bulk boiling occurs in the hot channel about 58 minutes following the loss of flow accident, even though all of the natural convection valves are opened to the flow. This requires two phase flow analysis for long term transient calculations. In Appendix D two phase flow parameters are suggested for future work.

A more detailed natural convection analysis of MITR-II could be made by combining the computer codes LOFA and COBRA-IV. COBRA-IV is capable of natural convection calculations if the pressure drop along the core or flow rate is given as input to the code. Since natural convection flow rate is governed by pressure drop along the core, neither one could be used as input to calculate the other one.

The computer code LOFA could be used to complete an iteration cycle with COBRA-IV. In other words, COBRA-IV can be used in stead of sub-program TRANS in LOFA for

transient calculations. The iteration cycle is completed in subroutine DOCO where the natural convection flow rate should be checked with the pressure drop along the loop.

Due to radial heat distribution in the core, pressure is not uniform at the top of the core in natural convection. To be able to use uniform pressure distribution in the computer code COBRA-IV, the height of the chimney could be added to the core length. This requires the cross flow calculations of COBRA-IV for the chimney, with zero heat generation, zero fuel thickness and water gap thickness equal to the fuel plate's.

This water gap allows cross flow between the nominal channels in the chimney due to density and pressure variation produced by different heat generations and different core channels.

APPENDIX A

COMPUTER CODE DESCRIPTION AND FLOW CHARTS

- A.1 Code Description
- A.2 Transient Pressure Drop in the Down Commer
- A.3 Transient Core Calculations
- A.4 Calculation of Core Entrance Properties

APPENDIX A

COMPUTER CODE DESCRIPTION AND FLOW CHARTS

A.1 Code Description

The Computer Code LOFA is written in FORTRAN and is able to follow the behavior of MITR-II after scram due to Loss of Flow Accident. It is capable therefore, of calculating the single channel steady state forced flow transient and natural convection.

Calculations start in Main program by evaluating the steady state operational conditions as is shown in Figure A.1.

Transient primary coolant mass velocity and pressure in the upper plenum is found in subroutine DOCO and the flow characteristic is decided and carried through by two factors NC and FFF. Positive values chosen by Natural Convection and Forced Flow Factor , NC and FFF respectively determine the domination of that flow.

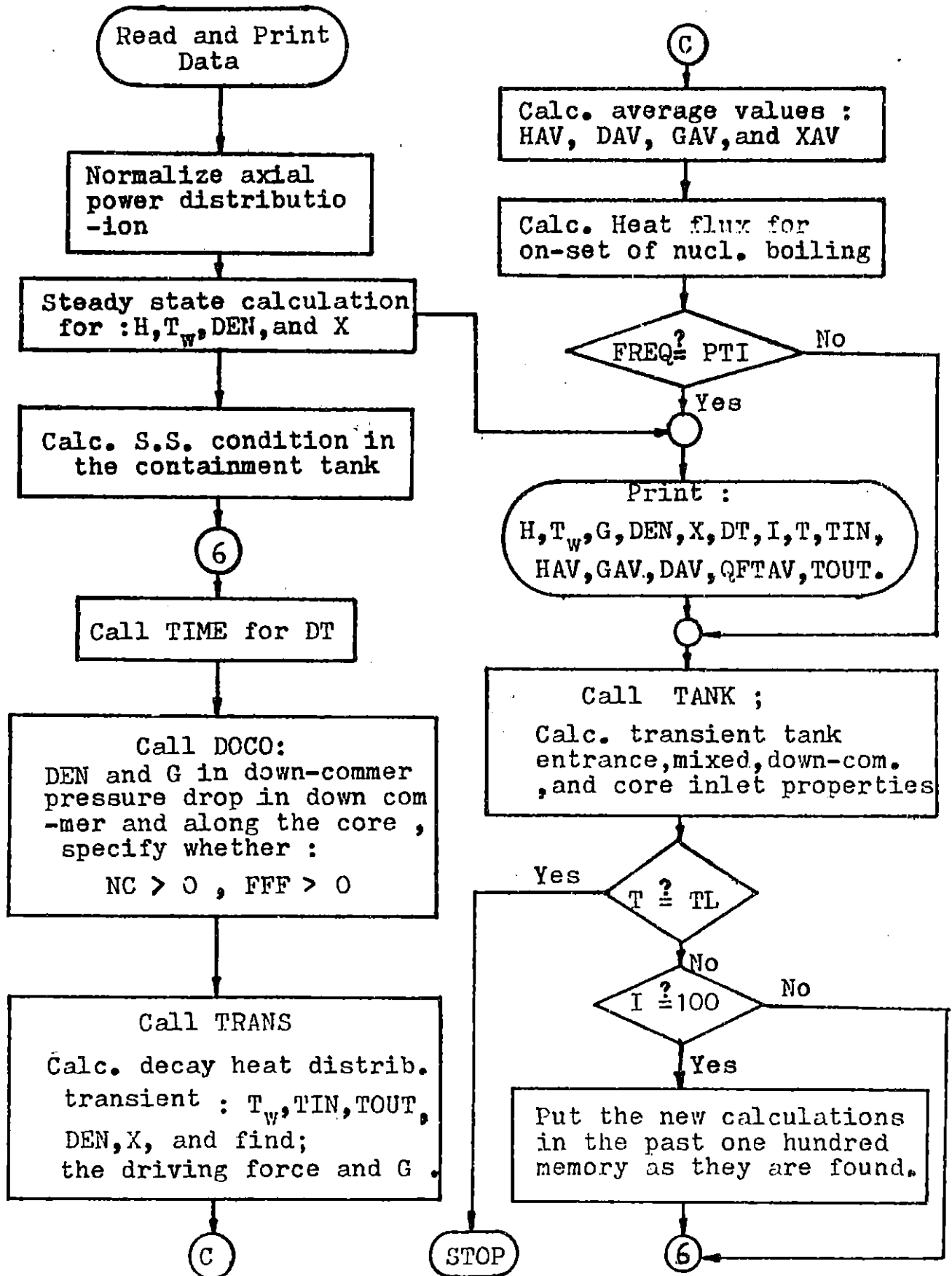
Transient thermal properties in the core are evaluated in subprogram TRANS and based on them, mass velocity is calculated.

Subroutine TANK calculates the containment tank mixed enthalpy and thermal properties at the core entrance.

Time step size is determined in subroutine TIME as the smallest time interval it takes for flow to sweep the corresponding mesh distance.

Subfunctions CP, VISCH and DENSH are used to tabulize constant pressure specific heat, absolute viscosity and density of water against enthalpy respectively.

FIG. A.1 Flow Diagram of MAIN Program



Heat Convection Coefficient is evaluated for different flow regimes in subprogram HCC as a function of enthalpy and mass velocity.

Function subprogram PDROP calculates pressure drop in the down comer for both forced flow and natural convective cooling.

Friction Coefficient is evaluated in Function FRIC for various flow cross sections, pipe as well as rectangular channels, for different flow regimes.

Average density in the down comer is found in subfunction DAVDC from containment tank mixed density and thermal properties in the lower plenum.

A.2 Transient Pressure Drop in the Down Comer

Starting with the steady state flow conditions at the main flow meter (MF-1), Figure 3.3, Coastdown Equation 2.1 and 2.2 give transient mass velocity and pressure at that point. Subroutine DOCO evaluates the pressure drop along the flow up to the upper plenum. The natural convection valve opens as soon as the static pressure at the top of the ball balances the hydraulic pressure at the bottom. When the ball drops there will be a pressure difference equal to the weight of the ball which causes upflow through the valve, until the driving force becomes zero due to flow coastdown.

The reverse flow in the natural convective valve can be found from conservation of mass and momentum through the valve:

$$G_{rv}^2 + G_{dc}^2 - G_{en}^2 + 2\rho g_c (P_{up} + \Delta P_{rv}) = 0 \quad (A.1)$$

$$A_{rv} G_{rv} + A_{dc} G_{dc} = A_{en} G_{en} \quad (A.2)$$

where

G is the mass velocity (lbm/sq.ft./sec.)

P_{up} is the pressure in the upper plenum at the time of opening

P_{rv} is the pressure drop in the valve due to reverse flow

$\Delta P_{rv} = K_{rv} G_{rv}^2 / 2\rho g_c$, with K being the form factor for reverse flow,

A is the flow cross sectional area,

ρ is the density of water (lbm/cu.ft.),

g_c is the conversion factor (32.2 lbm.ft./lb_f.sec.²),

and subscript rv , en , and dc refer to reverse flow, upper plenum entrance and down comer respectively. It is assumed that pressure at the bottom of the natural convection valve is equal to that of the entrance of the down comer. Solving Equations A.1 and A.2 simultaneously gives the upflow in the natural convection valve and mass velocity in the down comer right after the valves open.

Subroutine DOCO is shown as flow diagram in Figure A.2 to solve Equations A.1 and A.2. It also determines, after the valve opens, when natural convection will occur. The values for natural convection and forced flow factors, NC and FFF , discussed earlier in this chapter are also determined in this subprogram.

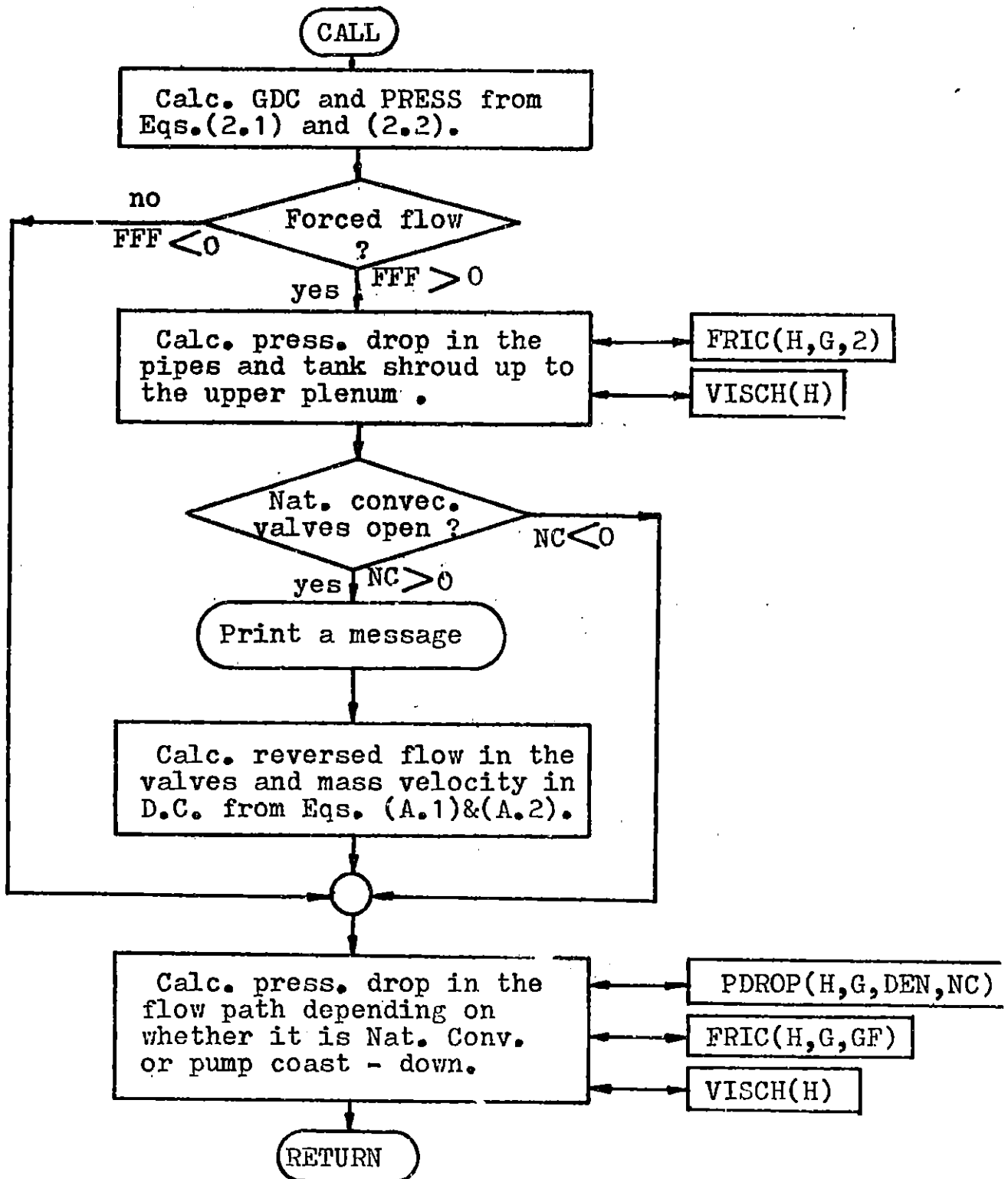


FIG. A.2 Flow Diagram of Subprogram DOCO

A.3 Transient Core Calculations

Decay heat generation is evaluated based on Equations 2.5, 2.7, 2.8 and 2.10 for delayed neutrons, delayed photoneutrons, fission products and activated core materials respectively. Transient core calculations are done in subroutine TRANS, whose flow diagram is shown in Figure A.3.

As discussed before, natural convection flow depends on the pressure drop in the loop as well as the driving force which is the density difference between down-flow and up-flow. These forces might balance and as a result there will be no flow in the loop for a while until the density in the core reduces due to release of decay heat into the water.

Another reason for no flow in the core is when flow reversal happens. For a short period of time there is no flow in the loop until one of the forces dominates and the fluid goes in that direction. Reverse flow is not included in the computer program, but to be conservative, its effect is considered in subprogram TRANS. In the case of reversed flow, the fluid is assumed to be stationary and transient calculations are performed in the direction of the reversed flow. In this case the core inlet properties are assumed to be those right at the top of the core, namely core outlet characteristics in the past time intervals. This yields more conservative values for core calculations and also makes the computer code more suitable for reverse flow transients.

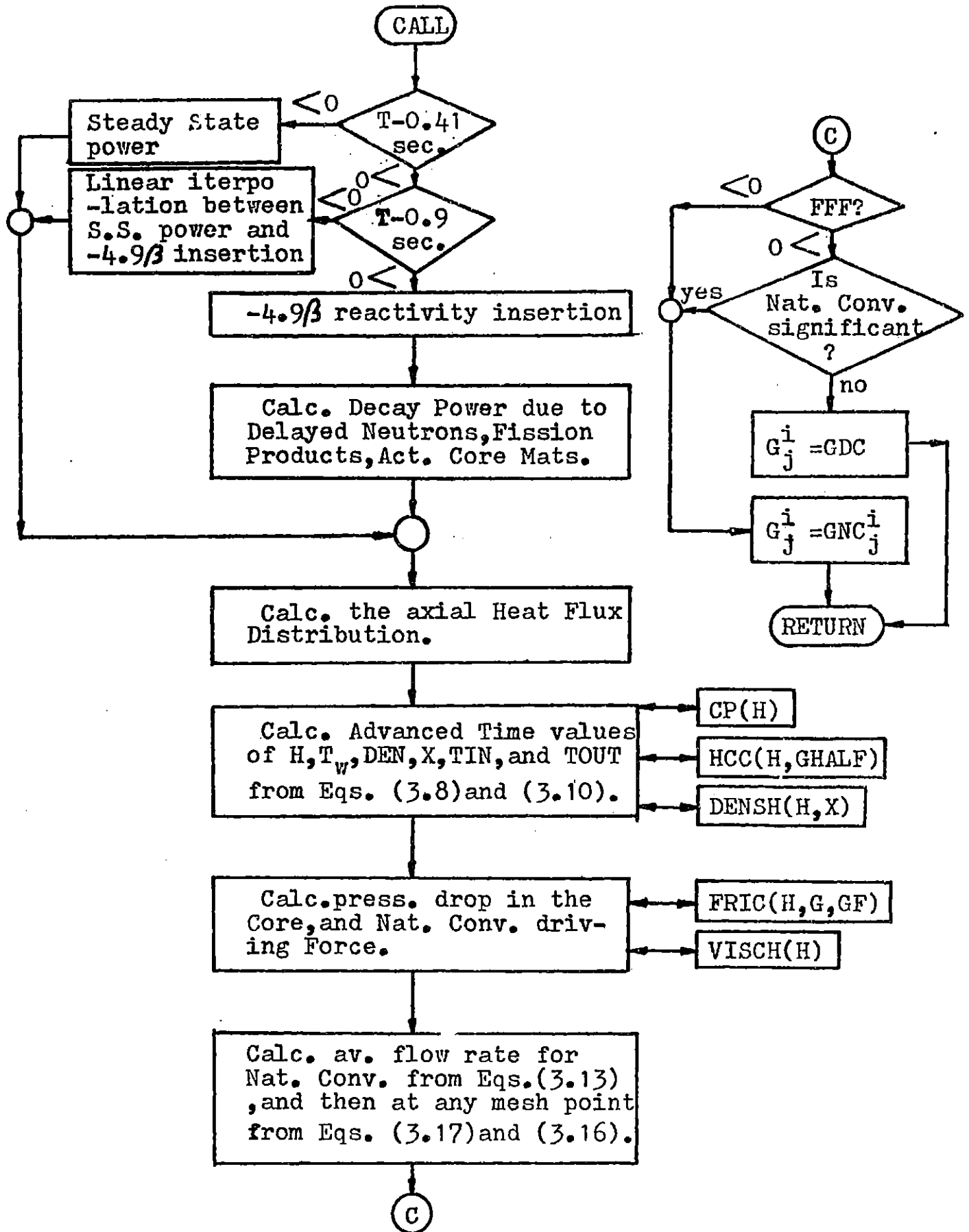


FIG. A.3 Flow Diagram of Subprogram TRANS

At any advanced time interval, t^{i+1} , average natural convective coolant flow is evaluated from Equation 3.13 by using thermal properties at time (i+1) and then corresponding mass velocity for each mesh point is calculated from Equations 3.17 and 3.16 as was shown in Figure 3.1. If the calculated flow is negative, which means that the flow is reversed the mass velocity is presumed to be zero or 0.0001 lbm/sq.ft./sec..

Logic START is used in this subprogram to specify the start of natural convection only. As soon as natural convection flow dominates, START picks positive values.

A.4 Calculation of Core Entrance Properties

Using Characteristic Method for enthalpy calculation, needs the core entrance enthalpy to be evaluated from the loop properties. Subroutine TANK is written to find the enthalpy and density of water in the lower plenum at any time to proceed the core calculations. Figure A.4 shows the Subprogram TANK.

In transient forced flow, neglecting the friction power transmission, the core entrance properties are the same as the heat exchangers outlet.

When natural convection starts, the relatively cold water in the down comer is removed by the hot water coming down the chimney

through the natural convection valves. At any time interval the amount of water entering the core is the same as that moving down from the containment tank into the chimney.

Stepwise enthalpy rise is considered for the tank mix calculations. A volume of $VF(L)$ is assumed to enter the down flow path at some mixed tank enthalpy of $HVF(L)$. This volume is moved down at constant temperature, by some amount of water $VF(L+1)$ entering in the next time interval with some temperature. This continues until $VF(L)$ reaches the lower plenum and enters the core gradually by natural convection. Depending on the flow rate, the temperature of the water entering the core is constant for a while until the next constant temperature volume of water reaches the lower plenum.

The amount of time it takes for any amount of water to reach the lower plenum is calculated from the down flow path volume, namely the volume between the containment tank and the chimney, $VCHY$, and the down comer volumes, VDC .

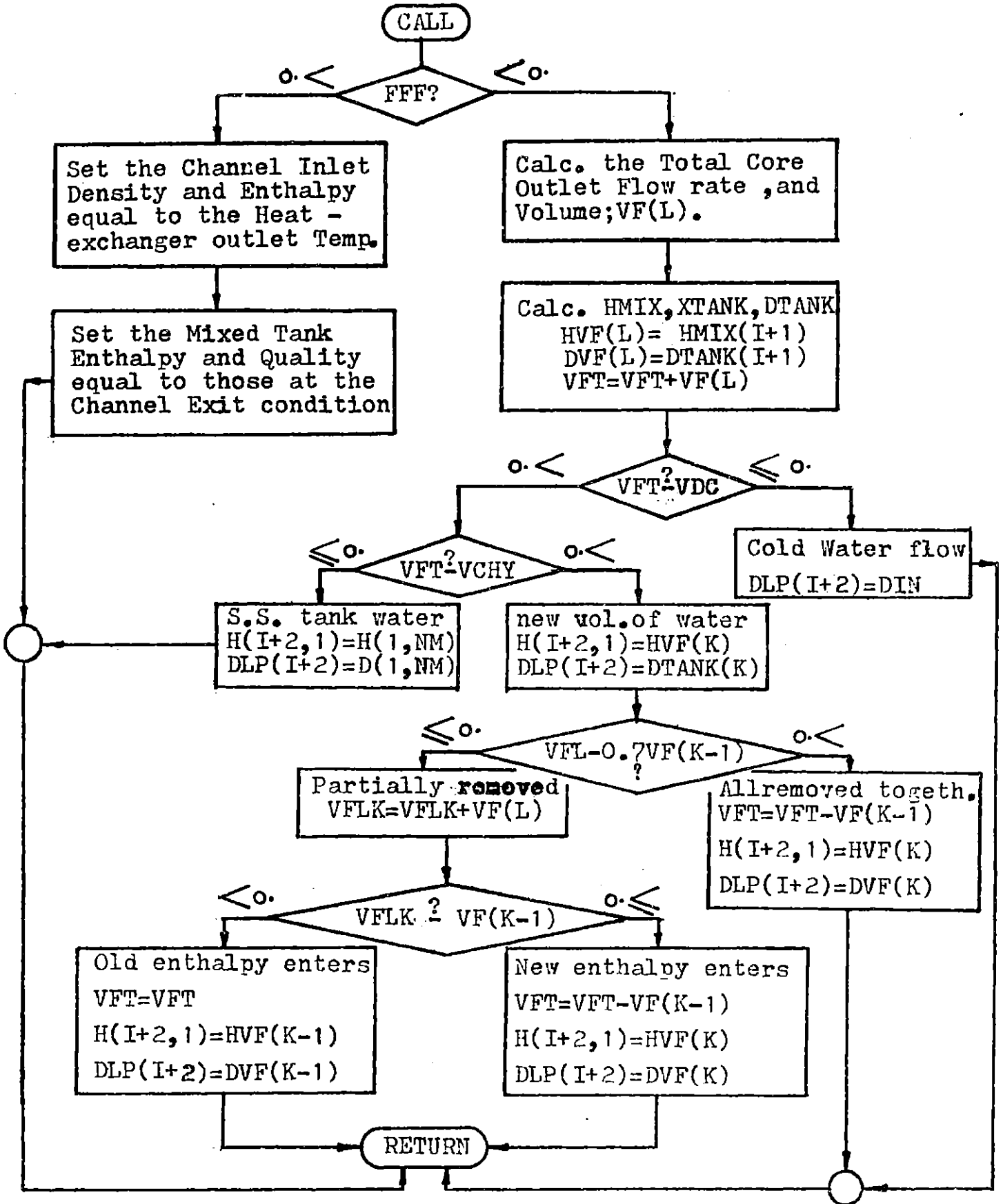


FIG . A.4 Flow Diagram of Subprogram TANK

APPENDIX B

B.1 Input Data Cards

B.2 Nomenclature to the Computer Code LOFA

Input Data Cards

<u>Card No.</u>	<u>Variable</u>	<u>Format and Explanation</u>
CARD 1		219,3F9.0
	NM	Number of axial mesh points, considering the first one to be in the lower plenum.
	NOV	Number of Natural Convection Valves open to the flow.
	TL	Time Limit for transient calculations, (sec.)
	PTI	Printing Time Interval, every PTI calculation will be printed in output.
	CHN	Total Number of heated channels in the core.
	CDT	Coast-down time which is from pump trip to zero flow of primary pumps, (seconds).
	DTS	Specified time intervals for transient calculations. This will be compared with time intervals determined in subroutine TIME and the minimum will be chosen, (seconds).
	ZL	Total axial length of fuel plates (heated and unheated), (ft.).

<u>Card No.</u>	<u>Variable</u>	<u>Format and Explanation</u>
CARD 2		7E9.5
	THMW	Thermal power of the reactor before scram, (MWth).
	GPM	Total primary flow rate of the reactor before scram, (gpm).
	HIN	Steady state enthalpy at the entrance of the core, (Btu/lbm).
	PIN	Total steady state pressure of the primary coolant measured at the nozzle MF-1, (psia).
	THE	Primary Heat Exchanger outlet temperature, (°C).
	SPV	Primary Heat Exchanger outlet specific volume, (ft. ³ /lbm).
	CPP	Primary Heat Exchanger outlet specific heat capacity at constant pressure, (Btu/lb°F).

<u>Card No.</u>	<u>Variable</u>	<u>Format and Explanation</u>
CARD 3		7E9.5
	HSAT	Saturation liquid enthalpy at the core exit pressure, (Btu/lbm).
	HFG	Latent heat of evaporatiOn of water at the core exit pressure, (Btu/lbm).
	RO	Total negative reactivity insertion, ($\Delta K/K$).
	BEFF	Effective total delayed neutrons fraction, (Beff).
	GAMA	Fraction of heat generated directly in the coolant.
	FR	Radial peaking factor.
	VTANK	Volume of the water in the containment tank, above the core.
CARD 4		6E9.5
	GA,GB, GC,GD	Constants which determine the curve fit to the flow as a function of time after pump coastdown; $G(t)=(GIN) \left[GA/\exp (GB)t + (GC) t-(GD) \right]$.
	PA,PB	Constants which determine pressure as a function of time after pump coastdown $PRESS(t)=(PIN) \left[(PA)t+1 / (PB)t+1 \right]$.

<u>Card No.</u>	<u>Variable</u>	<u>Format and Explanation</u>
CARD 5		8E9.5
	DSL	Hydraulic diameter of the shroud (shown* by cross section A_3), (ft.).
	DP	Primary coolant pipe diameter between nozzle MF-1 and the entrance to the reactor tank (shown as A_1), (ft.).
	DDC	Down Commer hydraulic diameter (shown as A_4), (ft.).
	DSA	Hydraulic diameter for the upper part of the reactor tank (shown as A_2), (ft.).
	DBL	Natural convection ball diameter (ft.).
	DCH	Core flow channel equivalent diameter(ft.).
	DCL	Down Coming flow passway length which is the summation of the height of the chimney, natural convection valve, and the down commer itself,(ft.).
	BP	Base perimeter of the coolant channel used in fin effectiveness calculation, (ft.).

* It is referred to Figure B.1

<u>Card No.</u>	<u>Variable</u>	<u>Format and Explanation</u>
CARD 6		8E9.5
	AP	Cross sectional area of the primary coolant pipe to the reactor, (ft ²).
	ASH	Reactor tank upper part flow pass (shown as A ₂), (ft ²).
	ASHL	Flow pass cross sectional area for the shroud (shown as A ₃), (ft ²).
	AUP	Upper plenum average cross sectional area (shown as A ₆), (ft ²) *.
	AVI	Natural convection valve inlet flow area (ft ²).
	AVO	Natural convection valve outlet flow area (ft ²).
	ACH	Core coolant channel flow area, (ft ²).
	AENT	Upper plenum entrance cross sectional area (shown as A ₅), (ft ²) *.

* These values are used for expansion pressure drop in the upper plenum

<u>Card No.</u>	<u>Variable</u>	<u>Format and Explanation</u>
CARD 7		8E9.5
	FKN	Friction coefficient for primary coolant pipe knee bends,(dimensionless).
	FKO	Orifice friction coefficient for flow meter MF-1.
	FKP	Primary coolant pipe surface friction coefficient.
	FKS	Shock friction coefficient for area change in reactor tank (shown as point P_3).
	FKD	Shock friction coefficient for flow entering the upper plenum,(shown as point P_4).
	FEN	Core entrance form coefficient.
	FKV	Form coefficient for the natural convection valve(down flow).
	FKR	Form coefficient for the natural convection valve (up flow).

<u>Card No.</u>	<u>Variable</u>	<u>Format and Explanation</u>
CARD 8		8E9.5
	HTK	Height of water in the tank above the natural convection valve,(ft.).
	HV	Height of the natural convection valve(ft.
	HC	Core height which includes fuel plate and endings,(ft.).
	HSU	Vertical height of the upper part of the reactor tank (shown as P_2P_3),(ft.).
	HSL	Vertical height of the shroud (shown as P_3P_4),(ft.).
	HLP	The length of the primary coolant pipeline from the Main flow meter (MF-1) to the reactor entrance (shown as P_1P_2),(ft.)
	HPI	Vertical height of the reactor entrance to the center line of the main flow meter (shown as H_0H_1),(ft.)
	CHYH	Total height of the chimney,(ft.).

<u>Card No.</u>	<u>Variable</u>	<u>Format and Explanation</u>
CARD 9		8E9.5
	HCH	Core coolant channel half width,(ft.).
	WFIN	Width of the fin(ft.).
	HFIN	Height of the fin,(ft.).
	FEX	Form coefficient of the core channel exit, (dimensionless).
	FKUP	Form coefficient at the exit of the natural convection valve to the upper plenum per unit area ratio.*
	AUC	Down comer flow cross sectional area, (ft. ²).
	ALK	Aluminum thermal conductivity used for fuel cladding, (Btu/ft.sec. ^o F).
	RSS	Stainless steel density used for natural convection valve,(lbm/ft. ³).

* Depending on how many valves are opened to flow, the total form coefficient is found as follows:

$$K=(1-FKUP \cdot AVO \cdot NOV / AUP)$$

<u>Card No.</u>	<u>Variable</u>	<u>Format and Explanation</u>
CARD 10		8E9.5
	HFGTK	Latent heat of evaporation of water at the average containment tank pressure, (Btu/lbm).
	HSATK	Saturation enthalpy of water at the average containment tank pressure, (Btu/lbm).
	VDC	Total volume of the down comer from the upper plenum to the lower plenum, (cu.ft.).
	VCHY	Total volume of the water between the chimney and the shroud, (cu.ft.).
	VG	Specific volume of saturated vapor at the core exit pressure, (cu.ft./lbm).
	VF	Specific volume of the saturated water at the core exit pressure, (cu.ft./lbm).
	TCF	Thermal conductivity of water at the average core pressure, (Btu/sec./ft./°F).
	CHNT	Total number of channels, heated plus unheated in the core.

<u>Card No.</u>	<u>Variable</u>	<u>Format and Explanation</u>
CARD 11		12F6.2 The number of input cards is equal to NM/12
	FQZ	Axial power distribution in the steady state condition. It does not need to be normalized because normalization will be performed in the code. Each valve should show the relative power at the mesh point starting from the lowest point of the fuel plate.
CARD 12		2F8.6 six cards for decay precursors
	BI,DLI	β_i and λ_i in Equation 2.5, namely delayed neutron yield and decay constant of the i th precursor.
CARD 13		2F10.8 eight cards for delayed photoneutrons
	Y,AL	γ_j and λ_j in Equation 2.7, i.e. the total number of photoneutrons and the decay constant of group j per fission of U-235

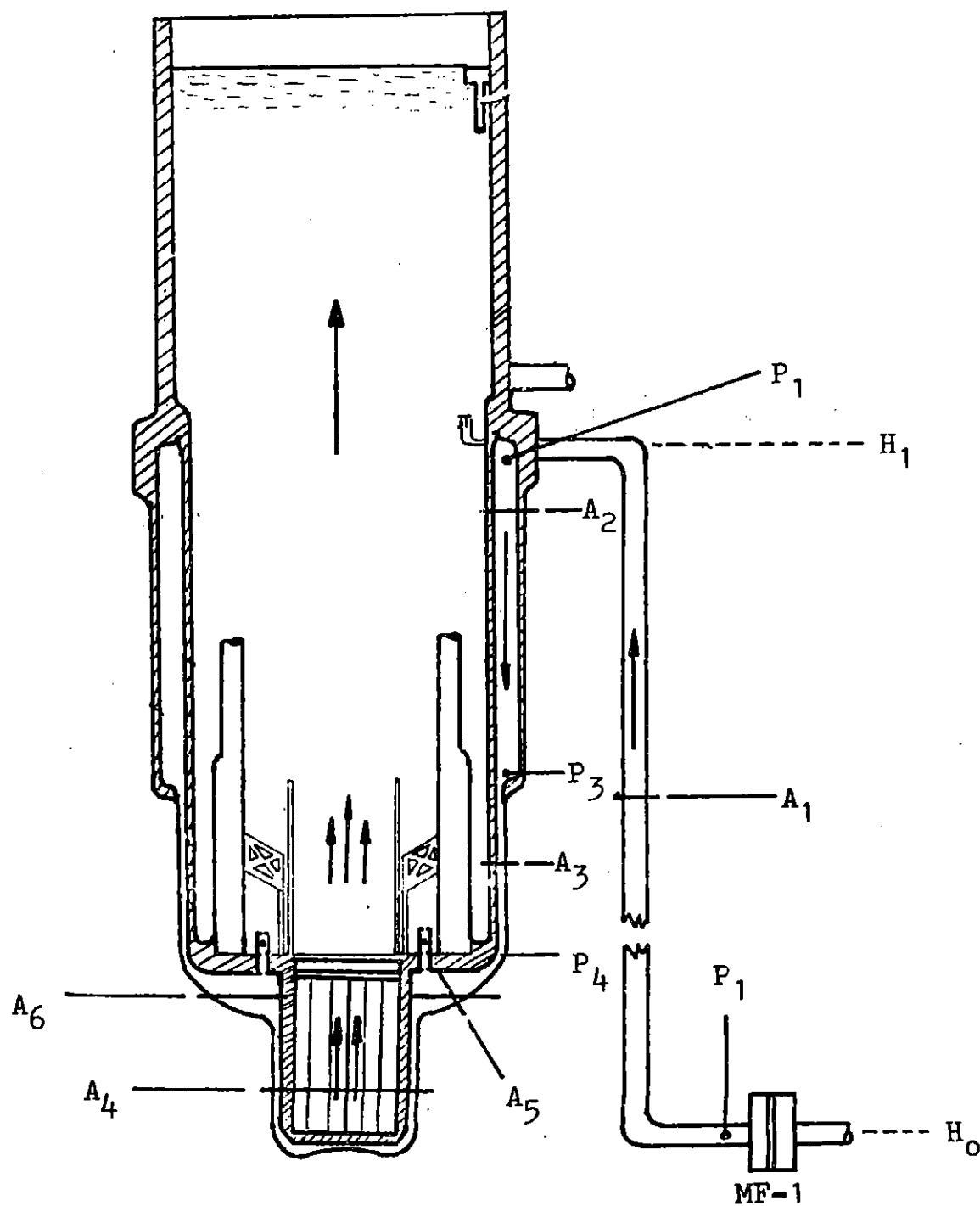


FIG . B-1

Nomenclature to the Computer Code LOFA

Throughout the computer program, the following parameters are used as defined below:

<u>Parameter</u>	<u>Description</u>
I	An array of hundreds of vectors to show time steps.
J	An array of NM vectors for mesh point.
POWER	Steady state thermal power, Btu/sec.
PRMTR	Parameter used in fin efficiency = $\frac{2(\text{HFIN} + \text{WFIN}/2)}{\text{ALK} \times \text{WFIN}}$
GIN	Steady state flow rate, lbm/ft. ² /sec.
GSCR	Scram set flow rate, lbm/ft. ² /sec.
DZ	Axial mesh distance, ft.
HWV=HTK	Height of water in the tank above the core equal to the height of the tank, ft.
FQZA(j)	Percentage of axial power produced at mesh point j, 1/ft.
QZF(j)	Axial power generated per unit length at mesh point j, Btu/ft/sec.
H(I,j)	Enthalpy at mesh point j at time I, Btu/lbm.

<u>Parameter</u>	<u>Description</u>
TW(I,J)	Wall temperature at mesh point J at time I, (°F).
X(I,J)	Steam quality at mesh point J at time I.
DEN(I,J)	Density at mesh point J at time I (lbm/ft. ³ .)
G(I,J)	Flow rate at mesh point J at time I (lbm/ft. ² /sec.)
T	Time passed after scram, (sec.)
QZAV	Average axial power deposited in the coolant between two mesh points per unit length, (Btu/ft./sec.).
RENO	Reynold's number.
HCCA	Convection heat coefficient in steady state power calculation, (Btu/ft. ² /sec./°F).
ETHA	Fin effectiveness defined in Equation 3.24.
P	Effective perimeter of finned fuel plate, (ft.).
QFAV	Average power flux deposited in the coolant between two mesh points, (Btu/ft. ² /sec.).
TIN	Core inlet coolant temperature, (°C).
TOUT	Core outlet coolant temperature, (°C).

<u>Parameter</u>	<u>Description</u>
DTANK(I)	Containment tank average density, (lbm/ft. ³).
T	Time passed after reactor scram, (sec).
DT	Time interval calculated in subroutine TIME from flow speed for transient calculation, (sec.).
HAV(I)	Average enthalpy, (Btu/lbm), flow rate, (lbm/ft. ² /sec.), and density, (lbm/ft. ³), respectively, over the core length at time step I.
GAV(I)	
DAV(I)	
PJ	Absolute pressure at mesh point J, (psia).
TSAT	Saturation temperature at mesh point J, (°F).
QONB	Heat flux for the onset of nucleation boiling, Equation 3.20, (Btu/sec./ft. ²).
HAVR=HAVP	Average enthalpy, (Btu/lbm), flow rate, (lbm/ft. ² /sec.), and density, (lbm/ft. ³), respectively over the length of the core in previous time interval.
GAVR=GAVP	
DAVR=DAVP	
HP(I,J)	Enthalpy, (Btu/lbm), flow rate, (lbm/ft. ² /sec.), and density, (lbm/ft. ³), respectively at mesh point J at previous time step I.
GP(I,J)	
DENP(I,J)	
HTAV	Average containment tank enthalpy, (Btu/lbm), flow rate, (lbm/ft. ² /sec.), and density, (lbm/ft. ³), respectively.
GTAV	
DTAV	

<u>Parameter</u>	<u>Description</u>
FREQ	Frequency of printing interval, computer calculation will be printed out whenever this variable becomes equal to PTI,(input).
DTP	Time interval calculated in the past time step, (sec.).
DELT(J)	Time interval it takes for flow rate to sweep the mesh distance J, J-1.
REF	Reference number, some large number used in subroutine TIME for comparison in order to find the minimum time interval, (sec.).
DTC	Minimum time interval it takes for flow to sweep some mesh distance. This value will be compared with the input time interval, (DTS)and the smaller value will be chosen, (sec.).
FKVO, FKVR	Total friction coefficient calcula ed for the number of natural convection valves open to the flow for downflow and reverseflow.
AVIN, AVOO	Total area open to natural convection at the top (inlet) and at the bottom (outlet) of natural convection valves respectively, (ft. ²).
GDC	Down commers flow rate in pump coast down, (forced flow), (lbm/ft. ² /sec.).

<u>Parameter</u>	<u>Description</u>
PRESS	Absolute pressure in pump coastdown at any time T, (lbf/ft. ²).
GDCP	Value of GDC in past time interval.
NC	Logic used for natural convection, it is positive whenever natural convection valves are open and negative when they are closed.
FFF	Forced Flow Factor, a logic which has a positive value when natural convection flow is dominant and it is negative when the flow is forced by a pump.
DPFP	Friction pressure drop in leading pipes, shroud of the containment tank, and down commers respectively, (lbf/ft. ²).
DPFS	
DPFD	
DPSP	Shock pressure drop due to area changes in leading pipes and shroud respectively, (lbf/ft. ²).
DPSS	
DPAS	Spacial acceleration drop to the upper plenum, (lbf/ft. ²).
DPEP	Pressure drop due to elevation in leading pipes and the shroud respectively, (lbf/ft. ²).
DPES	
PHV	Absolute pressure at the top of natural convection valves, (atmospheric plus height of water), (lbf/ft. ²).
PBAL	Pressure due to weight of natural convection balls, (lbf/ft. ²)

<u>Parameter</u>	<u>Description</u>
AA, BB, RAD, CC	Parameters used to calculate the upflow in the natural convection valves right after opening, if there is any.
GD1, GD2	Calculated values of flow rate which might upflow through the natural convection valves, ($\text{lbm}/\text{ft.}^2/\text{sec.}$)
GV, GD	Flow rate departed up into the natural convection valve as reverse flow, and down into the down comer right after opening, respectively, ($\text{lbm}/\text{ft.}^2/\text{sec.}$).
DPV	Friction pressure drop in natural convection valves due to reverse flow (upflow), ($\text{lbf}/\text{ft.}^2$).
DPDC	Total pressure drop in the down comer as far as core inlet, ($\text{lbf}/\text{ft.}^2$).
QACT	Heat generated due to activated core material, ($\text{Btu}/\text{sec.}$).
QDN	Energy reduced by delayed neutrons, ($\text{Btu}/\text{sec.}$).

<u>Parameter</u>	<u>Description</u>
QFP	Heat released from fission products after scram, (Btu/sec.).
Q	Total energy produced after the scram per unit time, (Btu/sec.).
QZT (I,J)	Decay power produced at time step I and mesh point J per unit length (Btu/ft. sec.).
GHALF, DHALF	Average flow rate over two mesh points, (lbm/ft. ² /sec.) and (lbm/ft. ³)
QZTAV	Average decay power deposited in the coolant per unit length, (Btu/ft./sec.).
QFTAV	Average effective decay power flux deposited in the coolant, (Btu/ft. ² /sec.).
ALFA	Dimensionless factor used in transient enthalpy calculation $= \frac{G \times T}{P \times Z}$
FFR	Average friction pressure drop in the core, (lbf/ft. ²).
FSH	Shock pressure drop due to area changes at the inlet and outlet of the core, (lbf/ft. ²).
FSA	Spacial acceleration pressure drop in the core, (lbf/ft. ²).

<u>Parameter</u>	<u>Description</u>
DFDEN	Pressure difference between the down comer and core due to density difference, (lbf/ft. ²).
DFCHY	Pressure difference between the two legs of the loop because of density difference in the chimney and the containment tank, (lbf/ft. ²).
DH, DDEN	Enthalpy and density difference between two succeeding mesh points.
AAV	Dimensionless factor used to calculate flow rate, $AAV = \frac{\frac{DDEN}{DH} + DH}{DENA V}$
AAL	λ , defined in Equation 3.15.
BAV	β , defined in Equation 3.15.
DD	δ , defined in Equation 3.16.
GG	γ , defined in Equation 3.16.
GGAV	$\bar{\gamma}$, defined in Equation 3.17.
DDAV	$\bar{\delta}$, defined in Equation 3.17.
AGRID	Total core cross sectional flow area, (ft. ²).
DLP(I)	Density in the lower plenum at time step I, (lbm/ft. ³).
HMIX(I)	Mixed containment tank enthalpy at time step I, (Btu/lbm).

<u>Parameter</u>	<u>Description</u>
XTANK(I) DTANK(I)	Containment tank mixed quality and density at time step I, (lbm/ft. ³).
AM	Total mass flow rate in the core, (lbm/sec.).
L	Variable used for enthalpy and density calculation in the lower plenum starting with the beginning of natural convection.
K	Variable used to balance the volume of hot water entering the tank and volume of cold water at constant enthalpy in the down comer ready to enter the core.
VF(L)	Volume of hot water entering the tank at time step L, (ft. ³).
HVF(L) DVF(L)	Enthalpy and density of hot water entering the down comer at time step L.
TNC	Logic used in subroutine TANK, it is positive if the relatively cold water in the chimney has all passed into the core and negative if it has not yet.
RNF RNH	Reynold's number defined for friction coefficient calculation.

<u>Variable</u>	<u>Description</u>
GF	Geometry factor used for friction coefficient calculation, it has a value of 0 for circular cross sections and 11 for rectangular ones.
F1	Friction coefficient for laminar flow $RNF < 2300$.
F3	Friction coefficient for transient flow $4000 \leq RNF < 51094$.
DAVDC	Average down comer density, $(\text{lbm}/\text{ft.}^3)$.
DPFD	Pressure drop in the down comer due to friction, $(\text{lbf}/\text{ft.}^2)$.
DPVL	Friction pressure drop in natural convection valves, $(\text{lbf}/\text{ft.}^2)$.
C_p	Constant pressure specific heat, $(\text{Btu}/\text{lbm}/\text{F})$.
VISCH	Absolute viscosity, $(\text{lbm}/\text{sec.}/\text{ft.})$.
HCC1	Heat convection coefficient for laminar and turbulent flow respectively, $(\text{Btu}/\text{ft.}^2/\text{sec.}/^\circ\text{F})$.
HCC2	

APPENDIX C

- C.1 Computer Code Listing
- C.2 Sample Output for Case-1 (4 In-Core Valves Open)

C
C
C
C
C
C
C

```
*****  
*  
*          COMPUTER CODE 'LOFA'  
*    FOR NATURAL CONVECTION CALCULATION OF MITR-II  
*          DURING LOSS OF FLOW ACCIDENT  
*  
*****  
DIMENSION H(100,50),TW(100,50),G(100,50),X(100,50),XAV(100)  
D ,FQZA(50),FQZ(50),QZF(50),DEN(100,50),BI(7),DLI(7),DTANK(100),  
D  GAV(100),DAV(100),HP(100,50),GP(100,50),DENP(100,50),HAV(100),  
D  DLP(100),QFTAV(100,50),DVF(10000),Y(8),AL(8),QONB(50)  
COMMON/TS/ITL,DLI,BI,RO,BEFP,POWER,FQZA,HSAT,HFG,GAMA,P,FEN,PEX,BP  
C      ,AL,Y  
COMMON/TI/H,DTS,DTC  
COMMON/FN/DCH,HCH,DZ,ZL,ETHA,VG,VF,TCF  
COMMON/TK/HIN,ACH,CHN,ADC,DCL,VTANK,START,HFGTK,HSATK,VDC,VCHY  
COMMON/PD/HC,DDC,DIN,FKVO,CHYH,DAV,TSCR,GSCR,CHNT  
COMMON/DK/ DLP,DTANK  
COMMON/LK/L,K,DVF,TNC  
COMMON/DC/ GA,GB,GC,GD,PA,PB,GIN,PIN,THE,CPP,CDT,RSS,HTK,HV,  
C      HSU,HSL,HLP,HPI,HVW,DSL,DP,DSA,DBL,AP,ASH,ASHL,AENT,  
C      AUP,AVI,AVO,FKN,FKO,FKP,PKS,PKD,FKV,PKR,FKUP,NOV  
READ(5,510) NM,NOV,TL,PTI,CHN,CDT,DTS,ZL,  
R      THMW,GPM,HIN,PIN,THE,SPV,CPP,  
R      HSAT,HFG,RO,BEFP,GAMA,FR,VTANK,  
R      GA,GB,GC,GD,PA,PB,  
R      DSL,DP,DDC,DSA,DBL,DCH,DCL,BP,  
R      AP,ASH,ASHL,AENT,AUP,AVI,AVO,ACH,  
R      FKN,FKO,FKP,PKS,PKD,PEN,FKV,PKR,  
R      HTK,HV,HC,HSU,HSL,HLP,HPI,CHYH,  
R      HCH,WFIN,HFIN,PEX,FKUP,ADC,ALK,RSS,  
R      HFGTK,HSATK,VDC,VCHY,VG,VF,TCF,CHNT  
READ(5,520) (FQZ(M),M=2,NM)  
READ(5,530) (BI(N),DLI(N),N=1,6)  
READ(5,540) (Y(N),AL(N),N=1,8)  
WRITE(6,601)
```

MAIN0001
MAIN0002
MAIN0003
MAIN0004
MAIN0005
MAIN0006
MAIN0007
MAIN0008
MAIN0009
MAIN0010
MAIN0011
MAIN0012
MAIN0013
MAIN0014
MAIN0015
MAIN0016
MAIN0017
MAIN0018
MAIN0019
MAIN0020
MAIN0021
MAIN0022
MAIN0023
MAIN0024
MAIN0025
MAIN0026
MAIN0027
MAIN0028
MAIN0029
MAIN0030
MAIN0031
MAIN0032
MAIN0033
MAIN0034
MAIN0035
MAIN0036

```

WRITE (6,602)
WRITE (6,603)
WRITE (6,604)
WRITE (6,605)
WRITE (6,606)
WRITE (6,610) NM,NOV,TL,PTI,CHN,CDT,DTS,ZL,
W      THMW,GPM,HIN,PIN,THE,SPV,CPP,
W      HSAT,HFG,RO,BEFP,GAMA,FR,VTANK,
W      GA,GB,GC,GD,PA,PB,
W      DSL,DP,DDC,DSA,DBL,DCH,DCL,BP,
W      AP,ASH,ASHL,AENT,AUP,AVI,AVO,ACH,
W      FKN,FKO,FKP,FKS,FKD,FEN,FKV,FKR,
W      HTK,HV,HC,HSU,HSL,HLP,HPI,CHYH,
W      HCH,WFIN,HFIN,FEF,FKUP,ADC,ALK,RSS,
W      HFGTK,HSATK,VDC,VCHY,VG,VF,TCF,CHNT
WRITE (6,620) (FQZ (M),M=2,NM)
WRITE (6,630) (BI (N),DLI (N),N=1,6)
WRITE (6,640) (Y (N),AL (N),N=1,8)
510 FORMAT (2I9,6F9.4/7E9.5/7E9.5/6E9.5/8E9.5/8E9.5/8E9.5/
F      8E9.5/8E9.5/8E9.5)
520 FORMAT (12F6.2)
530 FORMAT (2F8.6)
540 FORMAT (2F10.8)
601 FORMAT (' NM,NOV,TL,PTI,CHN,CDT,DTS,ZL' /
1      ' THMW,GPM,HIN,PIN,THE,SPV,CPP' )
602 FORMAT (' HSAT,HFG,RO,BEFP,GAMA,FR,VTANK' /
2      ' GA,GB,GC,GD,PA,PB' )
603 FORMAT (' DSL,DP,DDC,DSA,DBL,DCH,DCL,BP' )
604 FORMAT (' AP,ASH,ASHL,AENT,AUP,AVI,AVO,ACH' /
4      ' FKN,FKO,FKP,FKS,FKD,FEN,FKV,FKR' )
605 FORMAT (' HTK,HV,HC,HSU,HSL,HLP,HPI,CHYH' /
5      ' HCH,WFIN,HFIN,FEF,FKUP,ADC,ALK,RSS' )
606 FORMAT (' HFGTK,HSATK,VDC,VCHY,VG,VF,TCF,CHNT' )
610 FORMAT (2I15,6F15.4/7 (3X,E12.5) /7 (3X,E12.5) /6 (3X,E12.5) /8 (3X,E12.5)
F      /8 (3X,E12.5) /8 (3X,E12.5) /8 (3X,E12.5) /8 (3X,E12.5) /8 (3X,E12.5))
620 FORMAT (6 (3X,E12.5),2X,'FQZ')

```

```

MAIN0037
MAIN0038
MAIN0039
MAIN0040
MAIN0041
MAIN0042
MAIN0043
MAIN0044
MAIN0045
MAIN0046
MAIN0047
MAIN0048
MAIN0049
MAIN0050
MAIN0051
MAIN0052
MAIN0053
MAIN0054
MAIN0055
MAIN0056
MAIN0057
MAIN0058
MAIN0059
MAIN0060
MAIN0061
MAIN0062
MAIN0063
MAIN0064
MAIN0065
MAIN0066
MAIN0067
MAIN0068
MAIN0069
MAIN0070
MAIN0071
MAIN0072

```

```

630 FORMAT (2 (3X, E12.5) , 2X, 'BI, DLI')
640 FORMAT (2 (3X, E12.5) , 2X, 'Y, AL')
POWER=THMW*3412.2/3.6
PRMTR=SQRT (2. / (ALK*WFIN) ) * (HFIN+WFIN/2.)
GIN=GPM / (SPV*AP*448.86)
GSCR=1800. / (SPV*AP*448.86)
PIN=PIN*144.
TNC=-5.0
TSCR=0.0
DZ=ZL / (NM-2)
HWV=HTK
*****
C * NORMALIZATION OF FUEL AXIAL HEAT FLUX DISTRIBUTION *
C *****
C SUM=-0.5 * (FQZ (2) +FQZ (NM) )
DO 1 J=2, NM
1 SUM=SUM+FQZ (J)
DO 2 J=2, NM
FQZA (J) = (FQZ (J) / (SUM*DZ) ) *FR/CHN
2 QZF (J) =FQZA (J) *POWER
FQZA (1) =-FQZA (2)
QZF (1) =-QZF (2)
*****
C * STEADY STATE CALCULATIONS *
C *****
C H (1, 1) =HIN
H (2, 1) =HIN
H (3, 1) =HIN
X (1, 1) = (HIN-HSAT) /HFG
X (2, 1) = (HIN-HSAT) /HFG
G (1, 1) =GIN
G (1, NM) =GIN
TW (1, 1) =0.0
DEN (1, 1) =DENS (H (1, 1) , X (1, 1) )
WRITE (6, 3)
3 FORMAT (1H1, 25X, 'BTU/LBM' , 12X, 'O C' , 9X, 'LBM/S/FT**2' , 9X, 'LBM/FT**3'

```

```

MAIN0073
MAIN0074
MAIN0075
MAIN0076
MAIN0077
MAIN0078
MAIN0079
MAIN0080
MAIN0081
MAIN0082
MAIN0083
MAIN0084
MAIN0085
MAIN0086
MAIN0087
MAIN0088
MAIN0089
MAIN0090
MAIN0091
MAIN0092
MAIN0093
MAIN0094
MAIN0095
MAIN0096
MAIN0097
MAIN0098
MAIN0099
MAIN0100
MAIN0101
MAIN0102
MAIN0103
MAIN0104
MAIN0105
MAIN0106
MAIN0107
MAIN0108

```



```

F          /25X, 'H (I, J) ', 11X, 'TW (I, J) ', 10X, 'G (I, J) ', 11X, 'DEN (I, J) ',
F          9X, 'X (I, J) ', 11X, 'FQZA (J) ')
DO 5 J=2, NM
GCORE=GIN*AP / (CHNT*ACH)
RENO=DCH*GCORE / VISCH (H (1, J-1))
HCCA=0.000053 * (RENO**0.8) * (VISCH (H (1, J-1)) **0.333) / DCH
PRMT=PRMTR*SQRT (HCCA)
ETHA=0.5+1.5*TANH (PRMT) / PRMT
P=BP*ETHA
QZAV=0.5 * (QZF (J) + QZF (J-1)) + 0.5 * (GAMA*QZF (J) + GAMA*QZF (J-1))
QFAV=QZAV / (BP*0.5)
H (1, J) = H (1, J-1) + QFAV*DZ / (HCH*GIN)
TW (1, J) = (H (1, J) - 68.05) / CP (F (1, J)) + 100.0 + QZF (J) / (HCCA*P)
TW (1, J) = (TW (1, J) - 32.0) / 1.8
X (1, J) = (H (1, J) - HSAT) / HFG
DEN (1, J) = DENSH (H (1, J), X (1, J))
G (1, J) = GIN
WRITE (6, 4) H (1, J), TW (1, J), G (1, J), DEN (1, J), X (1, J), FQZA (J)
4  FORMAT (2X, 'INITIAL CONDITION', 6 (5X, E12.5) /)
5  CONTINUE
TIN= ((H (1, 2) - 68.05) / CP (H (1, 2)) + 100.) - 32.) / 1.8
TOUT= ((H (1, NM) - 68.05) / CP (H (1, NM)) + 100.) - 32.) / 1.8
WRITE (6, 105) TIN, TOUT
105 FORMAT (50X, 'TIN=', E12.5, 5X, 'TOUT=', E12.5)
DTANK (1) = DEN (1, NM)
DTANK (2) = DEN (1, NM)
T=0.0
DTP=0.006
I=1
FREQ=1.
NC=-5
START=-2.0
DIN=1. / SPV
GAVR=0.0
HAVR=0.0
DAVR=0.0

```

```

MAIN0109
MAIN0110
MAIN0111
MAIN0112
MAIN0113
MAIN0114
MAIN0115
MAIN0116
MAIN0117
MAIN0118
MAIN0119
MAIN0120
MAIN0121
MAIN0122
MAIN0123
MAIN0124
MAIN0125
MAIN0126
MAIN0127
MAIN0128
MAIN0129
MAIN0130
MAIN0131
MAIN0132
MAIN0133
MAIN0134
MAIN0135
MAIN0136
MAIN0137
MAIN0138
MAIN0139
MAIN0140
MAIN0141
MAIN0142
MAIN0143
MAIN0144

```

	GO TO 6	MAIN0145
6	CONTINUE	MAIN0146
C	*****	MAIN0147
C	* EVALUATION OF TIME STEP *	MAIN0148
C	*****	MAIN0149
	CALL TIME(I,G,DEN,DT,NM)	MAIN0150
	IF(DT.LT.0.0001) GO TO 24	MAIN0151
C	*****	MAIN0152
C	* CALCULATION OF AVERAGE VALUES *	MAIN0153
C	* AND SWITCHING THE CALCULATED VALUES TO PAST DESIGNATIONS *	MAIN0154
C	* FO LATER CALL *	MAIN0155
C	*****	MAIN0156
	IF(I-1) 7,7,8	MAIN0157
7	DO 71 J=1,NM	MAIN0158
	HAVR=HAVR+H(I,J)	MAIN0159
	GAVR=GAVR+G(I,J)	MAIN0160
	DAVR=DAVR+DEN(I,J)	MAIN0161
	HP(I,J)=H(I,J)	MAIN0162
	GP(I,J)=G(I,J)	MAIN0163
	DENP(I,J)=DEN(I,J)	MAIN0164
71	CONTINUE	MAIN0165
	GAVP=(DZ/(ZL+2.*DZ))*GAVR	MAIN0166
	DAVP=(DZ/(ZL+2.*DZ))*DAVR	MAIN0167
	HAVP=(DZ/(ZL+2.*DZ))*HAVR	MAIN0168
	GPP=GIN	MAIN0169
	GO TO 10	MAIN0170
8	GAVP=GAV(I)	MAIN0171
	DAVP=DAV(I)	MAIN0172
	HAVP=HAV(I)	MAIN0173
	DO 9 J=1,NM	MAIN0174
	HP(I,J)=H(I,J)	MAIN0175
	GP(I,J)=G(I,J)	MAIN0176
	DENP(I,J)=DEN(I,J)	MAIN0177
9	CONTINUE	MAIN0178
	GO TO 10	MAIN0179
10	CONTINUE	MAIN0180

```

HAVP=HP (I, NM)
GTAV=GP (I, NM)
DTAV=DAVDC (I, NC)
T=T+DT
C *****
C * TO FIND FORCED FLOW RATE , OPENNING OF NATURAL CONVECTION- *
C * VALVES AND PRESSURE-DROP ALONG THE DOWN-COMMER *
C *****
CALL DOCO (I, T, NC, DT, HAVP, GTAV, DTAV, GAVP, GDC, DPTDC, G, PFF)
II=I+1
C *****
C * TRANSIENT CALCULATION AND NATURAL CONVECTION FLOW RATE *
C * EVALUATION . *
C *****
CALL TRANS (T, DT, I, NM, NC, GDC, DPTDC, HP, GP, DENP, DTP, PFF,
T GAVP, DAVP, HAVP, H, G, DEN, X, TW, QPTAV)
TIN= (( (H (I+1, 2) -68.05) /CP (H (I+1, 2) ) +100.) -32.0) /1.8
TOUT= (( (H (I+1, NM) -68.05) /CP (H (I+1, NM) ) +100.0) -32.) /1.8
C *****
C * EVALUATION OF NEW AVERAGE VALUES . *
C *****
GAVN=0.0
DAVN=0.0
XAVN=0.0
HAVN=0.0
GAV (1) =GAVP
DAV (1) =DAVP
HAV (1) =HAVP
XAV (1) =0.0
DO 17 J=1, NM
GAVN=GAVN+G (I+1, J)
DAVN=DAVN+DEN (I+1, J)
HAVN=HAVN+H (I+1, J)
17 CONTINUE
DO 18 J=2, NM
18 XAVN=XAVN+X (I+1, J)

```

```

MAIN0181
MAIN0182
MAIN0183
MAIN0184
MAIN0185
MAIN0186
MAIN0187
MAIN0188
MAIN0189
MAIN0190
MAIN0191
MAIN0192
MAIN0193
MAIN0194
MAIN0195
MAIN0196
MAIN0197
MAIN0198
MAIN0199
MAIN0200
MAIN0201
MAIN0202
MAIN0203
MAIN0204
MAIN0205
MAIN0206
MAIN0207
MAIN0208
MAIN0209
MAIN0210
MAIN0211
MAIN0212
MAIN0213
MAIN0214
MAIN0215
MAIN0216

```

	GAV (I+1) = (DZ / (ZL+2.*DZ)) *GAVN	MAIN0217
	DAV (I+1) = (DZ / (ZL+2.*DZ)) *DAVN	MAIN0218
	HAV (I+1) = (DZ / (ZL+2.*DZ)) *HAVN	MAIN0219
	XAV (I+1) = (DZ / (ZL+1.*DZ)) *XAVN	MAIN0220
C	*****	MAIN0221
C	* EVALUATION OF ON-SET OF NUCLINATION BOILING *	MAIN0222
C	*****	MAIN0223
	DO 318 J=2, NM	MAIN0224
	HSATL=HSAT-2.8*(J-2)/(NM-2)	MAIN0225
	TSAT=(HSATL-68.05)/CP(HSATL)+100.	MAIN0226
	TW(I+1,J)=TW(I+1,J)*1.8+32.	MAIN0227
	DTSAT=TW(I+1,J)-TSAT	MAIN0228
	IF (DTSAT) 118, 118, 218	MAIN0229
118	QONB(J)=-0.1E-10	MAIN0230
	GO TO 318	MAIN0231
218	PJ=19.35-0.85*(J-2)/(NM-2)	MAIN0232
	A=0.00433*(PJ**1.156)	MAIN0233
	B=2.3/(PJ**0.0234)	MAIN0234
	QONB(J)=A*(DTSAT**B)	MAIN0235
	GO TO 318	MAIN0236
318	TW(I+1,J)=(TW(I+1,J)-32.)/1.8	MAIN0237
	RATIO=PREQ/PTI	MAIN0238
C	*****	MAIN0239
C	* PRINTING OF TRANSIENT VALUES . *	MAIN0240
C	*****	MAIN0241
	IF (RATIO-1.) 16, 11, 11	MAIN0242
11	WRITE(6,12) II,T,DT	MAIN0243
12	FORMAT(1H1,2X,I4,3X,'T=',F10.5,10X,'DT=',E12.5)	MAIN0244
	WRITE(6,13)	MAIN0245
13	FORMAT(/9X,'BTU/S/FT**2.',9X	MAIN0246
F	, 'BTU/LBM', 12X, 'O C', 11X, 'LBM/S/FT**2', 7X, 'LBM/FT**3'	MAIN0247
P	, 19X, 'HSAT=194.4 BTU/LBM'/3X, 'INCH', 8X, 'QPTAV', 12X,	MAIN0248
P	'H(I,J)', 10X, 'TW(I,J)', 10X, 'G(I,J)', 11X, 'DEN(I,J)',	MAIN0249
P	9X, 'X(I,J)', 11X, 'QONB(I,J)')	MAIN0250
	DO 14 J=2, NM	MAIN0251
	JJ=J-2	MAIN0252

14	WRITE (6,15) JJ, QFTAV (I+1, J), H (I+1, J), TW (I+1, J), G (I+1, J), DEN (I+1, J)	MAIN0253
	W , X (I+1, J), QONB (J)	MAIN0254
15	FORMAT (/4X, I2, 7(5X, E12.5))	MAIN0255
	WRITE (6,19) II, T, DT, HAV (I+1), GAV (I+1), DAV (I+1), TIN, TOUT	MAIN0256
19	FORMAT (32X, 60 ('='), 18X, 'HSAT=191.6 BTU/LBM')	MAIN0257
	F /2X, I3, 2X, 'T=', F7.3, 3X, 'DT=', E12.5, 7X, 'HAV=',	MAIN0258
	F E12.5, 1X, 'GAV=', E12.5, 1X, 'DAV=', E12.5, 1X, 'TIN=', E12.5, 2X,	MAIN0259
	F 'TOUT=', E12.5)	MAIN0260
	FREQ=0.0	MAIN0261
	GO TO 16	MAIN0262
16	FREQ=FREQ+1.	MAIN0263
	III=I+2	MAIN0264
C	*****	MAIN0265
C	* TO CALCULATE THE CORE INLET ENTHALPY AND DENSITY FOR PUETURE *	MAIN0266
C	* NEEDS :	MAIN0267
C	*****	MAIN0268
	CALL TANK (I, NM, NC, DT, H, G, DEN, X, PFF)	MAIN0269
	DTP=DT	MAIN0270
	I=I+1	MAIN0271
	IF (T-TL) 20, 20, 999	MAIN0272
C	*****	MAIN0273
C	* TO SAVE MEMORY SPACE AND SPECIFY OLD SPACES TO NEW *	MAIN0274
C	* CALCULATIONS :	MAIN0275
C	*****	MAIN0276
20	IF (I-100) 6, 21, 21	MAIN0277
21	I=10	MAIN0278
	H (9, NM+1) = H (99, NM)	MAIN0279
	DO 22 J=1, NM	MAIN0280
	H (10, J) = H (100, J)	MAIN0281
	G (10, J) = G (100, J)	MAIN0282
	DEN (10, J) = DEN (100, J)	MAIN0283
22	CONTINUE	MAIN0284
	DO 23 J=2, NM	MAIN0285
	TW (10, J) = TW (100, J)	MAIN0286
	X (10, J) = X (100, J)	MAIN0287
23	CONTINUE	MAIN0288

```
XAV(10)=XAV(100)
GAV(10)=GAV(100)
DAV(10)=DAV(100)
HAV(10)=HAV(100)
GO TO 6
24 WRITE(6,25)
25 FORMAT(3X,'TIME INTERVAL IS LESS THAN 0.001')
GO TO 999
999 STOP
END
```

```
MAIN0289
MAIN0290
MAIN0291
MAIN0292
MAIN0293
MAIN0294
MAIN0295
MAIN0296
MAIN0297
MAIN0298
```

	SUBROUTINE TIME(I,G,DEN,DT,NM)	TIME0001
	DIMENSION DELT(50),G(100,50),DEN(100,50),H(100,50)	TIME0002
	COMMON/TI/H,DTS,DTC	TIME0003
	COMMON/PN/DCH,HCH,DZ,ZL,ETHA,VG,VP,TCF	TIME0004
C	*****	TIME0005
C	* CALCULATION OF DIFFERENT TIME INTERVALS WHICH TAKES FOR FLOW *	TIME0006
C	* TO PASS THE MESH SPACES . *	TIME0007
C	*****	TIME0008
	DO 2 J=2,NM	TIME0009
2	DELT(J)=DZ*(DEN(I,J)+DEN(I,J-1))/(G(I,J)+G(I,J-1))	TIME0010
	REF=1.E+30	TIME0011
C	*****	TIME0012
C	* EVALUATION OF THE MIN. VALUES FOR TIME INTERVALS . *	TIME0013
C	*****	TIME0014
	DO 4 J=2,NM	TIME0015
	IF(DELT(J)-REF) 3,4,4	TIME0016
3	REF=DELT(J)	TIME0017
4	CONTINUE	TIME0018
	DTC=REF	TIME0019
C	*****	TIME0020
C	* SELECTION OF THE SMALLER VALUE OF THE MIN. TIME INTERVAL AND *	TIME0021
C	* THE SPECIFIED ONE AS INPUT TO THE CODE . *	TIME0022
C	*****	TIME0023
	IF(DTC-DTS) 5,5,6	TIME0024
5	DT=DTC	TIME0025
	GO TO 7	TIME0026
6	DT=DTS	TIME0027
	GO TO 7	TIME0028
7	RETURN	TIME0029
	END	TIME0030

	SUBROUTINE DOCO (I,T,NC,DT,HA VP,GTAV,DTAV,GAVP,GDC,DPTDC,G,FFP)	DOC00001
	DIMENSION DAV(100),G(100,50)	DOC00002
	COMMON/FN/DCH,HCH,DZ,ZL,ETHA,VG,VF,TCF	DOC00003
	COMMON/TK/HIN,ACH,CHN,ADC,DCL,VTANK,START,HFGTK,HSATK,VDC,VCHY	DOC00004
	COMMON/PD/HC,DDC,DIN,FKVO,CHYH,DAV,TSCR,GSCR,CHNT	DOC00005
	COMMON/DC/ GA,GB,GC,GD,PA,PB,GIN,PIN,THE,CPP,CDT,RSS,HTK,HV,	DOC00006
C	HSU,HSL,HLP,HPI,HV,DSL,DP,DSA,DBL,AP,ASH,ASHL,AENT,	DOC00007
C	AUP,AVI,AVO,FKN,FKO,PKP,PKS,PKD,PKV,PKR,FKUP,NOV	DOC00008
	ABL=0.785*DBL**2.	DOC00009
	FKVO=FKV/(NOV**2.)	DOC00010
	FKVR=FKR*((AVI/ADC)**2.)	DOC00011
	AVOO=AVO*NOV	DOC00012
	AVIN=AVI*NOV	DOC00013
	ALPA=AVO/AVI	DOC00014
	SPV=1./DIN	DOC00015
C	*****	DOC00016
C	* FLOW RATE AND PRESSURE FORCED VALUES AT MF1 AFTER PUMP *	DOC00017
C	* COAST-DOWN . *	DOC00018
C	*****	DOC00019
	GDC=GIN*(GA/(EXP(GB*T))+GC*T-GD)	DOC00020
	PRESS=PIN*(PA*T+1.)/(PB*T+1.)	DOC00021
	IF(GDC .LE. 0.0001) GO TO 7	DOC00022
	GDCP=GIN*(GA/(EXP(GB*(T-DT)))+GC*(T-DT)-GD)	DOC00023
	IF(T-CDT) 20,20,7	DOC00024
20	IF(NC) 1,1,30	DOC00025
30	DGG=GDCP-GAVP	DOC00026
	IF(DGG) 7,8,8	DOC00027
C	*****	DOC00028
C	* PRESSURE DROP CALCULATION IN THE SYSTEM FROM MF1 TO THE *	DOC00029
C	* UPPER PLENUM . *	DOC00030
C	*****	DOC00031
1	FFP=+5.0	DOC00032
	IF(GDC-GSCR) 21,21,41	DOC00033
21	IF(TSCR) 31,31,41	DOC00034
31	TSCR=T	DOC00035
41	CONTINUE	DOC00036


```

FRC=FRIC (HAVP,GTAV,2.)
DPFP=HLP*FRC*SPV* (GDC**2.) / (2.*DP*32.2)
DPSP=SPV* (GDC**2.) * (FKN+0.5*FKO) /32.2
DPEP=HPI/SPV
DPTP=DPFP+DPSP+DPEP
PRESS=PRESS-DPTP
DPFS=FRC*SPV* (GDC**2.) * (HSU/DSA+HSL/DSL) /64.4
DPSS=SPV* (GDC**2.) * (FKP+FKS+FKD) /64.4
DPES=- (HSU+HSL) /SPV
DPAS=SPV* (GDC**2.) *0.7761/32.2
DPTS=DPFS+DPSS+DPES+DPAS
PRESS=PRESS-DPTS
PHV=144.*14.7+HWV/SPV
PC=PHV+ (RSS- (1./SPV)) *3.14* (DBL**3.) /6.*AVI
DPC=PRESS-PC
*****
C * BALANCING THE PRESSURES TO SEE IF THE VALVES ARE OPENND . *
C *****
C IF (DPC-10.) 2,2,8
2 NC=+5
C *****
C *EVALUATION OF THE REVERSE FLOW IN THE VALVES RIGHT AFTER *
C * OPENNING , IF THERE IS ANY . *
C *****
SD=ADC/AVIN
SV=AENT/AVIN
AA= (ALFA+PKVR) *SD**2.+1.
BB=SD*SV* (ALFA+PKVR) *GDC
CC= ((ALFA+PKVR) *SV**2.-1.) * (GDC**2.) +2.*32.2*PHV/SPV
RAD= (BB**2.-AA*CC)
IF (RAD) 5,3,3
3 GD1= (BB+RAD**0.5) /AA
GD2= (BB-RAD**0.5) /AA
IF (GD1 .GE. GDC) GO TO 9
IF (GD1 .GE. 0.0 .AND. GD1 .LT. GDC) GD=GD1
IF (GD1 .GE. GDC .AND. GD2 .LT. GDC) CONTINUE

```

```

DOC00037
DOC00038
DOC00039
DOC00040
DOC00041
DOC00042
DOC00043
DOC00044
DOC00045
DOC00046
DOC00047
DOC00048
DOC00049
DOC00050
DOC00051
DOC00052
DOC00053
DOC00054
DOC00055
DOC00056
DOC00057
DOC00058
DOC00059
DOC00060
DOC00061
DOC00062
DOC00063
DOC00064
DOC00065
DOC00066
DOC00067
DOC00068
DOC00069
DOC00070
DOC00071
DOC00072

```

	IF (GD2 .GE. 0.0 .AND. GD2 .LE. GDC) GD=GD2	DOC00073
	GV=GDC*SV-GD*SD	DOC00074
	DPV=FKVO*SV*(GV**2.)/64.4	DOC00075
	PVO=PRESS-DPV	DOC00076
	PP=PVO-PHV	DOC00077
	IF (PP) 5,5,4	DOC00078
4	GDC=GD	DOC00079
	GO TO 5	DOC00080
5	WRITE (6,6)	DOC00081
6	FORMAT (/3X,'NATURAL CONVECTION VALVE OPENS'/32('*****'))	DOC00082
	GDC=GDC	DOC00083
	GO TO 7	DOC00084
C	*****	DOC00085
C	* DOWN-COMMER PRESSURE DROP CALCULATION FOR NATURAL CONVECTION *	DOC00086
C	*****	DOC00087
7	FFF=-5.0	DOC00088
	IF (GTAV .LE. 0.0001) GTAV=0.0001	DOC00089
	DPDC=PDROP (I,HAVP,GTAV,DTAV,NC,DT)	DOC00090
	DPTDC=DPDC	DOC00091
	GO TO 11	DOC00092
C	*****	DOC00093
C	* DOWN-COMMER PRESSURE DROP EVALUATION FOR FORCED FLOW . *	DOC00094
C	*****	DOC00095
8	FFF=+5.0	DOC00096
	IF (GDC .LE. 0.0001) GDC=0.0001	DOC00097
	DPDC=PDROP (I,HIN,GDC,DIN,NC,DT)	DOC00098
	DPTDC=PRESS-DPDC	DOC00099
	IF (DPTDC) 7,7,11	DOC00100
9	WRITE (6,10)	DOC00101
10	FORMAT (3X,'NEGATIVE FLOW')	DOC00102
	GO TO 11	DOC00103
11	RETURN	DOC00104
	END	DOC00105

	SUBROUTINE TRANS (T,DT,I,NM,NC,GDC,DPTDC,HP,GP,DENP,DTP,FFF,	TRNS0001
T	GAVP,DAVP,HAVP,H,G,DEN,X,TW,QPTAV)	TRNS0002
	DIMENSION H(100,50),G(100,50),DEN(100,50),TW(100,50),X(100,50),	TRNS0003
D	FQZA(50),QZT(100,50),GG(100,50),DD(100,50),GAV(100,50),	TRNS0004
D	HP(100,50),GP(100,50),DENP(100,50),DTANK(100),DLP(100),	TRNS0005
D	GT(100,50),BI(7),DLI(7),QPTAV(100,50),DVF(10000),	TRNS0006
D	DAV(100),GNC(100,50),Y(8),AL(8)	TRNS0007
	COMMON/TS/ITL,DLI,BI,RO,BEFP,POWER,FQZA,HSAT,HFG,GAMA,P,FEN,FEX,BP	TRNS0008
C	,AL,Y	TRNS0009
	COMMON/PD/HC,DDC,DIN,FKVO,CHYH,DAV,TSCR,GSCR,CHNT	TRNS0010
	COMMON/TK/HIN,ACH,CHN,ADC,DCL,VTANK,START,HFGTK,HSATK,VDC,VCHY	TRNS0011
	COMMON/FN/DCH,HCH,DZ,ZL,ETHA,VG,VF,TCF	TRNS0012
	COMMON/DK/ DLP,DTANK	TRNS0013
	COMMON/LK/L,K,DVF,TNC	TRNS0014
	COMMON/DC/ GA,GB,GC,GD,PA,PB,GIN,PIN,THE,CPP,CDT,RSS,HTK,HV,	TRNS0015
C	HSU,HSL,HLP,HPI,HVV,DSL,DP,DSA,DBL,AP,ASH,ASHL,AENT,	TRNS0016
C	AUP,AVI,AVO,PKN,PKO,PKP,FKS,PKD,PKV,PKR,PKUP,NOV	TRNS0017
	TSCR=0.0	TRNS0018
	DTSCR=TSCR+0.41	TRNS0019
	IF (T .LT. DTSCR) GO TO 3	TRNS0020
C	*****	TRNS0021
C	* EVALUATION OF THE DECAY HEAT .	TRNS0022
C	*****	TRNS0023
	STI=T-0.9	TRNS0024
	IF (STI .LT. 0.1) STI=0.1	TRNS0025
	QACT=0.000341*EXP(-0.0052*STI)	TRNS0026
	QACT=QACT*POWER	TRNS0027
	QDN=0.0	TRNS0028
	IF (STI .GT. 59.) GO TO 2	TRNS0029
	DO 1 N=1,6	TRNS0030
1	QDN=QDN+(BI(N)/(RO+BEFP))*EXP(-RO*DLI(N)*STI/(RO+BEFP))	TRNS0031
2	CONTINUE	TRNS0032
	QDN=QDN*POWER*1.153	TRNS0033
	IF (STI .LE. 10.) QFP=0.06025*(STI**(-0.0639))	TRNS0034
	IF (STI .GT. 10. .AND. STI .LE. 150.) QFP=0.07655*(STI**(-0.1807))	TRNS0035
	IF (STI .GT. 150.) QFP=0.1301*(STI**(-0.2834))	TRNS0036

	QFP=QFP*POWER	TRNS0037
	QDPHN=0.0	TRNS0038
	DO 102 N=1,8	TRNS0039
102	QDPHN=QDPHN+Y(N)*(1.-EXP(-AL(N)*STI))	TRNS0040
	QDPHN=QDPHN*POWER	TRNS0041
	Q=QACT+QDN+QFP+QDPHN	TRNS0042
	IF(T.GT.0.41.AND.T.LE.1.0) Q=POWER-(POWER-Q)*(T-0.41)/0.59	TRNS0043
	GO TO 4	TRNS0044
3	Q=POWER	TRNS0045
	GO TO 4	TRNS0046
4	CONTINUE	TRNS0047
C	*****	TRNS0048
C	*DECAY POWER DISTRIBUTION CALCULATION .	TRNS0049
C	*****	TRNS0050
	DO 5 J=2,NM	TRNS0051
5	QZT(I+1,J)=FQZA(J)*Q	TRNS0052
	QZT(I+1,1)=-QZT(I+1,2)	TRNS0053
	DO 6 J=1,NM	TRNS0054
	H(I,J)=HP(I,J)	TRNS0055
	G(I,J)=GP(I,J)	TRNS0056
	DEN(I,J)=DENP(I,J)	TRNS0057
6	CONTINUE	TRNS0058
	IF(I.GT.1) H(I,NM+1)=H(I-1,NM)	TRNS0059
	DTANK(1)=DEN(1,NM)	TRNS0060
	DTANK(2)=DEN(1,NM)	TRNS0061
	DO 7 J=2,NM	TRNS0062
	IF(GAVP-0.0001) 26,26,27	TRNS0063
C	*****	TRNS0064
C	* TRANSIENT CALCULATION FOR REVERSED OR NON FLOW ,	TRNS0065
C	*****	TRNS0066
26	JR=NM-J+2	TRNS0067
	H(I,NM+1)=H(I-1,NM)	TRNS0068
	H(I+1,NM+1)=H(I,NM)	TRNS0069
	DEN(I,NM+1)=DEN(I-1,NM)	TRNS0070
	G(I,NM+1)=GAVP	TRNS0071
	QZT(I+1,NM+1)=-QZT(I+1,NM)	TRNS0072

	GHALF=0.5*(G(I,JR)+G(I,JR-1))	TRNS0073
	DHALF=0.5*(DEN(I,JR)+DEN(I,JR-1))	TRNS0074
	QZTAV=0.5*((QZT(I+1,JR)+QZT(I+1,JR-1))+GAMA*(QZT(I+1,JR)+	TRNS0075
Q	QZT(I+1,JR-1)))	TRNS0076
	QPTAV(I+1,JR)=QZTAV/(BP*0.5)	TRNS0077
	ALFA=GHALF*DT/(DHALF*DZ)	TRNS0078
	IF (FPF .GT. 0.0) ALFA=ALFA*ADC/(CHNT*ACH)	TRNS0079
C	*****	TRNS0080
C	* EXPLICIT - CAUCHY POLYGON METHOD *	TRNS0081
C	*****	TRNS0082
	H(I+1,JR)=H(I,JR)-ALFA*(H(I,JR+1)-H(I,JR))+2.*DT*(QPTAV(I+1,JR)	TRNS0083
H)/(DHALF*HCH)	TRNS0084
	H(I+1,JR)=0.5*(H(I+1,JR)+H(I+1,JR-1))	TRNS0085
	X(I+1,JR)=(H(I+1,JR)-(HSAT-2.8*(JR-2))/(NM-2))/HFG	TRNS0086
	DEN(I+1,JR)=DENS(H(I+1,JR),X(I+1,JR))	TRNS0087
	TWH=(H(I+1,JR)-68.05)/CP(H(I+1,JR))+100.0	TRNS0088
	IF (FPF .LT. 0.0) TWH=(H(I+1,JR-1)-68.05)/CP(H(I+1,JR-1))+100.	TRNS0089
	TW(I+1,J)=TWH+QZT(I+1,JR)/(HCC(H(I+1,JR),GAVP)*P)	TRNS0090
	TW(I+1,JR)=(TW(I+1,JR)-32.)/1.8	TRNS0091
	GO TO 7	TRNS0092
C	*****	TRNS0093
C	* TRANSIENT CALCULATION FOR UPFLOW IN THE CORE , *	TRNS0094
C	*****	TRNS0095
27	GHALF=0.5*(G(I,J)+G(I,J-1))	TRNS0096
	DHALF=0.5*(DEN(I,J)+DEN(I,J-1))	TRNS0097
	QZTAV=0.5*((QZT(I+1,J)+QZT(I+1,J-1))+GAMA*(QZT(I+1,J)+	TRNS0098
Q	QZT(I+1,J-1)))	TRNS0099
	QPTAV(I+1,J)=QZTAV/(BP*0.5)	TRNS0100
	ALFA=GHALF*DT/(DHALF*DZ)	TRNS0101
	IF (FPF .GT. 0.0) ALFA=ALFA*ADC/(CHNT*ACH)	TRNS0102
C	*****	TRNS0103
C	* EXPLICIT - CAUCHY POLYGON METHOD *	TRNS0104
C	*****	TRNS0105
	H(I+1,J)=H(I,J)-ALFA*(H(I,J)-H(I,J-1))+2.*DT*(QPTAV(I+1,J))/	TRNS0106
H	(DHALF*HCH)	TRNS0107
	H(I+1,J)=0.5*(H(I+1,J)+H(I+1,J-1))	TRNS0108

	X (I+1,J) = (H (I+1,J) - (HSAT-2.8* (J-2) / (NM-2))) / HFG	TRNS0109
	DEN (I+1,J) = DENS (H (I+1,J) , X (I+1,J))	TRNS0110
	TWH = (H (I+1,J) - 68.05) / CP (H (I+1,J)) + 100.0	TRNS0111
	IF (FPF .LT. 0.0) TWH = (H (I+1,J-1) - 68.05) / CP (H (I+1,J-1)) + 100.	TRNS0112
	TW (I+1,J) = TWH + QZT (I+1,J) / (HCC (H (I+1,J) , GAVP) * P)	TRNS0113
	TW (I+1,J) = (TW (I+1,J) - 32.) / 1.8	TRNS0114
7	CONTINUE	TRNS0115
	DEN (I+1,1) = DENS (H (I+1,1) , X (I+1,1))	TRNS0116
	IF (FPF .LT. 0.0) GAVPC = GAVP	TRNS0117
	IF (NC) 17, 17, 107	TRNS0118
107	IF (START) 207, 207, 307	TRNS0119
207	GAVPC = 0.0	TRNS0120
	START = START + 4.	TRNS0121
	GO TO 307	TRNS0122
307	CONTINUE	TRNS0123
	IF (FPF .GT. 0.0) GAVP = GAVP * ADC / (CHNT * ACH)	TRNS0124
	ANOV = NOV	TRNS0125
C	*****	TRNS0126
C	* NATURAL CONVECTION FLOW EVALUATION . *	TRNS0127
C	*****	TRNS0128
	GAVC = GAVP	TRNS0129
	FFR = ZL * FRIC (HAVP, GAVC, 11.) * (GAVC ** 2.) / (2. * DCH * DAVP)	TRNS0130
	FSH = (FEN + FEX) * (GAVC ** 2.) / (2. * DAVP)	TRNS0131
	FSA = 0.0	TRNS0132
	DPTC = FFR + FSH + FSA	TRNS0133
	DFDEN = ZL * (DAVDC (I, NC) - DAVP) * 32.2	TRNS0134
	DFCHY = CHYH * (DAVDC (I, NC) - DTANK (I)) * 32.2	TRNS0135
	GAVNC = GAVPC + (DT / 2. * (HC + 0.00)) * ((DFDEN + DFCHY) - (DPTC + DPTDC))	TRNS0136
	GG (I+1, 1) = 1.0	TRNS0137
	DD (I+1, 1) = 0.0	TRNS0138
	DO 11 J = 2, NM	TRNS0139
	DH = H (I+1, J) - H (I+1, J-1)	TRNS0140
	IF (DH - 0.1) 8, 9, 9	TRNS0141
8	DH = H (I+1, 2) - H (I+1, NM)	TRNS0142
	DDEN = DEN (I+1, 2) - DEN (I+1, NM)	TRNS0143
	GO TO 10	TRNS0144

9	DH=H (I+1,J) -H (I+1,J-1)	TRNS0145
	DDEN=DEN (I+1,J) -DEN (I+1,J-1)	TRNS0146
	GO TO 10	TRNS0147
10	DRDH=DDEN/DH	TRNS0148
	DENAV=0.5 * (DEN (I+1,J) +DEN (I+1,J-1))	TRNS0149
	AAV=DRDH*DH/DENAV	TRNS0150
	AAL= (2.+AAV) / (2.-AAV)	TRNS0151
	BAV=2.0*DRDH*QPTAV (I+1,J) *DZ / (DENAV* (2.-AAV))	TRNS0152
	GG (I+1,J) =AAL*GG (I+1,J-1)	TRNS0153
11	DD (I+1,J) =AAL*DD (I+1,J-1) +BAV	TRNS0154
	GGAV=0.0	TRNS0155
	DDAV=0.0	TRNS0156
	GGs=-0.5*GG (I+1,NM)	TRNS0157
	DDs=-0.5*DD (I+1,NM)	TRNS0158
	DO 12 J=2,NM	TRNS0159
	GGAV=GGAV+GG (I+1,J)	TRNS0160
12	DDAV=DDAV+DD (I+1,J)	TRNS0161
	GGAV= (DZ / (ZL+2.*DZ)) * (GGAV+GGs)	TRNS0162
	DDAV= (DZ / (ZL+2.*DZ)) * (DDAV+DDs)	TRNS0163
	GNC (I+1,1) = (1./GGAV) * (GAVNC-DDAV)	TRNS0164
	DO 14 J=2,NM	TRNS0165
	GNC (I+1,J) =GG (I+1,J) *GNC (I+1,1) +DD (I+1,J)	TRNS0166
14	CONTINUE	TRNS0167
	DO 15 J=1,NM	TRNS0168
15	IF (GNC (I+1,J) .LE. 0.0001) GNC (I+1,J) =0.0001	TRNS0169
	GO TO 16	TRNS0170
16	IF (FFF) 19,19,17	TRNS0171
17	DO 18 J=1,NM	TRNS0172
18	G (I+1,J) =GDC	TRNS0173
	GO TO 21	TRNS0174
19	DO 20 J=1,NM	TRNS0175
20	G (I+1,J) =GNC (I+1,J)	TRNS0176
	GAVPC=GAVNC	TRNS0177
	GO TO 21	TRNS0178
21	RETURN	TRNS0179
	END	TRNS0180

```

SUBROUTINE TANK(I,NM,NC,DT,H,G,DEN,X,FFF)
DIMENSION H(100,50),HMIK(100),DEN(100,50),DAV(100),HVF(10000),
D DVF(10000),XTANK(100),DTANK(100),DLP(100),X(100,50),G(100,50),
D VF(10000)
COMMON/PD/HC,DDC,DIN,PKVO,CHYH,DAV,TSCR,GSCR,CHNT
COMMON/TK/HIN,ACH,CHN,ADC,DCL,VTANK,START,HPGTK,HSATK,VDC,VCHY
COMMON/DK/ DLP,DTANK
COMMON/LK/L,K,DVF,TNC
COMMON/DC/ GA,GB,GC,GD,PA,PB,GIN,PIN,THE,CPP,CDT,RSS,HTK,HV,
C HSU,HSL,HLP,HPI,HVV,DSL,DP,DSA,DBL,AP,ASH,ASHL,AENT,
C AUP,AVI,AVO,PKN,PKO,PKP,PKS,PKD,PKV,PKR,PKUP,NOV
IF(I .GE. 99) I99=100
IF(I .GE. 99) I=9
III=I+2
VSH=ASH*HSU+ASHL*HSL
VDCS=VDC+VCHY+VSH
AGRID=CHNT*ACH
IF(FFF) 9,1,1
C *****
C * EVALUATION OF THE TANK MIXED PROPERTIES DURING PUMP *
C * COAST-DOWN *
C *****
1 IF(III-10) 2,2,4
2 DO 3 N=1,III
H(N,1)=HIN
DLP(N)=DIN
HMIK(N)=H(1,NM)
XTANK(N)=X(1,NM)
3 DTANK(N)=DEN(1,NM)
GO TO 8
4 IF(III-100) 5,5,7
5 DO 6 N=10,III
H(N,1)=HIN
DLP(N)=DIN
XTANK(N)=X(1,NM)
HMIK(N)=H(1,NM)

```

```

TANK0001
TANK0002
TANK0003
TANK0004
TANK0005
TANK0006
TANK0007
TANK0008
TANK0009
TANK0010
TANK0011
TANK0012
TANK0013
TANK0014
TANK0015
TANK0016
TANK0017
TANK0018
TANK0019
TANK0020
TANK0021
TANK0022
TANK0023
TANK0024
TANK0025
TANK0026
TANK0027
TANK0028
TANK0029
TANK0030
TANK0031
TANK0032
TANK0033
TANK0034
TANK0035
TANK0036

```



```

6 DTANK (N) = DEN (1, NM)
GO TO 8
7 H (11, 1) = HIN
DLP (11) = DIN
XTANK (11) = X (1, NM)
HMIX (11) = H (1, NM)
DTANK (11) = DEN (1, NM)
GO TO 8
8 N=1
L=0
K=1
IF (I .LT. 99) I99=0
VPT=0.0
GO TO 25
C *****
C * EVALUATION OF TRANSPERING COLD WATER FROM D. C. TO THE LOWER *
C * PLENUM AFTER N. C. VALVES ARE OPENED . *
C *****
9 L=L+1
HMIX (9) = HMIX (99)
DTANK (9) = DTANK (99)
AH=G (I+1, NM) * AGRID
VP (L) = G (I+1, NM) * AGRID * DT / DEN (I+1, NM)
HMIX (I+1) = HMIX (I) + (AH * DT / (DTANK (I) * VTANK)) * (H (I+1, NM) - HMIX (I))
XTANK (I+1) = (HMIX (I+1) - HSATK) / HPGTK
DTANK (I+1) = DENSH (HMIX (I+1), XTANK (I+1))
HVF (L) = HMIX (I+1)
DVF (L) = DTANK (I+1)
VPT = VPT + VP (L)
IF (VPT - VDCS) 11, 11, 14
C *****
C * COLD WATER IS STILL MOVING DOWN . *
C *****
11 H (I+2, 1) = (VPT / VDCS) * (HVF (K) - HIN) + HIN
DLP (I+2) = (VPT / VDCS) * (DTANK (K) - DIN) + DIN
TNC = -0.5
TANK0037
TANK0038
TANK0039
TANK0040
TANK0041
TANK0042
TANK0043
TANK0044
TANK0045
TANK0046
TANK0047
TANK0048
TANK0049
TANK0050
TANK0051
TANK0052
TANK0053
TANK0054
TANK0055
TANK0056
TANK0057
TANK0058
TANK0059
TANK0060
TANK0061
TANK0062
TANK0063
TANK0064
TANK0065
TANK0066
TANK0067
TANK0068
TANK0069
TANK0070
TANK0071
TANK0072

```

	GO TO 25	TANK0073
C	*****	TANK0074
C	* TANK HOT WATER REACHES THE LOWER PLENUM . *	TANK0075
C	*****	TANK0076
14	IF (M-1) 15, 15, 17	TANK0077
15	H (I+2, 1) =HVF (K)	TANK0078
	DLP (I+2) =DTANK (K)	TANK0079
	TNC=+5.0	TANK0080
	M=M+1	TANK0081
	K=K+1	TANK0082
	K1=1	TANK0083
	VFLK=0.0	TANK0084
	GO TO 25	TANK0085
17	VFV=0.7*VF (K-1)	TANK0086
	TNC=+5.0	TANK0087
	IF (VF (L) -VFV) 19, 21, 21	TANK0088
C	*****	TANK0089
C	* THE VOLUME ENTERED THE TANK IS LESS THAN THE HOT WATER *	TANK0090
C	* VOLUME ENTERING THE CORE AT CONSTANT TEMP. . *	TANK0091
C	*****	TANK0092
19	IF (K1-1) 119, 119, 219	TANK0093
119	VFK1=VF (K-1)	TANK0094
	HVFK1=HVF (K-1)	TANK0095
	DVFK1=DVF (K-1)	TANK0096
	GO TO 219	TANK0097
219	VFLK=VFLK+VF (L)	TANK0098
	IF (VFLK-VFK1) 319, 419, 419	TANK0099
319	K1=K1+1	TANK0100
	VPT=VFT	TANK0101
	H (I+2, 1) =HVFK1	TANK0102
	DLP (I+2) =DVFK1	TANK0103
	GO TO 25	TANK0104
419	K1=1	TANK0105
	VPT=VFT-VFK1	TANK0106
	H (I+2, 1) =HVF (K)	TANK0107
	DLP (I+2) =DVF (K)	TANK0108

	K=K+1	TANK0109
	GO TO 25	TANK0110
C	*****	TANK0111
C	* THE VOLUME ENTERED THE TANK IS EQUAL TO OR LARGER THAN THE *	TANK0112
C	* VOLUME ENTERING THE CORE AT CONSTANT TEMP. . *	TANK0113
C	*****	TANK0114
21	VFT=VFT-VF (K-1)	TANK0115
	H (I+2, 1)=HVF (K)	TANK0116
	DLP (I+2)=DVF (K)	TANK0117
	K=K+1	TANK0118
	GO TO 25	TANK0119
25	IF (I .LE. 9 .AND. I99 .GE. 100) I=99	TANK0120
	RETURN	TANK0121
	END	TANK0122

	FUNCTION FRIC (HF, GAVP, GF)	FRIC0001
	DIMENSION DAV (100)	FRIC0002
	COMMON/PD/HC, DDC, DIN, FKVO, CHYH, DAV, TSCR, GSCR, CHNT	FRIC0003
	COMMON/PN/DCH, HCH, DZ, ZL, ETHA, VG, VF, TCF	FRIC0004
	IF (GF-5.) 1, 1, 2	FRIC0005
C	*****	FRIC0006
C	* FRICTION FACTOR CALCULATION FOR CIRCULAR CROSS SECTION *	FRIC0007
C	*****	FRIC0008
1	RNF=GAVP*DDC/VISCH (HF)	FRIC0009
	F1=64./RNF	FRIC0010
	GO TO 3	FRIC0011
C	*****	FRIC0012
C	* FRICTION FACTOR CALCULATION FOR RECTANGULAR CROSS SECTION . *	FRIC0013
C	*****	FRIC0014
2	RNF=GAVP*DCH/VISCH (HF)	FRIC0015
	F1=91.5/RNF	FRIC0016
	GO TO 3	FRIC0017
3	F3=0.3164/(RNF**0.25)	FRIC0018
	IF (RNF .LT. 2300.) FRIC=F1	FRIC0019
	IF (RNF .GE. 2300. .AND. RNF .LT. 4000.) FRIC=F1+ ((F3-F1)/(4000.-	FRIC0020
C	2300.))* (RNF-2300.)	FRIC0021
	IF (RNF .GE. 4000. .AND. RNF .LT. 51094.) FRIC=F3	FRIC0022
	IF (RNF .GE. 51094.) FRIC=0.184/(RNF**0.2)	FRIC0023
	RETURN	FRIC0024
	END	FRIC0025

```
FUNCTION DAVDC (I,NC)
DIMENSION DLP (100) ,DTANK (100) ,DAV (100) ,DVF (10000)
COMMON/PD/HC,DDC,DIN,FKVO,CHYH,DAV,TSCR,GSCR,CHNT
COMMON/DK/ DLP,DTANK
COMMON/LK/L,K,DVF,TNC
DLP (1) =1./0.0161
IF (NC) 1,1,2
1 DAVDC=DIN
GO TO 5
2 DAVDC=0.5* (DTANK (I) +DLP (I))
GO TO 5
5 RETURN
END
```

```
DVDC0001
DVDC0002
DVDC0003
DVDC0004
DVDC0005
DVDC0006
DVDC0007
DVDC0008
DVDC0009
DVDC0010
DVDC0011
DVDC0012
DVDC0013
```

FUNCTION PDROP(I, HAVP, GTAV, DTAV, NC, DT)	PDOP0001
DIMENSION DAV(100)	PDOP0002
COMMON/PD/HC, DDC, DIN, FKVO, CHYH, DAV, TSCR, GSCR, CHNT	PDOP0003
COMMON/TK/HIN, ACH, CHN, ADC, DCL, VTANK, START, HPGTK, HSATK, VDC, VCHY	PDOP0004
COMMON/FN/DCH, HCH, DZ, ZL, ETHA, VG, VF, TCF	PDOP0005
COMMON/DC/ GA, GB, GC, GD, PA, PB, GIN, PIN, THE, CPP, CDT, RSS, HTK, HV,	PDOP0006
C HSU, HSL, HLP, HPI, HWV, DSL, DP, DSA, DBL, AP, ASH, ASHL, AENT,	PDOP0007
C AUP, AVI, AVO, PKN, PKO, PKP, PKS, PKD, PKV, PKR, FKUP, NOV	PDOP0008
IF(NC) 1, 2, 2	PDOP0009
1 DPFD=(FRIC(HIN, GTAV, 2.)/DTAV)*(GTAV**2.)*(HC+30.*DDC)/2.0	PDOP0010
DPTD=DPFD	PDOP0011
GO TO 4	PDOP0012
2 DENS=DAVDC(I, NC)	PDOP0013
ANOV=NOV	PDOP0014
GDC=(CHNT*ACH*GTAV)/(ADC*ANOV/4.0)	PDOP0015
DPFD=(FRIC(HAVP, GDC, 2.)/DENS)*(GDC**2.)*(HC+30.*DDC)/(2.0*DDC)	PDOP0016
DPVL=FKVO*(GDC**2.)/(2.00*DENS)	PDOP0017
DPUP=(1.-FKUP*NOV*AVO/AUP)*(GDC**2.)/(2.*DENS)	PDOP0018
DPTD=DPFD+DPVL+DPUP	PDOP0019
GO TO 4	PDOP0020
4 PDROP=DPTD	PDOP0021
RETURN	PDOP0022
END	PDOP0023

```
FUNCTION CP(HCP)
  IF(HCP .LT. 68.05) CP=0.9976
  IF(HCP .GE. 68.05 .AND. HCP .LT. 117.95)
I   CP=0.9976+0.00004*(HCP-68.05)
  IF(HCP .GE. 117.95 .AND. HCP .LT. 168.05)
I   CP=0.9996+0.0001*(HCP-117.95)
  IF(HCP .GE. 168.05 .AND. HCP .LT. 218.52)
I   CP=1.0047+0.00019*(HCP-168.05)
  IF(HCP .GE. 218.52 .AND. HCP .LT. 269.61)
I   CP=1.0142+0.00029*(HCP-218.52)
  IF(HCP .GE. 269.61) CP=1.0289+0.00048*(HCP-269.61)
  RETURN
END
```

```
CPCP0001
CPCP0002
CPCP0003
CPCP0004
CPCP0005
CPCP0006
CPCP0007
CPCP0008
CPCP0009
CPCP0010
CPCP0011
CPCP0012
CPCP0013
```

```
FUNCTION VISCH (HV)
  IF (HV .LE. 65.)
1   VISCH=(4.3E-04) - (0.1E-06) * (HV-65.)
  IF (HV .GT. 65. .AND. HV .LE. 120.)
2   VISCH=(4.6E-04) - (3.27E-06) * (HV-65.)
  IF (HV .GT. 120. .AND. HV .LE. 175.)
3   VISCH=(2.8E-04) - (1.81E-06) * (HV-120.)
  IF (HV .GT. 175.)
4   VISCH=(1.8E-04) - (0.29E-06) * (HV-175.)
  RETURN
END
```

```
VISC0001
VISC0002
VISC0003
VISC0004
VISC0005
VISC0006
VISC0007
VISC0008
VISC0009
VISC0010
VISC0011
```



```
FUNCTION DENSH(HD,XD)
COMMON/PN/DCH,HCH,DZ,ZL,ETHA,VG,VF,TCF
IF(HD-194.4) 3,3,1
3 DENSH=62.5-0.0167*(HD-18.06)
GO TO 2
1 VH=XD*VG+(1.-XD)*VF
DENSH=1./VH
GO TO 2
2 RETURN
END
```

```
DENS0001
DENS0002
DENS0003
DENS0004
DENS0005
DENS0006
DENS0007
DENS0008
DENS0009
DENS0010
```

```

FUNCTION HCC(HH, GH)
COMMON/FN/DCH, HCH, DZ, ZL, ETHA, VG, VF, TCF
VISC=VISC(HH)
RNH=GH*DCH/VISC
IF (RNH-2300.) 3, 1, 1
3 HCC=7.0*TCF/DCH
GO TO 2
1 HCC1=7.0*TCF/DCH
HCC2=0.023*(GH**0.8)*(CP(HH)**0.33)*(TCF**0.66)/((DCH**0.2)*(VISC
C **0.47))
IF (RNH-4000.) 4, 5, 5
4 HCC=HCC1+((HCC2-HCC1)/(4000.-2300.))* (RNH-2300.)
GO TO 2
5 HCC=HCC2
GO TO 2
2 RETURN
END

```

```

HCCH0001
HCCH0002
HCCH0003
HCCH0004
HCCH0005
HCCH0006
HCCH0007
HCCH0008
HCCH0009
HCCH0010
HCCH0011
HCCH0012
HCCH0013
HCCH0014
HCCH0015
HCCH0016
HCCH0017

```

PRINT ON THE FOLLOWING PAGES IS PARTIALLY ILLEGIBLE

AF,ACV,TL,PTI,CHN,CDT,CTS,ZL
 THM,GPM,HIN,PIH,THE,SPV,CP
 HSAT,FG,RC,BEEF,GAMA,FR,VTANK
 GA,GR,GC,GC,PA,PE
 DSL,DF,DDG,DSA,DBL,DCH,DCL,PP
 AP,ASF,ASHL,AFNT,AUP,AVI,AVO,ACH
 FKA,FAG,FKP,FKS,FKD,FEN,FKV,FKR
 HTK,HV,HC,FSU,FSL,HLP,HPI,CHYH
 FCM,HFIN,HFIN,FEEX,FKUP,ADC,ALK,RSS
 HFGTK,HSATK,VDC,VCHY,VG,VF,TCF,CHNT

	25	4	180.0000	50.0000	322.0000	7.7000	0.1000	1.9166
	0.50000E+01	0.20000E+04	0.72050E+02	0.73200E+02	0.40000E+02	0.16100E-01	0.12000E+01	
	0.19440E+03	0.96260E+03	0.37300E-01	0.78000E-02	0.50000E-01	0.12650E+01	0.10180E+03	
	0.22830E+01	0.10000E+00	0.22830E-01	0.12830E+01	0.48000E+00	0.20000E+01		
	0.20643E+00	0.62500E+00	0.13000E+00	0.58550E+00	0.23960E+00	0.73400E-02	0.55000E+01	0.36670E+00
	0.30680E+00	0.36480E+01	0.11930E+01	0.35550E+00	0.22060E+01	0.20600E-01	0.49100E-01	0.14100E-02
	0.31100E+00	0.10450E+01	0.84000E+00	0.90000E+00	0.49000E+00	0.10500E+01	0.19040E+03	0.57880E+02
	0.70400E+01	0.10000E+01	0.23500E+01	0.40000E+01	0.22500E+01	0.24000E+02	0.15000E+02	0.25000E+01
	0.40000E-02	0.83300E-03	0.83300E-03	0.10000E+01	0.19000E+01	0.31000E+00	0.24860E-01	0.49330E+03
	0.95390E+03	0.19040E+03	0.89170E+00	0.50370E+01	0.20090E+02	0.16800E-01	0.10900E-03	0.40500E+03
	0.12400E+02	0.75000E+01	0.60500E+01	0.55000E+01	0.59200E+01	0.58500E+01	FCZ	
	0.57200E+01	0.54000E+01	0.51000E+01	0.46500E+01	0.42500E+01	0.38000E+01	FCZ	
	0.35500E+01	0.34000E+01	0.37800E+01	0.33000E+01	0.31200E+01	0.28500E+01	FCZ	
	0.25500E+01	0.21500E+01	0.18000E+01	0.18500E+01	0.24000E+01	0.33000E+01	FCZ	
	0.21500E-03	0.12000E-01	DI,DLI					
	0.14200E-02	0.30500E-01	BI,DLI					
	0.12740E-02	0.11100E+00	PI,DLI					
	0.25600E-02	0.30100E+00	PI,DLI					
	0.74800E-03	0.11400E+01	BI,DLI					
	0.27300E-03	0.30100E+01	PI,DLI					
	0.15800E-02	0.27700E+00	Y,AL					
	0.49500E-03	0.16500E-01	Y,AL					
	0.17000E-03	0.48100E-02	Y,AL					
	0.81400E-04	0.15000E-02	Y,AL					
	0.50100E-04	0.42800E-03	Y,AL					
	0.56500E-04	0.11700E-03	Y,AL					
	0.78000E-05	0.43700E-04	Y,AL					
	0.25000E-05	0.36700E-05	Y,AL					

Information Processing Center

Information Processing Center

Information Processing Center

Information Processing Center

	PTU/LBM P(I,J)	O C TW(I,J)	LBM/S/FT**2 G(I,J)	LBM/FT**3 DEN(I,J)	X(I,J)	FCZA(I)
INITIAL CONDITION	0.72050E+02	0.69679E+02	0.90207E+03	0.61598E+02	-0.12708E+00	0.59422E-02
INITIAL CONDITION	0.75039E+02	0.59617E+02	0.90207E+03	0.61548E+02	-0.12397E+00	0.35941E-02
INITIAL CONDITION	0.77073E+02	0.57131E+02	0.90207E+03	0.61514E+02	-0.12186E+00	0.28592E-02
INITIAL CONDITION	0.78868E+02	0.57675E+02	0.90207E+03	0.61484E+02	-0.12000E+00	0.28273E-02
INITIAL CONDITION	0.80643E+02	0.58621E+02	0.90207E+03	0.61455E+02	-0.11815E+00	0.28369E-02
INITIAL CONDITION	0.82417E+02	0.59450E+02	0.90207E+03	0.61425E+02	-0.11631E+00	0.28225E-02
INITIAL CONDITION	0.84160E+02	0.59939E+02	0.90207E+03	0.61396E+02	-0.11450E+00	0.27411E-02
INITIAL CONDITION	0.85830E+02	0.60049E+02	0.90207E+03	0.61368E+02	-0.11276E+00	0.25877E-02
INITIAL CONDITION	0.87497E+02	0.60165E+02	0.90207E+03	0.61342E+02	-0.11113E+00	0.24440E-02
INITIAL CONDITION	0.88872E+02	0.59891E+02	0.90207E+03	0.61317E+02	-0.10961E+00	0.22283E-02
INITIAL CONDITION	0.90200E+02	0.59674E+02	0.90207E+03	0.61295E+02	-0.10822E+00	0.20366E-02
INITIAL CONDITION	0.91417E+02	0.59288E+02	0.90207E+03	0.61275E+02	-0.10696E+00	0.18210E-02
INITIAL CONDITION	0.92521E+02	0.59304E+02	0.90207E+03	0.61257E+02	-0.10582E+00	0.17012E-02
INITIAL CONDITION	0.93565E+02	0.59517E+02	0.90207E+03	0.61239E+02	-0.10473E+00	0.16293E-02
INITIAL CONDITION	0.94587E+02	0.60007E+02	0.90207E+03	0.61222E+02	-0.10367E+00	0.16197E-02
INITIAL CONDITION	0.95586E+02	0.60357E+02	0.90207E+03	0.61205E+02	-0.10263E+00	0.15814E-02
INITIAL CONDITION	0.96550E+02	0.60469E+02	0.90207E+03	0.61189E+02	-0.10163E+00	0.14951E-02
INITIAL CONDITION	0.97447E+02	0.60350E+02	0.90207E+03	0.61174E+02	-0.10070E+00	0.13657E-02
INITIAL CONDITION	0.98258E+02	0.60125E+02	0.90207E+03	0.61161E+02	-0.99857E-01	0.12220E-02
INITIAL CONDITION	0.98964E+02	0.59631E+02	0.90207E+03	0.61149E+02	-0.99124E-01	0.10303E-02
INITIAL CONDITION	0.99557E+02	0.59191E+02	0.90207E+03	0.61139E+02	-0.98508E-01	0.86258E-03
INITIAL CONDITION	0.10010E+03	0.59593E+02	0.90207E+03	0.61130E+02	-0.97938E-01	0.88654E-03
INITIAL CONDITION	0.10074E+03	0.61121E+02	0.90207E+03	0.61119E+02	-0.97275E-01	0.11501E-02
INITIAL CONDITION	0.10160E+03	0.63512E+02	0.90207E+03	0.61105E+02	-0.96386E-01	0.15814E-02
			TIN= 0.40005E+02	TOUT= 0.56436E+02		

SI	T=	DT=						PSAT=194.4 BTU/LBM
INCH	BTU/S/FT**2. QFIAV	BTU/LBM H(L,J)	C C Th(L,J)	LBM/S/FT**2 G(L,J)	LBM/FT**3 DEN(L,J)	X(L,J)	CONS(L,J)	
0	0.0	0.72050E+02	0.57646E+02	0.84916E+03	0.61598E+02	-0.12708E+00	-0.10000E-10	
1	0.12941E+03	0.76132E+02	0.52792E+02	0.84916E+03	0.61530E+02	-0.12271E+00	-0.10000E-10	
2	0.88114E+02	0.78909E+02	0.52218E+02	0.84916E+03	0.61484E+02	-0.11970E+00	-0.10000E-10	
3	0.77709E+02	0.81357E+02	0.53297E+02	0.84916E+03	0.61443E+02	-0.11703E+00	-0.10000E-10	
4	0.76864E+02	0.83778E+02	0.54596E+02	0.84916E+03	0.61403E+02	-0.11439E+00	-0.10000E-10	
5	0.76799E+02	0.86195E+02	0.55824E+02	0.84916E+03	0.61362E+02	-0.11175E+00	-0.10000E-10	
6	0.75458E+02	0.88570E+02	0.56843E+02	0.84916E+03	0.61322E+02	-0.10916E+00	-0.10000E-10	
7	0.72312E+02	0.90844E+02	0.57612E+02	0.84916E+03	0.61285E+02	-0.10667E+00	-0.10000E-10	
8	0.58280E+02	0.92989E+02	0.58348E+02	0.84916E+03	0.61249E+02	-0.10432E+00	-0.10000E-10	
9	0.63403E+02	0.94579E+02	0.58812E+02	0.84916E+03	0.61215E+02	-0.10212E+00	-0.10000E-10	
10	0.57876E+02	0.96793E+02	0.59256E+02	0.84916E+03	0.61185E+02	-0.10011E+00	-0.10000E-10	
11	0.52348E+02	0.98431E+02	0.59550E+02	0.84916E+03	0.61158E+02	-0.98286E-01	-0.10000E-10	
12	0.47796E+02	0.99924E+02	0.60028E+02	0.84916E+03	0.61133E+02	-0.96609E-01	-0.10000E-10	
13	0.45195E+02	0.10133E+03	0.60593E+02	0.84916E+03	0.61109E+02	-0.95018E-01	-0.10000E-10	
14	0.44089E+02	0.10271E+03	0.61304E+02	0.84916E+03	0.61086E+02	-0.93465E-01	-0.10000E-10	
15	0.43439E+02	0.10406E+03	0.61929E+02	0.84916E+03	0.61064E+02	-0.91934E-01	-0.10000E-10	
16	0.41748E+02	0.10536E+03	0.62401E+02	0.84916E+03	0.61042E+02	-0.90459E-01	-0.10000E-10	
17	0.38822E+02	0.10656E+03	0.62714E+02	0.84916E+03	0.61022E+02	-0.89081E-01	-0.10000E-10	
18	0.35116E+02	0.10765E+03	0.62930E+02	0.84916E+03	0.61004E+02	-0.87826E-01	-0.10000E-10	
19	0.30563E+02	0.10859E+03	0.62949E+02	0.84916E+03	0.60986E+02	-0.86722E-01	-0.10000E-10	
20	0.25686E+02	0.10938E+03	0.62948E+02	0.84916E+03	0.60975E+02	-0.85780E-01	-0.10000E-10	
21	0.23735E+02	0.11010E+03	0.63403E+02	0.84916E+03	0.60963E+02	-0.84902E-01	-0.10000E-10	
22	0.27637E+02	0.11095E+03	0.64529E+02	0.84916E+03	0.60949E+02	-0.83896E-01	-0.10000E-10	
23	0.37066E+02	0.11209E+03	0.66230E+02	0.84916E+03	0.60930E+02	-0.82579E-01	-0.10000E-10	
*****							PSAT=191.6 BTU/LBM	
51	T= 0.290	DT= 0.59727E-02	NAV= 0.95671E+02	GAV= 0.84916E+03	DAV= 0.61204E+02	TIN= 0.40005E+02	TOUT= 0.62261E+02	

Information Processing Center

Information Processing Center

Information Processing Center

Information Processing Center

11 T= 0.59817 DT= 0.56987E-02							
INCH	BTU/S/FT**2. QETAU	BTU/LBM H(I,J)	C C T(I,J)	LBM/S/FT**2 G(I,J)	LBM/FT**3 DEN(I,J)	X(I,J)	HSAT=194.4 BTU/LBM SCNF(I,J)
0	0.0	0.72050E+02	0.52810E+02	0.79481E+03	0.61598E+02	-0.12708E+00	-0.10000E-10
1	0.97662E+02	0.75208E+02	0.45421E+02	0.79481E+03	0.61546E+02	-0.12367E+00	-0.10000E-10
2	0.66499E+02	0.77723E+02	0.45284E+02	0.79481E+03	0.61504E+02	-0.12093E+00	-0.10000E-10
3	0.58647E+02	0.80050E+02	0.50375E+02	0.79481E+03	0.61465E+02	-0.11839E+00	-0.10000E-10
4	0.58009E+02	0.82360E+02	0.51628E+02	0.79481E+03	0.61426E+02	-0.11586E+00	-0.10000E-10
5	0.57959E+02	0.84665E+02	0.52829E+02	0.79481E+03	0.61388E+02	-0.11334E+00	-0.10000E-10
6	0.56978E+02	0.86935E+02	0.53874E+02	0.79481E+03	0.61350E+02	-0.11086E+00	-0.10000E-10
7	0.54573E+02	0.89118E+02	0.54729E+02	0.79481E+03	0.61313E+02	-0.10846E+00	-0.10000E-10
8	0.51530E+02	0.91179E+02	0.55543E+02	0.79481E+03	0.61279E+02	-0.10620E+00	-0.10000E-10
9	0.47850E+02	0.93086E+02	0.56136E+02	0.79481E+03	0.61247E+02	-0.10409E+00	-0.10000E-10
10	0.43678E+02	0.94810E+02	0.56683E+02	0.79481E+03	0.61218E+02	-0.10217E+00	-0.10000E-10
11	0.39507E+02	0.96337E+02	0.57083E+02	0.79481E+03	0.61193E+02	-0.10046E+00	-0.10000E-10
12	0.36071E+02	0.97683E+02	0.57576E+02	0.79481E+03	0.61170E+02	-0.98936E-01	-0.10000E-10
13	0.34108E+02	0.98894E+02	0.58092E+02	0.79481E+03	0.61150E+02	-0.97553E-01	-0.10000E-10
14	0.33274E+02	0.10001E+03	0.58677E+02	0.79481E+03	0.61131E+02	-0.96268E-01	-0.10000E-10
15	0.32783E+02	0.10105E+03	0.59167E+02	0.79481E+03	0.61114E+02	-0.95060E-01	-0.10000E-10
16	0.31507E+02	0.10200E+03	0.59517E+02	0.79481E+03	0.61098E+02	-0.93947E-01	-0.10000E-10
17	0.29259E+02	0.10293E+03	0.59723E+02	0.79481E+03	0.61084E+02	-0.92955E-01	-0.10000E-10
18	0.26501E+02	0.10354E+03	0.59832E+02	0.79481E+03	0.61073E+02	-0.92098E-01	-0.10000E-10
19	0.23066E+02	0.10409E+03	0.59771E+02	0.79481E+03	0.61063E+02	-0.91396E-01	-0.10000E-10
20	0.19365E+02	0.10449E+03	0.59673E+02	0.79481E+03	0.61057E+02	-0.90852E-01	-0.10000E-10
21	0.17913E+02	0.10482E+03	0.59896E+02	0.79481E+03	0.61051E+02	-0.90388E-01	-0.10000E-10
22	0.20858E+02	0.10522E+03	0.60614E+02	0.79481E+03	0.61044E+02	-0.89842E-01	-0.10000E-10
23	0.27974E+02	0.10587E+03	0.61776E+02	0.79481E+03	0.61034E+02	-0.89045E-01	-0.10000E-10

11 T= 0.598 DT= 0.56987E-02 HAV= 0.93043E+02 GAV= 0.79480E+03 DAV= 0.61248E+02 TIN= 0.40005E+02 TGUT= 0.58806E+02							

Information Processing Center

Information Processing Center

Information Processing Center

Information Processing Center

61 T= 0.93034 DT= 0.69069E-02

INCH	BTU/S/FT**2. QFIAY	BTU/LBM H(L,J)	C C T(L,J)	LBM/S/FT**2 G(L,J)	LBM/FT**3 DEN(L,J)	X(L,J)	HSAT=194.4 BTU/LBM SCNP(L,J)
C	0.0	0.72050E+C2	0.46350E+02	0.73827E+03	0.61598E+02	-0.12708E+00	-0.10000E-10
1	0.41624E+02	0.73577E+C2	0.44672E+02	0.73827E+03	0.61573E+02	-0.12536E+00	-0.10000E-10
2	0.28342E+02	0.74643E+C2	0.44516E+02	0.73827E+03	0.61555E+02	-0.12413E+00	-0.10000E-10
3	0.24995E+02	0.75604E+C2	0.44964E+02	0.73827E+03	0.61539E+02	-0.12301E+00	-0.10000E-10
4	0.24723E+02	0.76571E+C2	0.45502E+02	0.73827E+03	0.61523E+02	-0.12188E+00	-0.10000E-10
5	0.24702E+02	0.77552E+C2	0.46022E+02	0.73827E+03	0.61506E+02	-0.12073E+00	-0.10000E-10
6	0.24284E+02	0.78532E+C2	0.46472E+02	0.73827E+03	0.61490E+02	-0.11959E+00	-0.10000E-10
7	0.23259E+02	0.79491E+C2	0.46835E+02	0.73827E+03	0.61474E+02	-0.11846E+00	-0.10000E-10
8	0.21962E+02	0.80415E+C2	0.47192E+02	0.73827E+03	0.61459E+02	-0.11739E+00	-0.10000E-10
9	0.20394E+02	0.81296E+C2	0.47451E+02	0.73827E+03	0.61444E+02	-0.11634E+00	-0.10000E-10
10	0.18616E+02	0.82123E+C2	0.47706E+02	0.73827E+03	0.61430E+02	-0.11535E+00	-0.10000E-10
11	0.16838E+02	0.82997E+C2	0.47909E+02	0.73827E+03	0.61417E+02	-0.11442E+00	-0.10000E-10
12	0.15374E+02	0.83626E+C2	0.48187E+02	0.73827E+03	0.61405E+02	-0.11354E+00	-0.10000E-10
13	0.14537E+02	0.84335E+C2	0.48503E+02	0.73827E+03	0.61393E+02	-0.11267E+00	-0.10000E-10
14	0.14181E+02	0.85038E+C2	0.48880E+02	0.73827E+03	0.61381E+02	-0.11182E+00	-0.10000E-10
15	0.13972E+02	0.85742E+C2	0.49228E+02	0.73827E+03	0.61370E+02	-0.11096E+00	-0.10000E-10
16	0.13428E+02	0.86434E+C2	0.49521E+02	0.73827E+03	0.61358E+02	-0.11011E+00	-0.10000E-10
17	0.12487E+02	0.87100E+C2	0.49757E+02	0.73827E+03	0.61347E+02	-0.10930E+00	-0.10000E-10
18	0.11295E+02	0.87729E+C2	0.49958E+02	0.73827E+03	0.61337E+02	-0.10852E+00	-0.10000E-10
19	0.98307E+01	0.88310E+C2	0.50086E+02	0.73827E+03	0.61327E+02	-0.10779E+00	-0.10000E-10
20	0.92620E+01	0.88835E+C2	0.50210E+02	0.73827E+03	0.61318E+02	-0.10711E+00	-0.10000E-10
21	0.76345E+01	0.89349E+C2	0.50516E+02	0.73827E+03	0.61309E+02	-0.10645E+00	-0.10000E-10
22	0.88895E+01	0.89910E+C2	0.51088E+02	0.73827E+03	0.61300E+02	-0.10575E+00	-0.10000E-10
23	0.11922E+02	0.90587E+C2	0.51891E+02	0.73827E+03	0.61289E+02	-0.10492E+00	-0.10000E-10

61 T= 0.930 DT= 0.69069E-02 HAV= 0.82152E+02 GAV= 0.73827E+03 DAV= 0.61430E+02 TIN= 0.40095E+02 TOUT= 0.50317E+C2

HSAT=191.6 ETU/LBM

Information Processing Center

Information Processing Center

Information Processing Center

Information Processing Center

21 T= 1.2E893 DT= 0.74937E-02								HSAT=194.4 BTU/LBM
INCH	BTU/S/FT**2. GFIAY	BTU/LBM H(I,J)	C C Tn(I,J)	LBM/S/FT**2 G(I,J)	LBM/FT**3 DEN(I,J)	X(I,J)	CCNR(I,J)	
C	C.0	0.72C5CE+C2	0.44487E+02	0.67956E+03	0.61598E+02	-0.12708E+00	-0.1CC0CE-10	
1	0.27521E+02	0.73137E+C2	0.42311E+02	0.67956E+03	0.61580E+02	-0.12582E+00	-0.1CC0CE-10	
2	0.18739E+02	0.73872E+C2	0.43195E+02	0.67956E+03	0.61568E+02	-0.12493E+00	-0.1CC0CE-10	
3	0.16527E+02	0.74530E+C2	0.42499E+02	0.67956E+03	0.61557E+02	-0.12412E+00	-0.1CC0CE-10	
4	0.16347E+02	0.75176E+C2	0.43861E+02	0.67956E+03	0.61546E+02	-0.12332E+00	-0.1CC0CE-10	
5	0.16333E+02	0.75822E+C2	0.44205E+02	0.67956E+03	0.61535E+02	-0.12253E+00	-0.1CC0CE-10	
6	0.16056E+02	0.76460E+C2	0.44495E+02	0.67956E+03	0.61525E+02	-0.12174E+00	-0.1CC0CE-10	
7	0.15379E+02	0.77077E+C2	0.44720E+02	0.67956E+03	0.61514E+02	-0.12097E+00	-0.1CC0CE-10	
8	0.14521E+02	0.77678E+C2	0.44942E+02	0.67956E+03	0.61504E+02	-0.12022E+00	-0.1CC0CE-10	
9	0.13484E+02	0.78262E+C2	0.45106E+02	0.67956E+03	0.61495E+02	-0.11949E+00	-0.1CC0CE-10	
10	0.12309E+02	0.78847E+C2	0.45207E+02	0.67956E+03	0.61485E+02	-0.11875E+00	-0.1CC0CE-10	
11	0.11133E+02	0.79455E+C2	0.45463E+02	0.67956E+03	0.61475E+02	-0.11800E+00	-0.1CC0CE-10	
12	0.10165E+02	0.80116E+C2	0.45740E+02	0.67956E+03	0.61464E+02	-0.11718E+00	-0.1CC0CE-10	
13	0.96117E+01	0.80867E+C2	0.46102E+02	0.67956E+03	0.61451E+02	-0.11628E+00	-0.1CC0CE-10	
14	0.93766E+01	0.81739E+C2	0.46576E+02	0.67956E+03	0.61437E+02	-0.11524E+00	-0.1CC0CE-10	
15	0.92383E+01	0.82742E+C2	0.47101E+02	0.67956E+03	0.61420E+02	-0.11408E+00	-0.1CC0CE-10	
16	0.88787E+01	0.83869E+C2	0.47661E+02	0.67956E+03	0.61401E+02	-0.11278E+00	-0.1CC0CE-10	
17	0.82564E+01	0.85100E+C2	0.48248E+02	0.67956E+03	0.61380E+02	-0.11137E+00	-0.1CC0CE-10	
18	0.74681E+01	0.86416E+C2	0.48872E+02	0.67956E+03	0.61358E+02	-0.10988E+00	-0.1CC0CE-10	
19	0.65000E+01	0.87787E+C2	0.49493E+02	0.67956E+03	0.61336E+02	-0.10833E+00	-0.1CC0CE-10	
20	0.54528E+01	0.89186E+C2	0.50148E+02	0.67956E+03	0.61312E+02	-0.10675E+00	-0.1CC0CE-10	
21	0.50479E+01	0.90612E+C2	0.50954E+02	0.67956E+03	0.61288E+02	-0.10514E+00	-0.1CC0CE-10	
22	0.5*777E+01	0.92089E+C2	0.51956E+02	0.67956E+03	0.61264E+02	-0.10348E+00	-0.1CC0CE-10	
23	0.72830E+01	0.93639E+C2	0.53111E+02	0.67956E+03	0.61238E+02	-0.10175E+00	-0.1CC0CE-10	
*****							HSAT=151.6 BTU/LBM	
21	T= 1.289	DT= 0.74937E-02	HAY= 0.80743E+02	GAY= 0.67956E+03	DAY= 0.61453E+02	TIN= 0.40005E+C2	TOUT= 0.52014E+C2	

Information Processing Center

Information Processing Center

Information Processing Center

Information Processing Center

71	T= 1.68312	DT= 0.82686E-02						HSAT=194.4 BTU/LBM
INCH	BTU/S/FT**2 Q(TAV)	BTU/LBM H(I,J)	C C T(I,J)	LBM/S/FT**2 G(I,J)	LBM/FT**3 DEN(I,J)	X(I,J)	CCR(I,J)	
0	0.0	0.72050E+02	0.44490E+02	0.61770E+03	0.61598E+02	-0.12708E+00	-0.10000E-10	
1	0.25521E+02	0.73161E+02	0.43324E+02	0.61770E+03	0.61580E+02	-0.12580E+00	-0.10000E-10	
2	0.17377E+02	0.73511E+02	0.43218E+02	0.61770E+03	0.61567E+02	-0.12488E+00	-0.10000E-10	
3	0.15325E+02	0.74584E+02	0.43530E+02	0.61770E+03	0.61556E+02	-0.12407E+00	-0.10000E-10	
4	0.15159E+02	0.75243E+02	0.42859E+02	0.61770E+03	0.61545E+02	-0.12325E+00	-0.10000E-10	
5	0.15146E+02	0.75502E+02	0.44250E+02	0.61770E+03	0.61534E+02	-0.12244E+00	-0.10000E-10	
6	0.14889E+02	0.76549E+02	0.44545E+02	0.61770E+03	0.61523E+02	-0.12165E+00	-0.10000E-10	
7	0.14261E+02	0.77169E+02	0.44771E+02	0.61770E+03	0.61513E+02	-0.12088E+00	-0.10000E-10	
8	0.13466E+02	0.77753E+02	0.44986E+02	0.61770E+03	0.61503E+02	-0.12014E+00	-0.10000E-10	
9	0.12504E+02	0.78296E+02	0.45126E+02	0.61770E+03	0.61494E+02	-0.11945E+00	-0.10000E-10	
10	0.11414E+02	0.78791E+02	0.45257E+02	0.61770E+03	0.61486E+02	-0.11881E+00	-0.10000E-10	
11	0.10324E+02	0.79238E+02	0.45345E+02	0.61770E+03	0.61478E+02	-0.11822E+00	-0.10000E-10	
12	0.94261E+01	0.79646E+02	0.45482E+02	0.61770E+03	0.61472E+02	-0.11767E+00	-0.10000E-10	
13	0.89131E+01	0.80032E+02	0.45642E+02	0.61770E+03	0.61465E+02	-0.11714E+00	-0.10000E-10	
14	0.86351E+01	0.80408E+02	0.45842E+02	0.61770E+03	0.61459E+02	-0.11663E+00	-0.10000E-10	
15	0.85668E+01	0.80778E+02	0.46018E+02	0.61770E+03	0.61453E+02	-0.11612E+00	-0.10000E-10	
16	0.82334E+01	0.81133E+02	0.46152E+02	0.61770E+03	0.61447E+02	-0.11562E+00	-0.10000E-10	
17	0.76563E+01	0.81464E+02	0.46240E+02	0.61770E+03	0.61441E+02	-0.11515E+00	-0.10000E-10	
18	0.69253E+01	0.81762E+02	0.46300E+02	0.61770E+03	0.61436E+02	-0.11471E+00	-0.10000E-10	
19	0.60276E+01	0.82021E+02	0.46304E+02	0.61770E+03	0.61432E+02	-0.11432E+00	-0.10000E-10	
20	0.50457E+01	0.82238E+02	0.46302E+02	0.61770E+03	0.61428E+02	-0.11397E+00	-0.10000E-10	
21	0.46810E+01	0.82439E+02	0.46430E+02	0.61770E+03	0.61425E+02	-0.11363E+00	-0.10000E-10	
22	0.54505E+01	0.82673E+02	0.46751E+02	0.61770E+03	0.61421E+02	-0.11326E+00	-0.10000E-10	
23	0.73100E+01	0.82588E+02	0.47238E+02	0.61770E+03	0.61416E+02	-0.11281E+00	-0.10000E-10	
*****							HSAT=191.6 BTU/LBM	
71	T= 1.683	DT= 0.82686E-02	HAV= 0.78491E+02	GAV= 0.61770E+03	DAV= 0.61491E+02	TIN= 0.40005E+02	TCUT= 0.46091E+02	

Information Processing Center

Information Processing Center

Information Processing Center

Information Processing Center

INCH	BTU/S/FT**2. QFIAY	BTU/LBM H(I,J)	C C T(I,J)	LBM/S/FT**2 G(I,J)	LBM/FT**3 DEN(I,J)	X(I,J)	HSAT=194.4 BTU/LBM (CNR(I,J))	
31	T= 2.11642		DT= 0.92332E-02					
0	0.0	0.72050E+C2	0.44597E+02	0.55283E+03	0.61596E+02	-0.12708E+00	-0.10000E-10	
1	0.23921E+02	0.73213E+C2	0.43419E+02	0.55283E+03	0.61579E+02	-0.12574E+00	-0.10000E-10	
2	0.16288E+02	0.74004E+C2	0.43318E+02	0.55283E+03	0.61566E+02	-0.12479E+00	-0.10000E-10	
3	0.14364E+02	0.74701E+C2	0.43645E+02	0.55283E+03	0.61554E+02	-0.12394E+00	-0.10000E-10	
4	0.14208E+02	0.75390E+C2	0.44031E+02	0.55283E+03	0.61543E+02	-0.12310E+00	-0.10000E-10	
5	0.14196E+02	0.76078E+C2	0.44397E+02	0.55283E+03	0.61531E+02	-0.12226E+00	-0.10000E-10	
6	0.13956E+02	0.76753E+C2	0.44706E+02	0.55283E+03	0.61520E+02	-0.12143E+00	-0.10000E-10	
7	0.13367E+02	0.77400E+C2	0.44944E+02	0.55283E+03	0.61509E+02	-0.12064E+00	-0.10000E-10	
8	0.12621E+02	0.78097E+C2	0.45171E+02	0.55283E+03	0.61499E+02	-0.11988E+00	-0.10000E-10	
9	0.11720E+02	0.78775E+C2	0.45318E+02	0.55283E+03	0.61486E+02	-0.11916E+00	-0.10000E-10	
10	0.10698E+02	0.79090E+C2	0.45458E+02	0.55283E+03	0.61481E+02	-0.11850E+00	-0.10000E-10	
11	0.95764E+01	0.79555E+C2	0.45591E+02	0.55283E+03	0.61473E+02	-0.11789E+00	-0.10000E-10	
12	0.88350E+01	0.79979E+C2	0.45695E+02	0.55283E+03	0.61466E+02	-0.11732E+00	-0.10000E-10	
13	0.83542E+01	0.80379E+C2	0.45862E+02	0.55283E+03	0.61459E+02	-0.11678E+00	-0.10000E-10	
14	0.81498E+01	0.80769E+C2	0.46070E+02	0.55283E+03	0.61453E+02	-0.11625E+00	-0.10000E-10	
15	0.80296E+01	0.81155E+C2	0.46254E+02	0.55283E+03	0.61446E+02	-0.11572E+00	-0.10000E-10	
16	0.77171E+01	0.81526E+C2	0.46394E+02	0.55283E+03	0.61440E+02	-0.11521E+00	-0.10000E-10	
17	0.71762E+01	0.81874E+C2	0.46490E+02	0.55283E+03	0.61434E+02	-0.11472E+00	-0.10000E-10	
18	0.64910E+01	0.82194E+C2	0.46560E+02	0.55283E+03	0.61429E+02	-0.11427E+00	-0.10000E-10	
19	0.56496E+01	0.82481E+C2	0.46576E+02	0.55283E+03	0.61424E+02	-0.11384E+00	-0.10000E-10	
20	0.47480E+01	0.82739E+C2	0.46594E+02	0.55283E+03	0.61420E+02	-0.11345E+00	-0.10000E-10	
21	0.43874E+01	0.82998E+C2	0.46755E+02	0.55283E+03	0.61416E+02	-0.11305E+00	-0.10000E-10	
22	0.51087E+01	0.83320E+C2	0.47129E+02	0.55283E+03	0.61410E+02	-0.11259E+00	-0.10000E-10	
23	0.68516E+01	0.83762E+C2	0.47693E+02	0.55283E+03	0.61403E+02	-0.11200E+00	-0.10000E-10	
31	T= 2.116		DT= 0.92332E-02	HAV= 0.78802E+02	GAV= 0.55282E+03	DAV= 0.61485E+02	TJN= 0.40005E+02	TCUT= C.46522E+C2

Information Processing Center

Information Processing Center

Information Processing Center

Information Processing Center

BI	T= 2.61017	DT= 0.10567E-01						HSAT=194.4 BTU/LBM
INCH	BTU/S/FT**2 QFTAV	BTU/LBM HLI,J)	C C TH(I,J)	LBM/S/FT**2 G(I,J)	LBM/FT**3 DEN(I,J)	X(I,J)	CCR(I,J)	
0	0.0	0.72050E+02	0.44818E+02	0.48271E+03	0.61598E+02	-0.12708E+00	-0.10000E-10	
1	0.22500E+02	0.73302E+02	0.43600E+02	0.48271E+03	0.61577E+02	-0.12565E+00	-0.10000E-10	
2	0.15320E+02	0.74153E+02	0.43506E+02	0.48271E+03	0.61563E+02	-0.12464E+00	-0.10000E-10	
3	0.13511E+02	0.74502E+02	0.42859E+02	0.48271E+03	0.61551E+02	-0.12374E+00	-0.10000E-10	
4	0.13364E+02	0.75443E+02	0.44273E+02	0.48271E+03	0.61538E+02	-0.12284E+00	-0.10000E-10	
5	0.13353E+02	0.76382E+02	0.44667E+02	0.48271E+03	0.61526E+02	-0.12195E+00	-0.10000E-10	
6	0.13127E+02	0.77108E+02	0.45000E+02	0.48271E+03	0.61514E+02	-0.12107E+00	-0.10000E-10	
7	0.12573E+02	0.77602E+02	0.45259E+02	0.48271E+03	0.61502E+02	-0.12022E+00	-0.10000E-10	
8	0.11872E+02	0.78457E+02	0.45505E+02	0.48271E+03	0.61491E+02	-0.11941E+00	-0.10000E-10	
9	0.11024E+02	0.79064E+02	0.45668E+02	0.48271E+03	0.61481E+02	-0.11865E+00	-0.10000E-10	
10	0.10063E+02	0.79616E+02	0.45821E+02	0.48271E+03	0.61472E+02	-0.11795E+00	-0.10000E-10	
11	0.91017E+01	0.80115E+02	0.45925E+02	0.48271E+03	0.61464E+02	-0.11731E+00	-0.10000E-10	
12	0.83102E+01	0.80569E+02	0.46081E+02	0.48271E+03	0.61456E+02	-0.11671E+00	-0.10000E-10	
13	0.78580E+01	0.80997E+02	0.46261E+02	0.48271E+03	0.61449E+02	-0.11614E+00	-0.10000E-10	
14	0.76658E+01	0.81414E+02	0.46484E+02	0.48271E+03	0.61442E+02	-0.11558E+00	-0.10000E-10	
15	0.75527E+01	0.81824E+02	0.46680E+02	0.48271E+03	0.61435E+02	-0.11503E+00	-0.10000E-10	
16	0.72537E+01	0.82219E+02	0.46830E+02	0.48271E+03	0.61429E+02	-0.11449E+00	-0.10000E-10	
17	0.67450E+01	0.82583E+02	0.46930E+02	0.48271E+03	0.61422E+02	-0.11399E+00	-0.10000E-10	
18	0.61055E+01	0.82912E+02	0.47000E+02	0.48271E+03	0.61417E+02	-0.11352E+00	-0.10000E-10	
19	0.53140E+01	0.83196E+02	0.47008E+02	0.48271E+03	0.61412E+02	-0.11310E+00	-0.10000E-10	
20	0.44660E+01	0.83433E+02	0.47009E+02	0.48271E+03	0.61408E+02	-0.11273E+00	-0.10000E-10	
21	0.41268E+01	0.83650E+02	0.47148E+02	0.48271E+03	0.61405E+02	-0.11237E+00	-0.10000E-10	
22	0.48052E+01	0.83906E+02	0.47494E+02	0.48271E+03	0.61400E+02	-0.11198E+00	-0.10000E-10	
23	0.64447E+01	0.84252E+02	0.48019E+02	0.48271E+03	0.61395E+02	-0.11150E+00	-0.10000E-10	
*****							HSAT=151.6 BTU/LBM	
BI	T= 2.610	DT= 0.10567E-01	HAV= 0.75264E+02	GAV= 0.48270E+03	DAV= 0.61472E+02	TIN= 0.40005E+02	TCUT= 0.46755E+02	

Information Processing Center

Information Processing Center

Information Processing Center

Information Processing Center

41	T= 3.17849	D1= 0.12524E-01						HSAT=194.4 BTU/LBM
INCH	BTU/S/FT**2 QF(AV)	BTU/LBM H(I,J)	C C Tb(I,J)	LBM/S/FT**2 G(I,J)	LBM/FT**3 DEN(I,J)	X(I,J)	CONB(I,J)	
0	0.0	0.72050E+C2	0.45198E+02	0.40677E+03	0.61598E+02	-0.12708E+00	-0.10000E-10	
1	0.21186E+02	0.73447E+C2	0.43908E+02	0.40677E+03	0.61575E+02	-0.12550E+00	-0.10000E-10	
2	0.14426E+02	0.74396E+C2	0.43823E+02	0.40677E+03	0.61559E+02	-0.12439E+00	-0.10000E-10	
3	0.12722E+02	0.75230E+C2	0.44218E+02	0.40677E+03	0.61545E+02	-0.12339E+00	-0.10000E-10	
4	0.12584E+02	0.76055E+C2	0.44678E+02	0.40677E+03	0.61531E+02	-0.12241E+00	-0.10000E-10	
5	0.12573E+02	0.76879E+C2	0.45116E+02	0.40677E+03	0.61518E+02	-0.12143E+00	-0.10000E-10	
6	0.12340E+02	0.77685E+C2	0.45488E+02	0.40677E+03	0.61504E+02	-0.12047E+00	-0.10000E-10	
7	0.11839E+02	0.78456E+C2	0.45780E+02	0.40677E+03	0.61491E+02	-0.11954E+00	-0.10000E-10	
8	0.11179E+02	0.79183E+C2	0.46054E+02	0.40677E+03	0.61479E+02	-0.11866E+00	-0.10000E-10	
9	0.10380E+02	0.79956E+C2	0.46242E+02	0.40677E+03	0.61468E+02	-0.11783E+00	-0.10000E-10	
10	0.94752E+01	0.80468E+C2	0.46416E+02	0.40677E+03	0.61458E+02	-0.11707E+00	-0.10000E-10	
11	0.85703E+01	0.81020E+C2	0.46537E+02	0.40677E+03	0.61449E+02	-0.11637E+00	-0.10000E-10	
12	0.78251E+01	0.81521E+C2	0.46712E+02	0.40677E+03	0.61440E+02	-0.11572E+00	-0.10000E-10	
13	0.73952E+01	0.81994E+C2	0.46911E+02	0.40677E+03	0.61432E+02	-0.11511E+00	-0.10000E-10	
14	0.72182E+01	0.82453E+C2	0.47157E+02	0.40677E+03	0.61425E+02	-0.11450E+00	-0.10000E-10	
15	0.71118E+01	0.82906E+C2	0.47374E+02	0.40677E+03	0.61417E+02	-0.11391E+00	-0.10000E-10	
16	0.68350E+01	0.83239E+C2	0.47540E+02	0.40677E+03	0.61410E+02	-0.11333E+00	-0.10000E-10	
17	0.63559E+01	0.83740E+C2	0.47653E+02	0.40677E+03	0.61403E+02	-0.11279E+00	-0.10000E-10	
18	0.57490E+01	0.84100E+C2	0.47731E+02	0.40677E+03	0.61397E+02	-0.11229E+00	-0.10000E-10	
19	0.50038E+01	0.84410E+C2	0.47743E+02	0.40677E+03	0.61392E+02	-0.11184E+00	-0.10000E-10	
20	0.42053E+01	0.84667E+C2	0.47745E+02	0.40677E+03	0.61388E+02	-0.11144E+00	-0.10000E-10	
21	0.38859E+01	0.84903E+C2	0.47895E+02	0.40677E+03	0.61384E+02	-0.11107E+00	-0.10000E-10	
22	0.45247E+01	0.85181E+C2	0.48268E+02	0.40677E+03	0.61379E+02	-0.11066E+00	-0.10000E-10	
23	0.60684E+01	0.85560E+C2	0.48836E+02	0.40677E+03	0.61373E+02	-0.11014E+00	-0.10000E-10	
41	T= 3.178	D1= 0.12524E-01	MAV= 0.80062E+02	GAV= 0.40677E+03	DAV= 0.61464E+02	TIN= 0.40005E+02	TCUT= 0.47522E+02	HSAT=191.6 BTU/LBM

Information Processing Center

Information Processing Center

Information Processing Center

Information Processing Center

91 T= 3.8820 DT= 0.15906E-01							
INCH	BTU/S/FT**2. QETA	BTU/LPM H(I,J)	C C Tn(I,J)	LRM/S/FT**2 G(I,J)	LBM/FT**3 DEN(I,J)	X(I,J)	PSAT=194.4 BTU/LBM CCNB(I,J)
0	0.0	0.72050E+02	0.45994E+02	0.31945E+03	0.61598E+02	-0.12708E+00	-0.10000E-10
1	0.19869E+02	0.73713E+02	0.44478E+02	0.31945E+03	0.61571E+02	-0.12522E+00	-0.10000E-10
2	0.13529E+02	0.74641E+02	0.44408E+02	0.31945E+03	0.61552E+02	-0.12393E+00	-0.10000E-10
3	0.11931E+02	0.75832E+02	0.44879E+02	0.31945E+03	0.61535E+02	-0.12277E+00	-0.10000E-10
4	0.11801E+02	0.76810E+02	0.45423E+02	0.31945E+03	0.61519E+02	-0.12163E+00	-0.10000E-10
5	0.11791E+02	0.77784E+02	0.45941E+02	0.31945E+03	0.61503E+02	-0.12049E+00	-0.10000E-10
6	0.11572E+02	0.78739E+02	0.46384E+02	0.31945E+03	0.61487E+02	-0.11937E+00	-0.10000E-10
7	0.11102E+02	0.79650E+02	0.46734E+02	0.31945E+03	0.61471E+02	-0.11830E+00	-0.10000E-10
8	0.10483E+02	0.80508E+02	0.47064E+02	0.31945E+03	0.61457E+02	-0.11728E+00	-0.10000E-10
9	0.97346E+01	0.81300E+02	0.47291E+02	0.31945E+03	0.61444E+02	-0.11637E+00	-0.10000E-10
10	0.88859E+01	0.82019E+02	0.47502E+02	0.31945E+03	0.61432E+02	-0.11546E+00	-0.10000E-10
11	0.80373E+01	0.82665E+02	0.47651E+02	0.31945E+03	0.61421E+02	-0.11466E+00	-0.10000E-10
12	0.73364E+01	0.83251E+02	0.47859E+02	0.31945E+03	0.61411E+02	-0.11393E+00	-0.10000E-10
13	0.69390E+01	0.83802E+02	0.48093E+02	0.31945E+03	0.61402E+02	-0.11323E+00	-0.10000E-10
14	0.67673E+01	0.84338E+02	0.48379E+02	0.31945E+03	0.61393E+02	-0.11254E+00	-0.10000E-10
15	0.66695E+01	0.84864E+02	0.48632E+02	0.31945E+03	0.61384E+02	-0.11187E+00	-0.10000E-10
16	0.64079E+01	0.85366E+02	0.48827E+02	0.31945E+03	0.61376E+02	-0.11122E+00	-0.10000E-10
17	0.59606E+01	0.85830E+02	0.48960E+02	0.31945E+03	0.61368E+02	-0.11061E+00	-0.10000E-10
18	0.53915E+01	0.86246E+02	0.49054E+02	0.31945E+03	0.61361E+02	-0.11004E+00	-0.10000E-10
19	0.46926E+01	0.86601E+02	0.49070E+02	0.31945E+03	0.61355E+02	-0.10956E+00	-0.10000E-10
20	0.39438E+01	0.86893E+02	0.49074E+02	0.31945E+03	0.61350E+02	-0.10913E+00	-0.10000E-10
21	0.36442E+01	0.87160E+02	0.49243E+02	0.31945E+03	0.61346E+02	-0.10873E+00	-0.10000E-10
22	0.42433E+01	0.87476E+02	0.49665E+02	0.31945E+03	0.61341E+02	-0.10827E+00	-0.10000E-10
23	0.56910E+01	0.87513E+02	0.50310E+02	0.31945E+03	0.61333E+02	-0.10769E+00	-0.10000E-10
*****							HSAT=191.6 BTU/LBM
91	T= 3.882	DT= 0.15906E-01	HAV= 0.81508E+02	GAV= 0.31945E+03	DAV= 0.61440E+02	TIN= 0.40005E+02	TOUT= 0.48830E+02

Information Processing Center

Information Processing Center

Information Processing Center

Information Processing Center

NATURAL CONVECTION VALVE OPENS

51	T= 5.60200	DT= 0.10000E+00						HSAT=194.4 BTU/LBM
INCH	BTU/S/FT**2. QF(TAV)	BTU/LBM H(I,J)	C C TMI(I,J)	LBM/S/FT**2 G(I,J)	LBM/FT**3 DEN(I,J)	X(I,J)	(CNR(I,J))	
0	0.0	0.72111E+C2	0.68653E+02	0.78968E+01	0.61597E+02	-0.12701E+C0	-0.10000E-10	
1	0.17505E+02	0.84604E+C2	0.57343E+02	0.78695E+01	0.61385E+02	-0.11391E+C0	-0.10000E-10	
2	0.11919E+02	0.93273E+C2	0.60949E+02	0.78508E+01	0.61244E+02	-0.10478E+C0	-0.10000E-10	
3	0.10512E+02	0.10098E+C3	0.65423E+02	0.78341E+01	0.61115E+02	-0.96651E-C1	-0.10000E-10	
4	0.10397E+02	0.10853E+C3	0.69750E+02	0.78176E+01	0.60989E+02	-0.88679E-01	-0.10000E-10	
5	0.10389E+02	0.11586E+C3	0.72875E+02	0.78017E+01	0.60867E+02	-0.80938E-C1	-0.10000E-10	
6	0.10213E+02	0.12270E+C3	0.77551E+02	0.77869E+01	0.60753E+02	-0.73716E-C1	-0.10000E-10	
7	0.97817E+01	0.12869E+C3	0.80593E+02	0.77738E+01	0.60652E+02	-0.67361E-C1	-0.10000E-10	
8	0.92363E+01	0.13366E+C3	0.83212E+02	0.77629E+01	0.60569E+02	-0.62075E-C1	-0.10000E-10	
9	0.85766E+01	0.13746E+C3	0.84914E+02	0.77546E+01	0.60506E+02	-0.59003E-01	-0.10000E-10	
10	0.78289E+01	0.14002E+C3	0.86084E+02	0.77490E+01	0.60463E+02	-0.55216E-01	-0.10000E-10	
11	0.70812E+01	0.14139E+C3	0.86456E+02	0.77459E+01	0.60440E+02	-0.53667E-C1	-0.10000E-10	
12	0.64654E+01	0.14175E+C3	0.86634E+02	0.77450E+01	0.60434E+02	-0.53169E-C1	-0.10000E-10	
13	0.61136E+01	0.14140E+C3	0.86485E+02	0.78587E+01	0.60440E+02	-0.53407E-C1	-0.10000E-10	
14	0.59640E+01	0.14061E+C3	0.86246E+02	0.79740E+01	0.60453E+02	-0.54101E-C1	-0.10000E-10	
15	0.58761E+01	0.13955E+C3	0.85626E+02	0.80911E+01	0.60471E+02	-0.55078E-C1	-0.10000E-10	
16	0.56474E+01	0.13822E+C3	0.84626E+02	0.82098E+01	0.60493E+02	-0.56322E-C1	-0.10000E-10	
17	0.52515E+01	0.13652E+C3	0.83276E+02	0.83302E+01	0.60520E+02	-0.57858E-C1	-0.10000E-10	
18	0.47501E+01	0.13474E+C3	0.81702E+02	0.84523E+01	0.60551E+02	-0.59685E-C1	-0.10000E-10	
19	0.41344E+01	0.13256E+C3	0.79743E+02	0.85762E+01	0.60588E+02	-0.61829E-01	-0.10000E-10	
20	0.34746E+01	0.13007E+C3	0.77731E+02	0.87018E+01	0.60629E+02	-0.64284E-C1	-0.10000E-10	
21	0.32197E+01	0.12759E+C3	0.76475E+02	0.88292E+01	0.60671E+02	-0.66734E-C1	-0.10000E-10	
22	0.37385E+01	0.12569E+C3	0.76375E+02	0.89584E+01	0.60702E+02	-0.68579E-C1	-0.10000E-10	
23	0.50140E+01	0.12492E+C3	0.77404E+02	0.90893E+01	0.60715E+02	-0.69251E-C1	-0.10000E-10	

51	T= 5.602	DT= 0.10000E+00	MAV= 0.12261E+03	GAV= 0.80898E+01	DAV= 0.60754E+02	TIN= 0.40039E+02	TCUT= 0.69365E+C2	

Information Processing Centre

Information Processing Centre

Information Processing Centre

Information Processing Centre

11 T= 10.43512 DT= 0.10000E+00							
INCH	BTU/S/FT**2 Q(TAV)	BTU/LBM H(I,J)	C C T(I,J)	LBM/S/FT**2 G(I,J)	LBM/FT**3 DEN(I,J)	X(I,J)	PSAT=194.4 BTU/LBM CORR(I,J)
C	0.0	C.72555E+C2	0.62473E+02	0.11237E+02	0.61583E+02	-0.12614E+00	-0.10000E-10
1	0.13876E+02	C.81576E+C2	0.54225E+02	0.11209E+02	0.61433E+02	-0.11664E+00	-0.10000E-10
2	0.94484E+01	C.88197E+C2	0.56593E+02	0.11190E+02	0.61329E+02	-0.11005E+00	-0.10000E-10
3	0.83327E+01	C.93158E+C2	0.56779E+02	0.11173E+02	0.61236E+02	-0.10415E+00	-0.10000E-10
4	0.82421E+01	C.99313E+C2	0.62907E+02	0.11155E+02	0.61143E+02	-0.98255E-01	-0.10000E-10
5	0.82351E+01	0.10420E+C3	0.65938E+02	0.11138E+02	0.61050E+02	-0.92325E-01	-0.10000E-10
6	0.80957E+01	C.11043E+C3	0.66731E+02	0.11121E+02	0.60957E+02	-0.86460E-01	-0.10000E-10
7	C.77540E+01	C.11575E+C3	0.71213E+02	0.11105E+02	0.60869E+02	-0.80806E-01	-0.10000E-10
8	0.73216E+01	0.12080E+C3	0.73617E+02	0.11089E+02	0.60784E+02	-0.75432E-01	-0.10000E-10
9	0.67787E+01	0.12552E+C3	0.75591E+02	0.11075E+02	0.60705E+02	-0.70403E-01	-0.10000E-10
10	0.62000E+01	0.12586E+C3	0.77467E+02	0.11061E+02	0.60633E+02	-0.65770E-01	-0.10000E-10
11	0.56103E+01	C.13281E+C3	0.75039E+02	0.11049E+02	0.60567E+02	-0.61536E-01	-0.10000E-10
12	0.51252E+01	0.13745E+C3	0.80762E+02	0.11038E+02	0.60506E+02	-0.57628E-01	-0.10000E-10
13	0.43462E+01	0.14092E+C3	0.82494E+02	0.11027E+02	0.60448E+02	-0.53899E-01	-0.10000E-10
14	0.47277E+01	0.14433E+C3	0.84368E+02	0.11017E+02	0.60391E+02	-0.50234E-01	-0.10000E-10
15	0.46580E+01	C.14771E+C3	0.86096E+02	0.11006E+02	0.60335E+02	-0.46602E-01	-0.10000E-10
16	0.44767E+01	0.15098E+C3	0.87623E+02	0.10996E+02	0.60280E+02	-0.43076E-01	-0.10000E-10
17	0.41629E+01	C.15406E+C3	0.88928E+02	0.10987E+02	0.60229E+02	-0.39752E-01	-0.10000E-10
18	0.37654E+01	0.15689E+C3	0.90070E+02	0.10978E+02	0.60182E+02	-0.36688E-01	-0.10000E-10
19	0.32773E+01	C.15540E+C3	0.90891E+02	0.10970E+02	0.60140E+02	-0.33949E-01	-0.10000E-10
20	0.27543E+01	0.16158E+C3	0.91631E+02	0.10964E+02	0.60103E+02	-0.31560E-01	-0.10000E-10
21	0.25451E+01	C.16363E+C3	0.92917E+02	0.10957E+02	0.60069E+02	-0.29299E-01	-0.10000E-10
22	0.29635E+01	0.16600E+C3	0.95049E+02	0.10950E+02	0.60029E+02	-0.26719E-01	-0.10000E-10
23	0.39746E+01	0.16507E+C3	0.97989E+02	0.10941E+02	0.59978E+02	-0.23355E-01	-0.10000E-10

11	T= 10.435	DT= 0.10000E+00	HAV= 0.12811E+C3	GAV= 0.11055E+02	DAV= 0.60662E+02	TIN= 0.40509E+02	TCUT= 0.93629E+02

Information Processing Center

Information Processing Center

Information Processing Center

Information Processing Center

61 T= 15.435 CT= 0.10CCCE+CC HAV= 0.12116E+03 GAV= 0.95541E+01 DAV= 0.60778E+02 TIN= 0.41113E+02 LGUT= C.84125E+02

HSAT=151.6 BTU/LBM

0.33139E+01 0.15531E+03 0.85791E+02 0.94715E+01 0.60207E+02 -0.37636E-01 -0.10CCCE-10

0.24708E+01 0.15288E+03 0.87379E+02 0.94781E+01 0.60245E+02 -0.44034E-01 -0.10CCCE-10

0.21220E+01 0.15096E+03 0.86373E+02 0.94831E+01 0.60280E+02 -0.42437E-01 -0.10CCCE-10

0.22764E+01 0.14934E+03 0.84594E+02 0.94875E+01 0.60308E+02 -0.44271E-01 -0.10CCCE-10

0.27324E+01 0.14758E+03 0.83966E+02 0.94922E+01 0.60337E+02 -0.44622E-01 -0.10CCCE-10

0.31394E+01 0.14552E+03 0.83321E+02 0.94977E+01 0.60371E+02 -0.44849E-01 -0.10CCCE-10

0.34707E+01 0.14319E+03 0.82271E+02 0.95035E+01 0.60410E+02 -0.51049E-01 -0.10CCCE-10

0.37323E+01 0.14063E+03 0.81279E+02 0.95107E+01 0.60453E+02 -0.53823E-01 -0.10CCCE-10

0.38835E+01 0.13790E+03 0.79595E+02 0.95180E+01 0.60499E+02 -0.56787E-01 -0.10CCCE-10

0.39416E+01 0.13507E+03 0.78541E+02 0.95255E+01 0.60546E+02 -0.55850E-01 -0.10CCCE-10

0.40405E+01 0.13221E+03 0.76961E+02 0.95331E+01 0.60594E+02 -0.62947E-01 -0.10CCCE-10

0.42730E+01 0.12929E+03 0.75455E+02 0.95405E+01 0.60642E+02 -0.66105E-01 -0.10CCCE-10

0.46800E+01 0.12622E+03 0.74030E+02 0.95490E+01 0.60694E+02 -0.65421E-01 -0.10CCCE-10

0.51741E+01 0.12268E+03 0.72686E+02 0.95579E+01 0.60750E+02 -0.73019E-01 -0.10CCCE-10

0.56683E+01 0.11921E+03 0.71077E+02 0.95677E+01 0.60811E+02 -0.76962E-01 -0.10CCCE-10

0.61043E+01 0.11520E+03 0.69383E+02 0.95784E+01 0.60877E+02 -0.81246E-01 -0.10CCCE-10

0.64547E+01 0.11091E+03 0.67329E+02 0.95888E+01 0.60945E+02 -0.85828E-01 -0.10CCCE-10

0.67456E+01 0.10633E+03 0.65204E+02 0.96018E+01 0.61025E+02 -0.90654E-01 -0.10CCCE-10

0.68659E+01 0.10168E+03 0.62814E+02 0.96144E+01 0.61104E+02 -0.95667E-01 -0.10CCCE-10

0.68717E+01 0.96914E+02 0.60217E+02 0.96271E+01 0.61183E+02 -0.10075E+00 -0.10CCCE-10

0.69473E+01 0.92158E+02 0.57233E+02 0.96397E+01 0.61263E+02 -0.10591E+00 -0.10CCCE-10

0.78715E+01 0.87366E+02 0.54242E+02 0.96525E+01 0.61353E+02 -0.11092E+00 -0.10CCCE-10

0.11569E+02 0.81954E+02 0.52545E+02 0.96669E+01 0.61433E+02 -0.11666E+00 -0.10CCCE-10

0.7441E+02 0.60226E+02 0.60226E+02 0.96879E+01 0.61565E+02 -0.12501E+00 -0.10CCCE-10

0.0 0.0 0.0 0.0 0.0 0.0 0.0

BTU/5/FT**2 C C BTU/LBM FT(L,J) LBM/5/FT**2 DEN(L,J) LBM/FT**3 X(I,J) HSAT=194.4 BTU/LBM

61 T= 15.435C9 DT= 0.10CCCE+00

CGNBI(J)

21	T= 20.43469	CT= 0.10CC0E+00					
INCH	BTU/S/FT**2. QETAV	BTL/LBM E(I,J)	C C TW(I,J)	LBM/S/FT**2 G(I,J)	LBM/FT**3 DEN(I,J)	X(I,J)	HSAT=194.4 BTL/LBM CCNR(I,J)
0	0.0	0.74570E+C2	0.58199E+02	0.89114E+01	0.61556E+02	-0.12446E+C0	-0.1CC0CE-10
1	0.10271E+02	0.81685E+C2	0.51561E+02	0.88939E+01	0.61437E+02	-0.11694E+C0	-0.1CC0CE-10
2	0.69937E+01	0.86545E+C2	0.53557E+02	0.88820E+01	0.61356E+02	-0.11177E+C0	-0.1CC0CE-10
3	0.61679E+01	0.90646E+C2	0.56057E+02	0.88715E+01	0.61284E+02	-0.10718E+00	-0.1CC0CE-10
4	0.61008E+01	0.95111E+C2	0.58475E+02	0.88610E+01	0.61213E+02	-0.10262E+C0	-0.1CC0CE-10
5	0.60956E+01	0.99384E+C2	0.60805E+02	0.88506E+01	0.61142E+02	-0.98055E-01	-0.1CC0CE-10
6	0.59924E+01	0.10360E+C3	0.62949E+02	0.88402E+01	0.61072E+02	-0.93554E-01	-0.1CC0CE-10
7	0.57395E+01	0.10764E+C3	0.64855E+02	0.88303E+01	0.61004E+02	-0.89224E-01	-0.1CC0CE-10
8	0.54195E+01	0.11148E+C3	0.66696E+02	0.88209E+01	0.60940E+02	-0.85117E-01	-0.1CC0CE-10
9	0.50324E+01	0.11505E+C3	0.68214E+02	0.88122E+01	0.60880E+02	-0.81281E-01	-0.1CC0CE-10
10	0.45937E+01	0.11832E+C3	0.69654E+02	0.88042E+01	0.60826E+02	-0.77754E-01	-0.1CC0CE-10
11	0.41549E+01	0.12129E+C3	0.70860E+02	0.87969E+01	0.60776E+02	-0.74539E-01	-0.1CC0CE-10
12	0.37936E+01	0.12402E+C3	0.72166E+02	0.87902E+01	0.60730E+02	-0.71580E-01	-0.1CC0CE-10
13	0.35872E+01	0.12661E+C3	0.73470E+02	0.87838E+01	0.60687E+02	-0.68764E-01	-0.1CC0CE-10
14	0.34994E+01	0.12915E+C3	0.74873E+02	0.87776E+01	0.60645E+02	-0.66005E-01	-0.1CC0CE-10
15	0.34478E+01	0.13165E+C3	0.76163E+02	0.87715E+01	0.60603E+02	-0.63276E-01	-0.1CC0CE-10
16	0.33136E+01	0.13407E+C3	0.77301E+02	0.87656E+01	0.60563E+02	-0.60639E-01	-0.1CC0CE-10
17	0.30814E+01	0.13633E+C3	0.78269E+02	0.87600E+01	0.60525E+02	-0.58165E-01	-0.1CC0CE-10
18	0.27872E+01	0.13839E+C3	0.79108E+02	0.87550E+01	0.60491E+02	-0.55900E-01	-0.1CC0CE-10
19	0.24259E+01	0.14020E+C3	0.79701E+02	0.87506E+01	0.60460E+02	-0.53895E-01	-0.1CC0CE-10
20	0.20388E+01	0.14174E+C3	0.80223E+02	0.87468E+01	0.60435E+02	-0.52168E-01	-0.1CC0CE-10
21	0.18839E+01	0.14317E+C3	0.81139E+02	0.87433E+01	0.60411E+02	-0.50551E-01	-0.1CC0CE-10
22	0.21936E+01	0.14483E+C3	0.82673E+02	0.87392E+01	0.60383E+02	-0.48703E-01	-0.1CC0CE-10
23	0.22420E+01	0.14702E+C3	0.84803E+02	0.87338E+01	0.60346E+02	-0.46302E-01	-0.1CC0CE-10

21	T= 20.435	CT= 0.1CC0CE+00	HAV= 0.11669E+03	GAV= 0.88012E+01	DAV= 0.60853E+02	TIN= 0.41408E+C2	IGUT= 0.61541E+C2
							HSAT=191.6 BTL/LBM

Information Processing Center

Information Processing Center

Information Processing Center

Information Processing Center

71	T= 25.43422	CT= 0.10000E+00						MSAT=194.4 BTU/LBM
INCH	BTU/S/FT**2. QETA	BTU/LBM F(I,J)	C C T(I,J)	LBM/S/FT**2 G(I,J)	LBM/FT**3 DEN(I,J)	X(I,J)	CCNE(I,J)	
0	0.0	0.75059E+C2	0.56995E+02	0.83706E+01	0.61549E+02	-0.12395E+00	-0.10000E-10	
1	0.93681E+01	0.81605E+C2	0.50940E+02	0.83555E+01	0.61439E+02	-0.11703E+00	-0.10000E-10	
2	0.63788E+01	0.86075E+C2	0.52792E+02	0.83452E+01	0.61264E+02	-0.11226E+00	-0.10000E-10	
3	0.56256E+01	0.90028E+C2	0.55093E+02	0.83361E+01	0.61298E+02	-0.10803E+00	-0.10000E-10	
4	0.55644E+01	0.93547E+C2	0.57316E+02	0.83271E+01	0.61233E+02	-0.10303E+00	-0.10000E-10	
5	0.55597E+01	0.97872E+C2	0.59457E+02	0.83180E+01	0.61167E+02	-0.99625E-01	-0.10000E-10	
6	0.54655E+01	0.10174E+C3	0.61428E+02	0.83091E+01	0.61103E+02	-0.95481E-01	-0.10000E-10	
7	0.52348E+01	0.10546E+C3	0.63182E+02	0.83006E+01	0.61040E+02	-0.91496E-01	-0.10000E-10	
8	0.49430E+01	0.10897E+C3	0.64874E+02	0.82925E+01	0.60982E+02	-0.87716E-01	-0.10000E-10	
9	0.45899E+01	0.11225E+C3	0.66271E+02	0.82849E+01	0.60927E+02	-0.84187E-01	-0.10000E-10	
10	0.41898E+01	0.11525E+C3	0.67596E+02	0.82780E+01	0.60877E+02	-0.80943E-01	-0.10000E-10	
11	0.37896E+01	0.11797E+C3	0.68706E+02	0.82717E+01	0.60831E+02	-0.77987E-01	-0.10000E-10	
12	0.34601E+01	0.12047E+C3	0.69908E+02	0.82660E+01	0.60790E+02	-0.75267E-01	-0.10000E-10	
13	0.32718E+01	0.12294E+C3	0.71103E+02	0.82605E+01	0.60750E+02	-0.72680E-01	-0.10000E-10	
14	0.31917E+01	0.12516E+C3	0.72368E+02	0.82552E+01	0.60711E+02	-0.70147E-01	-0.10000E-10	
15	0.31447E+01	0.12745E+C3	0.73569E+02	0.82499E+01	0.60673E+02	-0.67644E-01	-0.10000E-10	
16	0.30223E+01	0.12955E+C3	0.74610E+02	0.82448E+01	0.60636E+02	-0.65226E-01	-0.10000E-10	
17	0.29104E+01	0.13171E+C3	0.75494E+02	0.82401E+01	0.60602E+02	-0.62960E-01	-0.10000E-10	
18	0.25421E+01	0.13359E+C3	0.76260E+02	0.82357E+01	0.60571E+02	-0.60888E-01	-0.10000E-10	
19	0.22126E+01	0.13523E+C3	0.76799E+02	0.82320E+01	0.60543E+02	-0.59055E-01	-0.10000E-10	
20	0.18595E+01	0.13662E+C3	0.77272E+02	0.82287E+01	0.60520E+02	-0.57480E-01	-0.10000E-10	
21	0.17183E+01	0.13792E+C3	0.78103E+02	0.82258E+01	0.60498E+02	-0.56006E-01	-0.10000E-10	
22	0.20007E+01	0.13942E+C3	0.79498E+02	0.82223E+01	0.60473E+02	-0.54321E-01	-0.10000E-10	
23	0.26933E+01	0.14141E+C3	0.81434E+02	0.82177E+01	0.60440E+02	-0.52128E-01	-0.10000E-10	

Information Processing Center

Information Processing Center

Information Processing Center

Information Processing Center

71 T= 25.434 DT= 0.10000E+00 HAV= 0.11371E+03 GAV= 0.82756E+01 DAV= 0.60902E+02 TIN= 0.41680E+02 ICUT= 0.78455E+02

MSAT=191.8 BTU/LBM

31 T= 30.43376 DT= 0.10000E+00							
INCH	BTU/S/FT**2. QFTAV	BTU/LBM F(I,J)	C C T(I,J)	LBM/S/FT**2 G(I,J)	LBM/FT**3 DEN(I,J)	X(I,J)	HSAT=194.4 BTU/LBM CCN9(I,J)
0	0.0	0.75523E+C2	0.56136E+02	0.79585E+01	0.61540E+02	-0.12347E+00	-0.10000E-10
1	0.86845E+01	0.81633E+C2	0.50523E+02	0.79451E+01	0.61438E+02	-0.11700E+00	-0.10000E-10
2	0.59133E+01	0.85604E+C2	0.52263E+02	0.79360E+01	0.61369E+02	-0.11254E+00	-0.10000E-10
3	0.52151E+01	0.89491E+C2	0.54411E+02	0.79279E+01	0.61307E+02	-0.10858E+00	-0.10000E-10
4	0.51584E+01	0.93145E+C2	0.56484E+02	0.79159E+01	0.61246E+02	-0.10466E+00	-0.10000E-10
5	0.51540E+01	0.96804E+C2	0.58481E+02	0.79118E+01	0.61185E+02	-0.10073E+00	-0.10000E-10
6	0.50667E+01	0.10041E+C3	0.60319E+02	0.79039E+01	0.61125E+02	-0.96864E-01	-0.10000E-10
7	0.48529E+01	0.10387E+C3	0.61956E+02	0.78963E+01	0.61067E+02	-0.93143E-01	-0.10000E-10
8	0.45823E+01	0.10715E+C3	0.63534E+02	0.78892E+01	0.61012E+02	-0.89614E-01	-0.10000E-10
9	0.42550E+01	0.11020E+C3	0.64838E+02	0.78825E+01	0.60961E+02	-0.86320E-01	-0.10000E-10
10	0.38840E+01	0.11299E+C3	0.66073E+02	0.78764E+01	0.60915E+02	-0.83293E-01	-0.10000E-10
11	0.35131E+01	0.11552E+C3	0.67108E+02	0.78708E+01	0.60872E+02	-0.80536E-01	-0.10000E-10
12	0.32076E+01	0.11784E+C3	0.68227E+02	0.78657E+01	0.60834E+02	-0.77999E-01	-0.10000E-10
13	0.30330E+01	0.12004E+C3	0.69343E+02	0.78609E+01	0.60797E+02	-0.75588E-01	-0.10000E-10
14	0.27589E+01	0.12219E+C3	0.70536E+02	0.78562E+01	0.60761E+02	-0.73228E-01	-0.10000E-10
15	0.29152E+01	0.12431E+C3	0.71623E+02	0.78515E+01	0.60726E+02	-0.70896E-01	-0.10000E-10
16	0.28017E+01	0.12636E+C3	0.72600E+02	0.78470E+01	0.60691E+02	-0.68646E-01	-0.10000E-10
17	0.26054E+01	0.12827E+C3	0.73420E+02	0.78429E+01	0.60660E+02	-0.66537E-01	-0.10000E-10
18	0.23566E+01	0.13000E+C3	0.74130E+02	0.78391E+01	0.60631E+02	-0.64610E-01	-0.10000E-10
19	0.20511E+01	0.13152E+C3	0.74629E+02	0.78357E+01	0.60605E+02	-0.62907E-01	-0.10000E-10
20	0.17238E+01	0.13281E+C3	0.75065E+02	0.78329E+01	0.60584E+02	-0.61445E-01	-0.10000E-10
21	0.15929E+01	0.13400E+C3	0.75832E+02	0.78303E+01	0.60564E+02	-0.60078E-01	-0.10000E-10
22	0.18547E+01	0.13538E+C3	0.77120E+02	0.78273E+01	0.60541E+02	-0.58515E-01	-0.10000E-10
23	0.24875E+01	0.13722E+C3	0.78912E+02	0.78232E+01	0.60510E+02	-0.56478E-01	-0.10000E-10

31	T= 30.434	DT= 0.10000E+00	HAV= 0.11152E+03	GAV= 0.78743E+01	DAV= 0.60939E+02	TIN= 0.41938E+02	TOUT= 0.76148E+02
HSAT=191.6 BTU/LBM							

Information Processing Center

Information Processing Center

Information Processing Center

Information Processing Center

APPENDIX D

TWO PHASE FLOW ANALYSIS

- D.1 Friction Coefficient
- D.2 Void Fraction
- D.3 Boiling Criteria

APPENDIX D

TWO PHASE FLOW

D.1 Friction Coefficient

Due to small dimensions of flow channels, one dimensional uniform velocity can be assumed for the coolant in upward motion. Mesh point calculation showed that considering the density variation along the fuel plate, the variation in fluid velocity is negligibly small. Therefore, one can consider constant but not equal velocities for vapour and liquid.

The maximum pressure in the lower plenum in the case of pump coast-down and natural convection, which is the probable case for boiling to occur, is about 19.5 psia. This means that in the case of boiling, steam bubbles are free to have relative velocity with respect to the liquid, therefore, the Separated Flow Model could be applied, whereas at high pressures that vapour and liquid could not have any relative velocity, the Homogeneous Model is a better assumption.

With these assumptions, Lockhart-Martinelle Correlation (Ref, D,1) could be used as the first step:

$$\left. \frac{dP}{dz} \right|_{\text{friction}} = [(2f_f G (1-x)v_f)/D] \phi_f^2 \quad (D.1)$$

where

$$\phi_f = 1 + C/X + 1/X^2 \quad (D.2)$$

and C is a constant of fluid conditions (turbulent or viscous) and

$X = (dP/dz)_f / (dP/dz)_g$ is the ratio of liquid phase to vapour phase friction pressure gradient assuming each one is flowing alone in the channel

G total mass flow rate per unit area

x mass quality

D hydraulic diameter

ν_f liquid volume density, and

f_f liquid friction coefficient

For laminar flow in rectangular channels $f = C(GD/\mu)^{-n}$

therefore

$$X = [f_f G^2 (1-x)^2 \nu_f / D] / [f_g G^2 x^2 \nu_g / D] = (1-x)^2 \nu_f / x^2 \nu_g \quad f_f / f_g$$

Since

$$f_f / f_g = C(GD(1-x)/\mu_f)^{-n} / C(GDx/\mu_g)^{-n} = (\mu_f/\mu_g)^n (x/(1-x))^n$$

$$X = (\nu_f/\nu_g) (\mu_f/\mu_g)^n ((1-x)/x)^{2-n} \quad (D.3)$$

Because of the relative velocity between vapour and liquid, Chisholm (Ref. .2) corrected the L.M. method by allowing for the interfacial shear force between the phases. He also used Equation D.2 to introduce the influence of mass velocity on ϕ_f (Ref. D.3). A most convenient general expression (Ref D.4) for the coefficient C, used by Collier (Ref. D.5) is:

$$C = [\lambda + (C_2 - \lambda)(\nu_{fg}/\nu_f)^{0.5}] [(\nu_g/\nu_f)^{0.5} + (\nu_f/\nu_g)^{0.5}] \quad (D.4)$$

where $\lambda = (2^{2-n} - 2)/2$

and for smooth tube of $G \leq 1.47 \times 10^6 \text{ lb}_m/\text{hr ft}^2$ $C_2 = 1.47 \times 10^6/G$

$n = 1$ for laminar flow

$n = 0.25$ for transition region

D.2 Void Fraction

Lockhart and Martinelli suggested the following correlation for void fraction as a function of pressure for separated flow model:

$$\alpha = (1 + X^{0.8})^{-0.378} \quad (\text{D.5})$$

The the slip ratio can be found from the general equation:

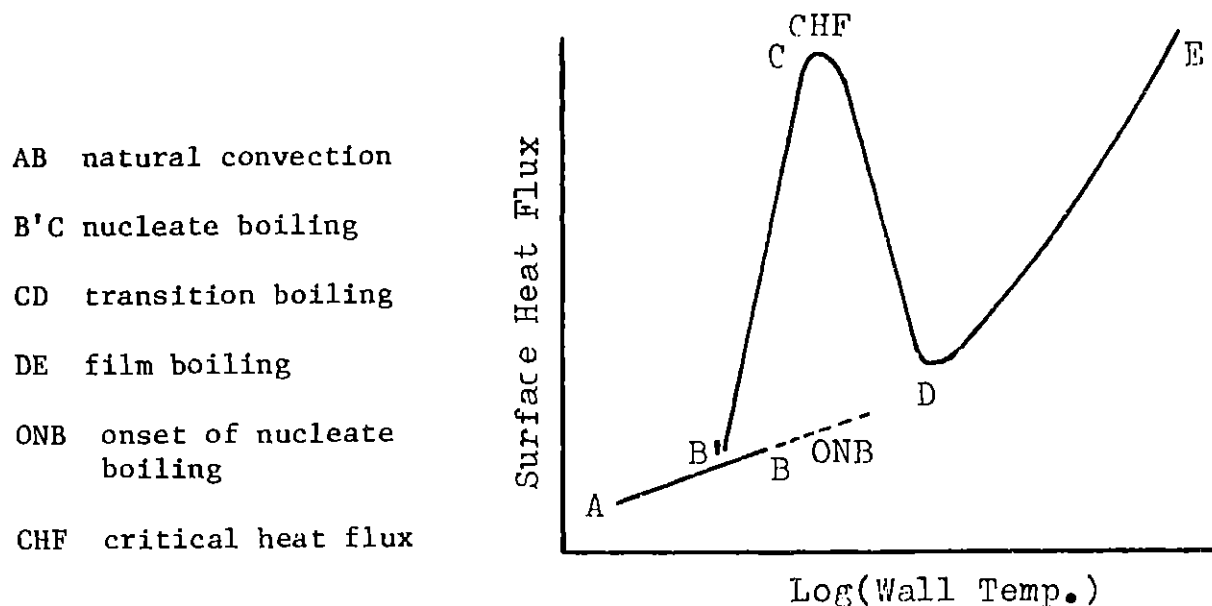
$$S = (x/(1-x))((1-\alpha/\alpha)(v_g/v_f)) \quad (\text{D.6})$$

where as defined before

$$X = (v_f/v_g)(\mu_f/\mu_g)^n((1-x)/x)^{2-n}$$

D.3 Boiling Criteria

Following a pump coast down, the decay energy released into the coolant will increase the enthalpy to a point that may exceed the saturation enthalpy, and therefore Saturated Pool Boiling occurs. If the heat flux is large enough, Subcooled Pool Boiling may occur, even though the enthalpy is below saturation. These can be shown on the characteristic curve of pool boiling; surface heat flux versus wall temperature.



In the natural convection region, the liquid is at or below the saturation temperature, therefore, in this region fluid can be treated as a single phase liquid and in the case of convection, natural convection formulas can be applied correctly.

In the nucleate boiling region, the surface temperature increases slowly for a large increase in surface heat flux. Several equations are known for this condition, but the Rohsenow Correlation (Ref. D.6) gives a conservative results for pressures around atmospheric:

$$T_w = T_{sat} + C_{sf} (\mu_f H_{fg} / k) [(q'' / \mu_f H_{fg}) \sqrt{(\sigma / g(\rho_f - \rho_g))}]^{0.33} \quad (D.7)$$

where

σ is surface tension, lb/ft

H_{fg} is the latent enthalpy, Btu/lbm

q'' surface heat flux, Btu/ft²hr

μ dyn. viscosity, lb/ft hr

k thermal conductivity, Btu/hr ft °F and

C_{sf} surface fluid constant, conservatively taken to be 0.013

Critical Heat Flux

High increase in surface heat flux will result in a sudden drop in heat transfer coefficient which causes a surface temperature surge, that usually ends up to melt the heating surface.

Several equations are offered for pool boiling crisis, but only two of them are taken here and the most conservative result should be used.

Rohsenow and Griffith (Ref. D.7) obtained the following correlation for the critical heat flux

$$q_c'' = 143 H_{fg} \rho_v ((\rho_f - \rho_v) / \rho_v)^{0.6} (g/g_0)^{0.25} \quad (D.8)$$

where

ρ is the mass density lbm/ft³

H_{fg} latent enthalpy Btu/lbm, and

q_c'' Btu/hr ft²

The other equation is for low velocity convection, obtained by Mcbeth (Ref. D.8):

$$q_c'' / 10^6 = 0.00633 H_{fg} De^{-0.1} (G/10^6)^{0.51} (1 - x_{exit}) \quad (D.9)$$

which is valid over the range of

$P = 15$ to 2000 psia

$G/10^6 = 0,1$ to 7.7 lb/hr ft²

$De = 0.1$ to 0.94 in ; equivalent wetted diameter

$L = 6$ to 123 in ; length of heated chamber

and x_{exit} = negative to positive ; quality.

APPENDIX E

STARTUP INCORE TEMPERATURE MEASUREMENTS

NOTE : Thermocouple Positions are Describe in Table 4.1

Table E-1

STARTUP INCORE TEMPERATURE MEASUREMENTS (° C)

STEADY STATE POWER OF 2.5 MWth FOR 3 hrs.

T/C no.	15	19	8 [*]	10	11	12	13	14
S. 0.0	44.8	54.4	52.0	53.0	45.8	48.0	44.8	44.0
3.0			48.2					
43.0			61.8					
60.0			66.7					
80.0			68.2					
110.0			65.2					
120.0				49.0				
130.0					41.2			
150.0						42.2		
160.0							38.7	
190.0								38.5
235.0		50.8						
265.0			61.8					
346.0				54.4				
347.0					43.5			
348.0						41.0		
348.5							38.5	
349.5								38.4
350.0	38.4							
352.0			60.2					

* Thermocouple no. 8 is the same as 9 for the other Tables

Table E-2

STARTUP INCORE TEMPERATURE MEASUREMENTS ($^{\circ}\text{C}$)

STEADY STATE POWER OF 3.0 MWth FOR 3hrs. (run #3)

T/C no.	6	7	9	10	11	12	13	16
S.								
0.0		38.8	40.8		33.3	39.5		
11.0						49.3		
20.0		52.0						
27.0						43.3		
32.0					35.8			
50.0						40.5		
56.0					36.0			
68.0			62.4					
75.0		58.8						
83.0						38.5		
90.0					36.4			
95.0						38.3		
115.0			57.5					
122.0		53.5						
min.								
2.5						36.8		
3.5					36.0			
4.0			54.0					
4.5		50.8						
5.5					36.2			
7.8			53.8					

Table E-2 Cont.

STARTUP INCORE TEMPERATURE MEASUREMENTS (° C)

STEADY STATE POWER OF 3.0 MWth FOR 3hrs. (run #3)

T/C no.									
		6	7	9	10	11	12	13	16
min.	8.5		50.5						
	9.5						36.8		
	12.0					36.8			
	12.1			53.2					
	12.5		50.7						
	13.5						37.3		
	15.5					37.3			
	16.5			53.3					
	17.0		50.8						

Table E-3

STARTUP INCORE TEMPERATURE MEASUREMENTS (° C)

STEADY STATE POWER OF 3.5 MWth FOR 6.0 hrs.37 min.

T/C no.	6	7	9	10	11	12	13	16
S.								
0.0	40.2	39.3	41.3	132.3	32.6	41.9	35.4	
25.0						45.0		
30.0						44.0		
33.0			69.0					
42.0					35.8			
48.0						45.5		
55.0						40.5		
70.0		60.5						
75.0			63.3					
93.0					38.5			
105.0						38.5		
133.0			58.5					
142.0		54.6						
150.0					36.6			
min. 165.0						37.5		
3.5						37.3		
4.0					35.8			
4.5			55.8					
5.0		52.5						
7.5						36.8		

Table E-3 Cont.

STARTUP INCORE TEMPERATURE MEASUREMENTS (°C)

STEADY STATE POWER OF 3.5 MWth FOR 6.0 hrs., 37 min.

T/C no.	6	7	9	10	11	12	13	16
Time								
min.								
10.0						37.3		
12.0						37.5		
12.5					37.3			
14.0		52.0						
15.0			54.4					
16.5		52.0						
17.5						37.8		
18.0					38.5			
20.0						38.0		
21.0					38.5			
21.5				119.3				
22.0			54.8					
22.5		53.0						
25.0	53.0							
26.0							35.5	
27.0						38.5		
40.0						38.6		
40.5							35.9	
42.0					40.9			
43.0				112.5				

Table E-4 Cont.

STARTUP INCORE TEMPERATURE MEASUREMENTS (° C)

STEADY STATE POWER OF 4.0 MWth FOR 10.0 min.

T/C no.	6	7	9	10	11	12	13	16
Time mins.								
3.4						38.1		
5.0	53.3							
5.6		52.8						
6.0			55.0					
7.4					38.9			
8.5						37.5		
9.5							34.8	
14.5						37.4		
14.8	52.0							
15.2		52.5						
15.5			54.0					
15.9					38.5			
16.7						37.0		
17.2							33.9	
17.7				82.3				
19.7	51.8							
20.0		52.0						
20.4			54.0					
21.0					38.6			
21.3						36.6		

Table E-5

STARTUP INCORE TEMPERATURE MEASUREMENTS (° C)

STEADY STATE POWER OF 4.0 MWth FOR 11.5 hrs.

Time	T/C no.	6	7	9	10	11	12	13	16
	S.	0.0	50.8	49.8	52.3	152.8	42.5	49.0	43.0
	13.0						50.5		
	17.0					44.3			
	20.0			73.3					
	25.0						53.3		
	28.0					55.5			
	34.0			78.3					
	38.0						49.0		
	43.0					45.5			
	47.0			73.8					
	50.0						48.0		
	65.0					46.8			
	75.0			70.5					
	82.0		66.0						
	90.0					47.3			
	100.0						46.3		
	105.0			68.5					
	112.0		64.8						
	120.0						45.8		
	125.0					46.3			

Table E-5 Cont.

STARTUP INCORE TEMPERATURE MEASUREMENTS (° C)

STEADY STATE POWER OF 4.0 MWth FOR 11.5 hrs.

T/C no.	6	7	9	10	11	12	13	16
S.								
160.0					46.5			
170.0						45.5		
190.0			65.8					
200.0		62.8						
210.0	63.0							
230.0						45.5		
250.0							41.5	
280.0				148.5				
290.0								78.3
310.0						45.5		
360.0			65.3					
370.0		62.3						
380.0					47.0			
390.0						45.8		
510.0						46.3		
530.0	62.5							
550.0		62.5						
570.0			65.3					
585.0				143.3				
610.0					48.8			

Table E-5 Cont.

STARTUP INCORE TEMPERATURE MEASUREMENTS (° C)

STEADY STATE POWER OF 4.0 MWth FOR 11.5 hrs.

T/C no.	6	7	9	10	11	12	13	16
S.								
610.0					48.8			
640.0						46.6		
660.0							43.3	
680.0								72.8
700.0	63.0							
730.0		63.3						
760.0			66.0					
790.0				140.0				
820.0					50.0			
850.0						47.3		
870.0							44.3	
900.0								70.5
910.0	63.5							
930.0						47.5		

Table E-6

STARTUP INCORE TEMPERATURE MEASUREMENTS (° C)

STEADY STATE POWER OF 4.5 MWth FOR 3.25 hrs.

Time	T/C no.	6	7	9	10	11	12	13	16
	s.	0.0	44.8	43.5	46.3	152.5	35.0	45.8	38.3
	12.0						44.3		
	14.0						46.6		
	18.0						47.8		
	22.0						48.8		
	30.0			75.4					
	40.0					38.3			
	45.0						45.5		
	50.0						44.5		
	60.0					38.8			
	70.0			68.0					
	80.0						42.8		
	90.0		61.0						
	100.0			65.3					
	105.0					39.3			
	110.0						42.0		
	150.0		58.3						
	160.0			63.0					
	170.0					38.3			
	190.0						40.3		

Table E-6 Cont.

STARTUP INCORE TEMPERATURE MEASUREMENTS (° C)

STEADY STATE POWER OF 4.5 MWth FOR 3.25 hrs.

T/C no.	6	7	9	10	11	12	13	16
S.								
210.0							36.0	
225.0	57.3							
230.0		56.5						
240.0			60.5					
250.0				149.0				
270.0					39.0			
285.0						40.3		
300.0							36.4	
320.0								78.2
350.0	56.8							
360.0		56.3						
365.0			59.8					
375.0				146.9				
380.0					40.5			
385.0						41.2		
400.0							37.3	
410.0								76.0
425.0	57.5							
430.0		57.2						
450.0			60.5					

Table E-6 Cont.

STARTUP INCORE TEMPERATURE MEASUREMENTS (° C)

STEADY STATE POWER OF 4.5 MWth FOR 3.25 hrs.

T/C no.	6	7	9	10	11	12	13	16
S.								
455.0				142.5				
460.0					42.0			
470.0						42.0		
480.0							38.3	
490.0								72.3
515.0	57.5							
525.0		57.5						
530.0			60.3					
540.0				139.8				
545.0					43.3			
555.0						42.8		
560.0							39.0	
570.0								70.0
580.0						42.5		

Table E-7

STARTUP INCORE TEMPERATURE MEASUREMENTS (° C)

STEADY STATE POWER OF 4.9 MWth FOR 10.0 mins.

T/C no.	6	7	9	10	11	12	13	16
S.								
0.0	50.3	49.0	51.8		40.0	51.5	43.0	55.5
9.0						46.8		
11.0						47.5		
14.0						49.3		
20.0						52.3		
26.0					42.8			
35.0					43.8			
43.0			76.8					
51.0						47.8		
56.0						47.3		
60.0					43.8			
70.0			70.3					
75.0			64.5					
85.0						45.5		
90.0		63.5						
95.0			66.5					
100.0					45.0			
104.0						44.8		
128.0		62.0						
131.0			63.0					

Table E-7 Cont.

STARTUP INCORE TEMPERATURE MEASUREMENTS (°C)

STEADY STATE POWER OF 4.9 MWth FOR 10.0 mins.

T/C no.	6	7	9	10	11	12	13	16
Time mins.								
5.7							39.0	
6.0								57.3
8.6	58.0							
8.65		58.0						
8.7			60.5					
8.8				99.3				
8.9					43.3			
9.0						42.5		
9.2							39.8	
9.3								56.0
10.5	58.3							
10.6		58.3						
10.75			60.5					
10.95				97.8				
11.1					44.8			
11.3						43.5		
11.5							40.0	
12.0								55.3
12.5						43.3		
13.5					44.5			

Table E-7 Cont.

STARTUP INCORE TEMPERATURE MEASUREMENTS (° C)

STEADY STATE POWER OF 4.9 MWth FOR 10.0 mins.

T/C no.	6	7	9	10	11	12	13	16
S.								
134.0					44.3			
135.0					44.0			
137.0						42.8		
140.0							39.5	
146.0								59.5
150.0				103.0				
152.0	58.8							
154.0		58.8						
156.0			60.8					
158.0				102.8				
160.0					44.0			
163.0						42.5		
164.0							39.0	
170.0								58.8
270.0	57.8							
mins.								
4.8		58.0						
5.0			60.3					
5.2				101.0				
5.4					43.8			
5.5						42.8		

Table E-8 Cont.

STARTUP INCORE TEMPERATURE MEASUREMENTS (°C)

STEADY STATE POWER OF 4.83 MWth FOR 18 hrs.

T/C no.	6	7	9	10	11	12	13	16
S.								
115.0						47.0		
120.0					46.8	46.8		
122.0					45.8			
130.0					46.2			
140.0			68.8					
145.0		66.3						
180.0								92.0
188.0							41.5	
200.0						46.0		
210.0					46.5			
230.0				125.0				
235.0			67.3					
250.0		65.5						
255.0	65.3							
265.0								90.0
270.0							40.3	
270.0						46.3		
300.0					46.8			
310.0				173.5				
315.0			67.5					

Table E-8 Cont.

STARTUP INCORE TEMPERATURE MEASUREMENTS (°C)

STEADY STATE POWER OF 4.83 MWth FOR 18 hrs.

Time	T/C no.	6	7	9	10	11	12	13	16
	S.	330.0		64.8					
	335.0	64.5							
	340.0						46.8		
	400.0								86.3
	405.0							36.6	
	415.0						47.8		
	430.0					49.3			
	450.0				169.5				
	455.0			68.0					
	465.0		65.3						
	475.0	65.5							
min.	15.2								81.8
	15.3							45.8	
	15.5						49.0		
	15.75					52.0			
	15.8				164.8				
	16.0			69.0					
	16.2		66.5						
	16.3	66.5							
	16.5						49.3		

REFERENCES

- 1.1 Choi, D.K., "Temperature Distribution and Natural Convective Shutdown Cooling of the MITR-II", SM Thesis, Nuclear Engineering Department, MIT, May 1970.
- 1.2 Choi, D.K., "Natural Convective Core Cooling of the MITR-II Including the Effect of Scram Delay Time", Special Project Report, 22.90, Nuclear Engineering Department, MIT, May 1970.
- 1.3 MIT Reactor Staff, "Operational Manual for the MITR-II", Massachusetts Institute of Technology, June 1973.
- 1.4 Allen, G.C.Jr., Clark, L.Jr., Gosnell, J.W., Lanning, D.D., "The Reactor Engineering of the MITR-II Construction and Startup", Nuclear Engineering Department, MIT, June 1976, MITNE-186.
- 2.1 MIT Reactor Staff, "Safety Analysis Report for the MIT Research Reactor(MITR-II)", MIT, October 1970, MITNE-115.
- 2.2 Henry, A.F., "Nuclear Reactor Analysis", The MIT Press, 1975.
- 2.3 MIT Reactor Staff, "Primary Coolant Flow Scram Calibration", MITR Procedure Manual, Section 6.1.3.3 SR no. O-75-68, April 1975.
- 2.4 Zubarev, T.N., Sokolov, A.K., "Calculations of the Heat Release in a Shutdown Reactor", Letter to the Editor, J. Nuclear Energy, Part A. Reactor Science, Vol.13, pp.72-92, 1960-1961.
- 2.5 Afonso-Morales, M., "Natural Convective Cooling of the MITR-II After a Scram Due to a Loss of Flow", SM Thesis, Nuclear Engineering Department, MIT, December 1971.
- 2.6 Lamarsh, J.R., "Introduction to Nuclear Reactor Theory", Addison-Wesley Publishing Co. Inc., 1966.

- 2.7 Shure, K., "Fission Product Decay Energy", Bettis Technical Review, WAPV-BT-24, Reactor Technology, pp.1-17, December 1971.
- 2.8 Dudziak, D.J., Private Communication with K.Shure, (Ref.2.7).
- 2.9 Bernard, J., Three Dimensional CITATION Calculation for Shim Bank at 7.9 and 16.9 Inches From the Bottom of the Core, JHO 629, and JHO 736, November 1976.
- 2.10 Eckert, E.R.G., "Heat and Mass Transfer", McGraw-Hill Book Co. Inc., 1956.
- 2.11 Addae, A.K., "The Reactor Physics of the Massachusetts Institute of Technology Research Reactor Redesign", Ph.D. Thesis, Nuclear Engineering Department, MIT, July 1970, MITNE-118.
- 2.12 Yarman, N.T., "The Reactivity and Transient Analysis of the MITR-II", Ph.D. Thesis, Nuclear Engineering Department, MIT, July 1972, MITNE-139.
- 2.13 Keepin, R.C., "Physics of Nuclear Kinetics",
- 3.1 Eselgroth, P.W., Griffith, P., "Natural Convection Flows in Parallel Connected Vertical Channels with Boiling", Department of Mechanical Engineering, MIT, AT (30-1) 3496, July 1967.
- 3.2 Meyer, J.E., Williams, J.S.Jr., "A Momentum Integral Model for the Treatment of Transient Fluid Flow", Bettis Technical Review, WAPD-BT-25, pp. 47-72, 1962.
- 3.3 Meyer, J.E., "Conservation Laws in One-Dimensional Hydrodynamics", Bettis Technical Review, WAPD-BT-20, pp.61-72, September 1960.
- 3.4 Birkhoff, G., Kimes, T.F., "CHIC Program for Thermal Transients", WAPD-TM-245, February 1962.
- 3.5 Collier, J.G., "Convective Boiling and Condensation", McGraw-Hill Book Co. Lt. (UK), 1972.

- 3.6 Bergles, A.E., Rohsenow, W.M., "The Determination of Forced Convection Surface Boiling Heat Transfer", Paper 63-HT-22, Paper Presented at the Sixth National Heat Transfer Conference of the ASME-AICHE at Boston, August 1963.
- 3.7 Dittus, F.W., Boelter, L.M.K., University of California Publ. Eng., Vol.2, p.443, 1930.
- 3.8 Rohsenow, W.M., Choi, H.Y., "Heat, Mass and Momentum Transfer", Prentice Hall Inc., 1961.
- 3.9 Taborda-Romero, J.A., "Design of MITR-II Fuel Plates, Heat Transfer in Longitudinal Finned Narrow Channels", SM Thesis, Nuclear Engineering Department, MIT, September 1971.
- 3.10 Kays, W.M., "Loss Coefficients for Abrupt Changes in Flow Cross-Section with Low Reynold's Number Flow in Single and Multiple Tube System ", Transaction of ASME, 72:8, pp. 1067-1074, November 1950.
- 3.11 Etherington, H., editor, "Nuclear Engineering Handbook", McGraw-Hill Book Co., 1958.
- 3.12 El-Wakil, M.M., "Nuclear Heat Transport", International Text Book Co., 1971.
- 4.1 MIT Reactor Staff, "Step-Wise Rise to Five Megawatts", Procedure Manual, Subprocedure 5.10.1, SR no. O-75-143, December 1975.
- 4.2 Szymzak, W.J., "Experimental Investigation of Heat Transfer Characteristics of MITR-II Fuel Plates-In-Channel Thermocouple Response and Calibration", SM Thesis, Nuclear Engineering Department, MIT, September 1975.
- 5.1 Meagher, P.C., "Design of Central Irradiation Facilities for the MITR-II Research Reactor", SM Thesis, Nuclear Engineering Department, MIT, September 1976.

- D.1 Lockhart, R.W., Martinelli, R.C., "Proposed Correlation of Data for Isothermal Two-Phase Two-Component Flow in Pipes", Chem. Eng. Prog., 45,39, 1949.
- D.2 Chisholm, D., "A Theoretical Basis for the Lockhart-Martinelli Correlation for Two-Phase Flow", N.E.L. Report, no.310, 1967.
- D.3 Chisholm, D., "The Influence of Mass Velocity on Friction Pressure Gradients During Steam-Water Flow", Paper 35 Presented at 1968 Thermodynamic and Fluid Mechanics Convention I, Mech. Eng. Bristol, March 1968.
- D.4 Chisolm, D., Sutherland, L.A., "Prediction of Prssure Gradients in Pipe Line Systems During Two-Phase Flow", Paper 4 Presented at Symposium on Fluid Mechanics and Measurements in Two-Phase Flow Systems, Univ. of Leeds, September 1969.
- D.5 Collier, J.G., "Convective Boiling and Condensation", McGraw-Hill Co. (UK) Pub. 1972.
- D.6 Rohsenow, W.M., "A Method of Correllating Heat Transfer Data for Surface Boiling of Liquids", Transaction ASME, Vol.74, pp.969-975, 1952.
- D.7 Rohsenow, W.M., Griffith, P., "Correllation of Maximum Heat Transfer Data for Boiling of Saturated Liquids", Chem. Eng. Prog., Symp. Series, 52, no.18, 47, 1956.
- D.8 McBeth, R.V., British Report on Two-Phase Flow, United Kingdom Atomic Energy Authority, AEEW-R-267, 1963.